Innovative approaches to mineral exploitation: the cases of manganese enrichment and pyrite recycling

PhD Thesis

Shpetim Kastrati

Matr. N. R08877

[Digitare il testo]

Indice

Abstract

Turkey is an important manganese ore producer and a major target for new manganese deposits exploration. The two Mn deposits prospected for the present work are Mn-rich lenses within the melange zone of the Eskişehir ophiolite and the Manisa metamorphic deposit. Both deposits are subeconomic due to the relatively low Mn content but underwent metamorphic textural and mineralogical modifications that could allow applying separation techniques to produce a final commercial Mn concentrate.

The Eskişehir ophiolite is located in the western part of the Izmir-Ankara-Erzincan Suture Zone (IAESZ) that crosses Turkey from the west (Izmir area) to the east (border with Georgia) (Uysal et al., 2009). Manganese deposits within the IAESZ are classified by Ozturk (1997) as radiolarian chert-hosted deposits. They are related to Neo-Tethyan suture and form the epi-ophiolitic sediment succession together with associated radiolarite, radiolarian chert, siliceous shale and brown claystone. The deposits show high Mn, variable Si and low Al contents and, as a rule, cannot be enriched due to their very fine grain size.. The Taycilar Mn deposit has never been mined and the local geology is not well known due to paucity of outcrops and absence of investigation. Mn-rich rocks are different from those typical of manganese deposits within IAESZ having undergone a strong metamorphic overprint, and now they consist of strongly deformed braunite-rich quartzites, with NW-SE trend of layering.

Mineralogy and texture of the Taycilar deposit show conditions that can favour magnetic enrichment of ore at relatively coarse grain size, providing the opportunity to produce a high grade sand final product.

Braunite shows a paramagnetic behaviour that is strongly affected by incorporation of elements, like Mg and Fe, substituting Mn. In addition the Taycilar deposit shows a metamorphic recrystallization with grain size increase that allows significative separation of Mn-rich phases and quartz at relatively coarse grainsize of crushed ore.

For the experiment two samples, about 25 kg each, were taken from two outcrops and mixed in equal proportions. Ore was crushed at grain size 95 wt% +4 mm and 100% -20 mm.

Magnetic separation tests were carried out with a Permroll dry magnetic separator at University of Eskisehir, using constant roll speed and magnetic field. Two tests were done for this experiments.

Mn enrichment is respectively 6.55 wt% and 4.86 wt% for ESK2C and ESK10C, that corresponds to 8.46 wt% and 6.28 wt% on a MnO basis, respectively. Mn recovery is very high for ESK2C, 93.7 %, and much lower for ESK10C, 77.7 %.

In conclusion tests show that braunite-rich metamorphic manganese deposits can be successfully enriched magnetically, with a metal recovery that is inversely correlated to grain size. Minimum grain size is hence chosen on the basis of crushing costs and market demand.

Manisa manganese deposit shows a texture with relatively large scale Mn-rich and Mn-poor domains, differently from typical fine grained homogeneous Mn deposits within cherts. This texture can allow gravitational enrichment of the ore due to the high liberation that can be attained through comminution. To test

the feasibility of such enrichment a stock of 10 Mt of run of mine was taken to a 5 km away enrichment plant, that comprises a jaw crusher, a ball mill, a jig and two shaking tables.

Jig final concentrate has 46,76 wt% Mn while concentrate from tables is poorer (around 38,6 wt% Mn). That is because at millimeter scale the jig works very well and the grains have a good grade of liberation. The final concentrate, resulting from mixture of jig and table concentrates has a good commercial quality, with 45,04 wt% Mn, where 70,97 wt% of the material comes from the jig and only 29,03 wt% from the tables The separation efficiency is 70,60 %.

As a conclusion, according to this test, Manisa Mn ore can be successfully enriched at a grain size - 6 mm.

Pyrite (FeS_2) is one of the most ubiquitous minerals of the earth crust. It is found in igneous, metamorphic and sedimentary rocks and crystallizes at both high and low temperatures.

Pyrite was widely used in the past for the production of sulfuric acid, but nowadays this use is limited to China and pyrite lost its value as an industrial mineral. The present work deals with projects for the extraction of pyrite in Albania and Kosovo for new industrial applications that re-opened pyrite market.

For the projects three different ways to recover pyrite were considered: a) as a by-product of pyrite-bearing active mines (Trepça, Kosovo; Fusharrez, Albania); b) re-opening abandoned pyrite mines used in past for sulfuric acid production (Spaç, Albania); c) exploitation of a new pyrite deposit (Lunik, Albania).

Pyrite is an important sulfide phase in the active lead and zinc Trepça Mine, Kosovo. Trepça Belt belongs to the Kosovo sector of the Serbo-Kosovo-Macedonian-Rhodope Metallogenic belt of Oligocene-Miocene age, which includes base and precious-metal districts in Kosovo, southern and western Serbia, northern Greece and southern Bulgaria (Heinrich and Neubauer, 2002).

In northern Albania pyrite can be recovered within the Mirdita ophiolite belt, in similar geological settings, as a by-product and from the tailings of the Fusharrez copper mine and from the abandoned Spaç pyrite mine.

Mirdita is located in the Jurassic age Mirdita-Pindos ophiolite belt of Albania-Greece that ranges from ultramafic to mafic rocks with a number of andesitic and felsic volcanic domes in the central portion. The volcanic rocks are overlain by a sedimentary melange (Beccaluva et al., 1994).

Finally in eastern Albania the never exploited Lunik pyrite deposit is placed inside volcanic rocks. It was formed underwater together with pillow basalts and at low temperature hydrothermal conditions.

The demanding quality parameters for the new industrial applications concern grain size (90% between 10 and 50 mm), S content (48 +/- 2 wt%) and Fe (above 44 wt%). The preliminary study of the above mentioned deposits led to rank them in order of decreasing geologic, technical and logistic feasibility. The application of the results led to begin exploitation at Spac abandoned mine where about 1000 MT of pyrite ore were taken and exported to Italy in 2012.

1 Introduction

During these years we have worked in many countries of the world. Many studies have been conducted on prospection, extraction and enrichment tests of chromite ore, and some articles have been published on the results that we have achieved. Chrome is one of the most demanding industrial products of the world market. At the same time, given the requirements of the steel market, although in smaller quantities, of other minerals that used to be produced, we tried to find new resources that will give us the opportunity to exploit new types of mineral deposits that, until today, are left in limbo. Working on mines and reserves of chrome we saw the opportunity to join further exploration for manganese and pyrites in Turkey, Albania and Kosovo. And we tried to find out all the possibilities for implementing the market of these minerals through enrichment tests to reach the parameters and attributes that are required for today's technology in the steel market, doing tests that have never been performed before. This work contains also a study on the possibility to re-cycle pyrite stocks and pyrite-rich dumps that started from an environmental study regarding pyrite mines and dumps, that was one of the reasons for the closure of the mines. Work in Turkey was done in collaboration with UT Group srl., Sigma metal LTD., 4 Mevsim Madencilik LTD and Politechnic University of Eskisehir, work in Albania and Kosovo was done in collaboration with UT Group srl, Trepca Mine coroporation and the universities of Pristina, Kosovo and Tirana, Albania.

Chapter 1

2 Enrichment tests of manganese deposits

In general manganese ore has never been enriched because of the very fine grain size of particles, although few enrichment experiments have been made. In this work we tested two specific typologies of manganese deposits that can be enriched, because of their mineralogical and textural characteristics.

Two specific deposits of the two different typologies were chosen for the test, both of them located in Turkey.

2.1 Manganese and manganese deposits

Manganese (Mn) is the twelfth most abundant element in the earth crust, where it occurs with an average content of about 1000 ppm (Emsley, 2001) compared to a slightly lower concentration (700 ppm) within the continental crust (Wedepohl, 1985). Manganese is a minor constituent of most rocks, either magmatic, sedimentary or metamorphic. Although manganese is a siderophile element it has a strong affinity for oxygen, thus forming a great variety of oxides, even if relatively common Mn minerals belong also to the classes of carbonates, sulphides and silicates.

Due to its large use in the iron and steel industry manganese is a major commodity in the metal mining industry. Cox and Singer (1986) describe four types of Mn mineral deposits: replacement, volcanogenic, epithermal and sedimentary. Volcanogenic Mn deposits are formed by a combination of volcanic and hydrothermal processes related to hot springs activity in oceanic environments (Mosier and Page, 1988). As a consequence of tectonic displacement such type of deposits can, nowadays, be found in the sedimentary cover of ophiolite complexes or as sedimentary slices within ophiolite melanges, with a metamorphic overprint that can range from nearly absent to high grade.

Ore associations of volcanogenic Mn deposits mainly comprise Mn oxides and/or hydroxides with minor silicates and carbonates (Mosier and Page, 1988). Most common Mn oxides are pyrolusite, psilomelane and manganite, while hydroxides are usually present as amorphous phases. The main characters of these deposits are the high Mn content (usually higher than 40 wt% MnO) and the lithological association with chert. Due to their high grade and very fine mixing of manganese oxides and silica grains Mn ores are not enriched and are sold as lumpy or, after ,comminution, as gravels.

The metamorphic overprint on these deposits usually leads to formation of the Mn silicate braunite (Dasgupta et al., 1993; Vason and Martin, 1993). Experimental data (Abs-Wurmbach and Peters, 1999) show that braunite is the stable Mn phase in a Mn-Al-Si-O system at 600 °C and 4 kbar for a wide range of fO_2 (log fO_2 between -11 and +2). Metamorphic overprint can also lead to re-crystallization of quartz (Dasgupta et al., 1993), thereby giving rise to a general grain size increase and, sometimes, a metamorphic layered to nodular

textured rock, where Mn minerals and quartz are physically separated at centimetric scale. As braunite is a Mn-rich mineral, containing as much as 63.60 nominal wt% Mn, more than the Mn content of pyrolusite and manganite, physical separation of it from gangue phases can be a very effective way to produce commercial manganese concentrate.

Metamorphic braunite-rich Mn deposits are well known in literature (e.g. Dasgupta and Manickavasagam, 1981; Ostwald and Nayak, 1993; Buhn et al., 1995; Velilla and Jimenez-Millan, 2003) but the possibility of braunite magnetic separation has not been investigated in detail yet. In the present study preliminary results on magnetic enrichment of braunite-rich Mn ore of volcanogenic type, that underwent metamorphism, are presented.

2.2 Geography of Turkey

Turkey is situated in Anatolia and the Balkans, bordering the Black Sea, between Bulgaria and Georgia, and bordering the Aegean Sea and the Mediterranean Sea, between Greece and Syria(Fig.1). The area of Turkey is 783,562 km^2; land: 770,760 km^2, water: 9,820 km^2.

Turkey extends more than 1,600 km from west to east but generally less than 800 km from north to south. Total land area of about 783,562 km^2 extends for 756,816 km^2 in Asia and for 23,764 km^2 in Europe.

Fig. 1. Map of Turkey.

2.3 Geology of Turkey

Turkey is characterized by a very complex geology, whose main features are still poorly understood despite an increasing amount of geological data that have become available in the last 25 years. The complex geology has resulted in widely different views on the geological evolution of Turkey.

Turkey is geologically divided into three main tectonic units: the Pontides, the Anatolides-Taurides and the Arabian Platform (Fig. 2, Ketin 1966). These tectonic units, which were once
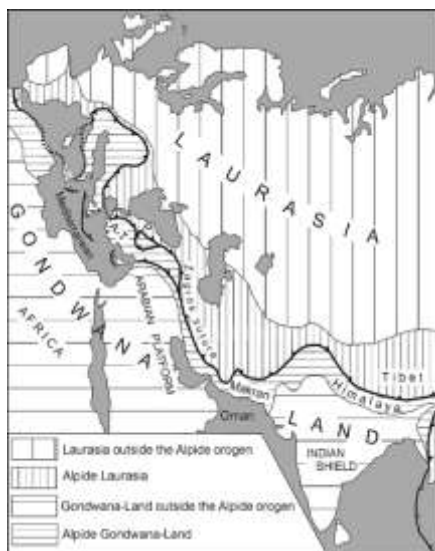
Fig. 2. Tectonic setting of Turkey within the Alpide-Himalayan chain (modified after Şengör 1987). A-T: Anatolides-Taurides; P: Pontides.

surrounded by oceans, are now separated by sutures, which mark the tectonic lines or zones along which these oceans have disappeared. The Pontides exhibit Laurasian affinities and are comparable to the tectonic units in the Balkans and the Caucasus, as well as those in the central Europe (Fig. 2). They all were located north of the northern branch of the Neo-Tethys. The complete closure of this ocean resulted in the İzmir-Ankara-Erzincan suture, which marks the boundary between the Pontides and the Anatolides-Taurides (Fig. 3). The Anatolides-Taurides show Gondwana affinities but were separated from the main mass of Gondwana by the southern branch of Neo-Tethys. They are in contact with the Arabian Platform along the Assyrian suture (Fig. 3). The northern margin of the Arabian Platform is represented by southeast Anatolia south of the Assyrian suture. The Anatolian peninsula is surrounded on three sides by seas, which exhibit widely differing geological features. The Black Sea in the north is an oceanic back-arc basin. It formed during the Cretaceous behind and north of the Pontide magmatic arc as a result
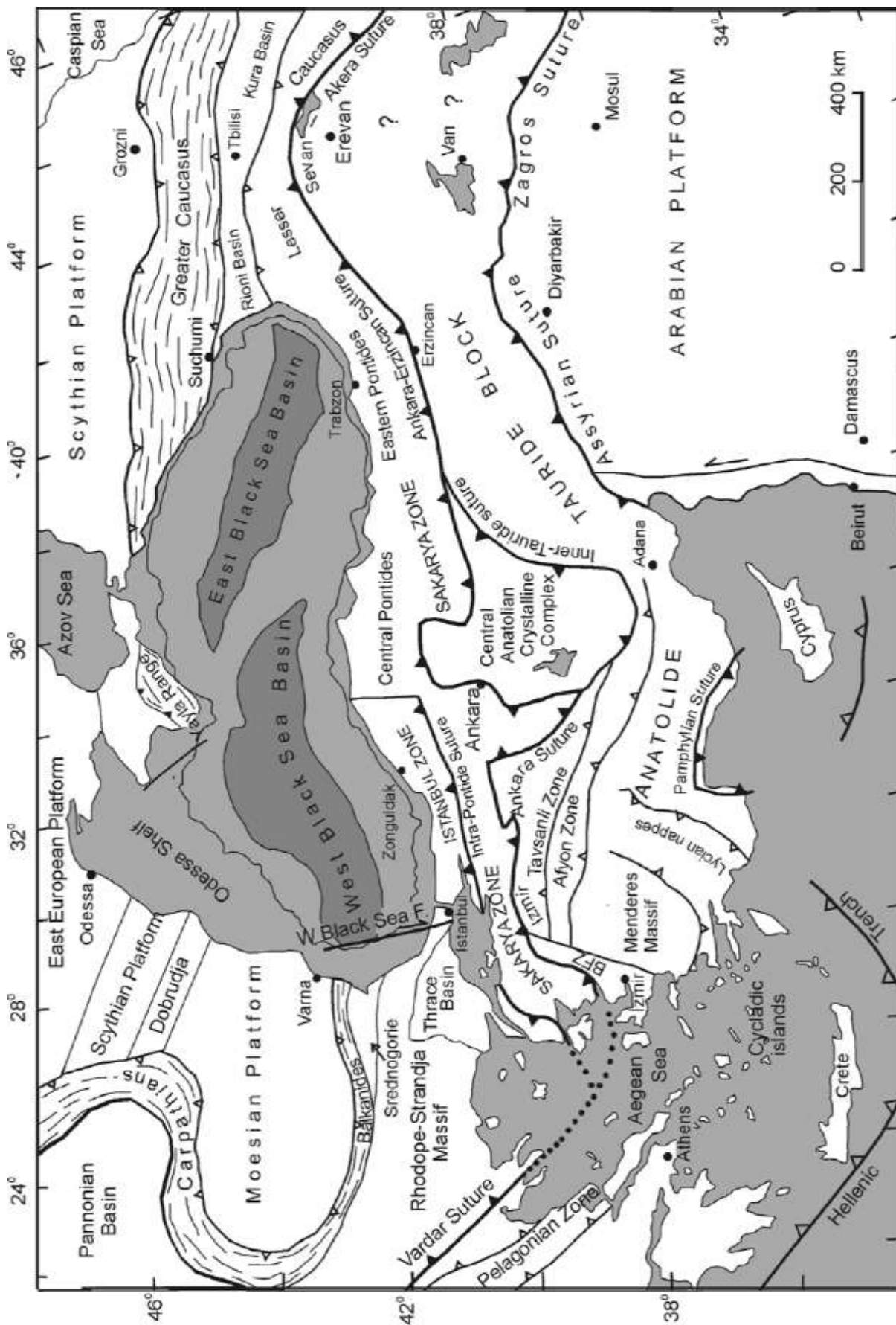
Fig. 3. Tectonic map of north-eastern Mediterranean region showing the major sutures and continental blocks. Sutures are shown by heavy lines with the polarity of former subduction zones indicated by filled triangles. Heavy lines with open triangles represent active subduction zones. The Late Cretaceous oceanic crust in the Black Sea is shown by grey tones. Small open triangles indicate the vergence of the major fold and thrust belts. BFZ denotes the Bornova Flysch Zone (modified after Okay & Tüysüz 1999).

of the subduction of the northern Neo-Tethys ocean (e.g. Görür 1988). In the pre-Cretaceous times, the Pontides were adjacent to Dobrugea and Crimea. The Aegean is a geologically young sea, which started to develop during the Oligo-Miocene as a result of north-south extension above the retreating Hellenic subduction zone (e.g. Jolivet 2001). The Eastern Mediterranean represents a relic of the southern branch of the Neo-Tethys (Fig. 1), and is much older than the other seas (e.g. Garfunkel 2004).

2.4 Manganese deposits of Turkey

Turkey is mainly composed of west to east trending orogenic belts belonging to the Alpine-Hymalaian range, and provides a section across a Tethyan ocean basin from the African plate to the Eurasian continent. This orogenic belt contains a large number of interesting manganese or ferromanganese deposits which lie in east – west to northeast – southwest trending belts (Fig. 4). Their occurrence and distribution patterns are closely associated with the evolution of the Tethyan Ocean, and therefore the metallogenic zones of manganese of Turkey are overprinted with its major tectonostratigraphic units. Manganese deposits in Turkey are also important in regard to the correlation of marine polymetallic oxides of the Alpine belt which were described by several workers.
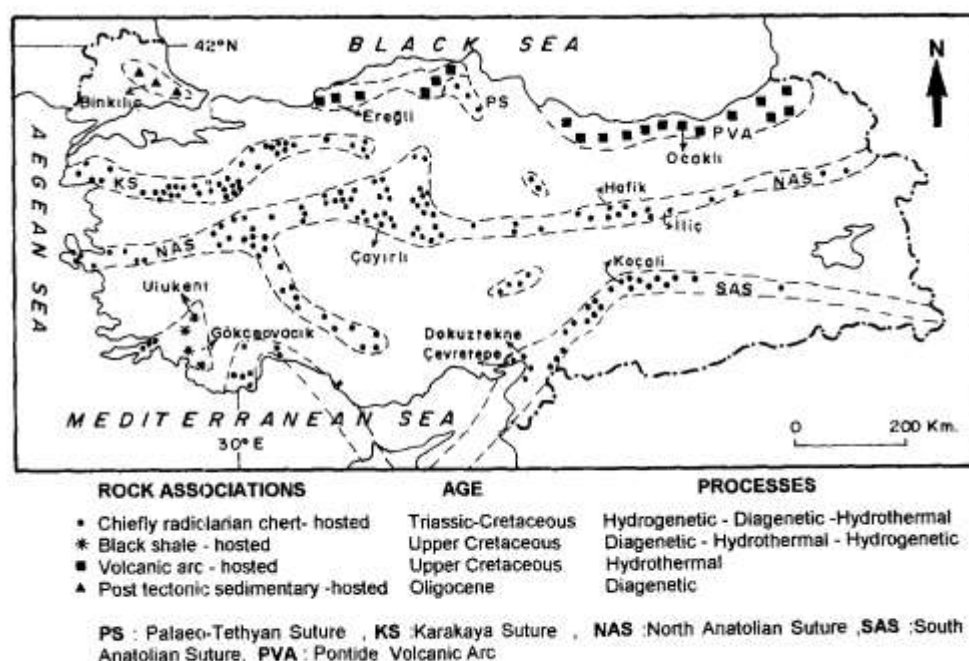
Fig. 1. Distributions and types of manganese deposits in Turkey.

Fig.4. Distribution and types of manganese deposits in Turkey Ozturk (1997).

Manganese deposits in Turkey are divided into four main groups on the basis of their age, host rocks and processes of formation (Ozturk 1997). The first is hydrothermal-hydrogenetic and rarely diagenetic-type manganese deposits which are chiefly associated with radiolarian chert series (Eskisehir deposists). These deposits occur as lenses and small ore beds within ophiolitic mélange zones of Paleo-Tethyan, Karakaya and

7

Neo Tethyan (North Anatolian and South Anatolian) suture belts. The second is black shale-hosted manganese deposits that are found in black shale, calcareous shale and calciturbiditic limestone horizons of the passive margin sediments of Late Cretaceous age in the western Taurides. These deposits generally are metamorphosed to greenschist facies and include Mn carbonate- silicate and oxide minerals. The third is volcanic arc – hosted ores along the Black Sea margin which occur in different types of metasomatic, hydrothermal and stratabound settings. Rock associations include Upper Cretaceous dacitic tuff, reddish limestone, marl and hemipelagic claystone. The fourth is Oligocene – hosted ores in the Thrace Basin. These deposits are similar to those of the Paratethyan Oligocene belt which occur on the eastern and northern margin of Black Sea and include the Chiatura (Georgia), Nikopol (Ukraine) and Varna (Bulgaria) deposits, respectively. The Oligocene Mn deposits of the Thrace basin were formed by diagenetic replacement processes during a marine regression.

2.5 Enrichment test on the Manisa manganese deposit

2.5.1 Geology and mineralogy of Manisa deposit

The geomorphology of western Anatolia is a good example of a post-collisional extensional region, dominated by approximately E–W trending active normal faults with typical maximum segment lengths in the range of 10–25 km (Fig. 5) (Eyidoğan and Jackson, 1985; Şengör et al., 1985; Seyitoğlu and Scott, 1991; Paton, 1992; the İzmir–Balıkesir Fault Zone (IBTZ) that accommodated N-S extension in the region (Özkaymak and Sözbilir, 2008; Sözbilir et al., 2008, 2009; Uzel and Sözbilir, 2008; Özkaymak et al., 2011; Uzel et al., 2012). This transversely oriented strike–slip-dominated zone was a deep crustal transform fault in the Late Cretaceous that later acted as a transfer fault zone during the Neogene and Quaternary (Okay and Siyako, 1993; Okay et al., 1996; Ring et al., 1999; Özkaymak and Sözbilir, 2008; Uzel and Sözbilir, 2008; Özkaymak et al., 2011; Uzel et al., 2012). In the central part of the zone, the Spildağı High Range is elevated by the Manisa Fault Zone (MFZ) to up to 1500 m.
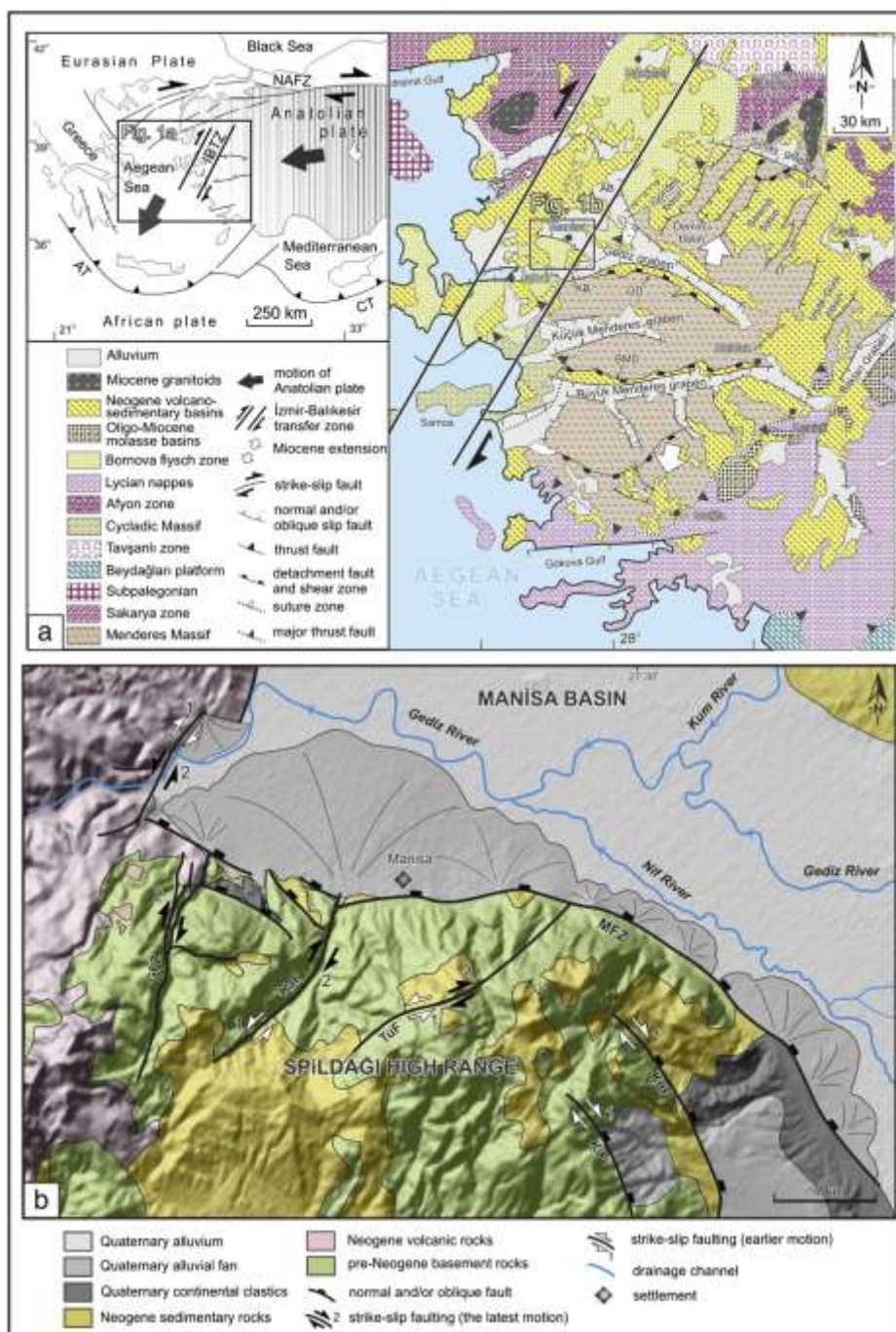
Fig. 5. (a) Simplified tectonic map showing the main fault system of western Anatolia, with locations of structures described in this study (compiled from Şengör et al., 1985; Sözbilir, 2002; Bozkurt and Sözbilir, 2004, 2006; Özkaymak and Sözbilir, 2008; Uzel and Sözbilir, 2008; Sözbilir et al., 2011 and the present work). Double arrows indicate reactivation of the IBTZ as a sinistral and later a dextral zone. Abbreviations: AB, Akhisar Basin; KB, Kemalpaşa Basin; GD, Gediz Detachment Fault; BMD, Büyük Menderes Detachment Fault; AT, Aegean Trench; CT, Cyprus Trench; İAZ, İzmir–Ankara Suture Zone. The regional map (inset) shows the main tectonic structures in Turkey and surrounding regions; (b) Simplified geological and relief map showing the arc-shaped nature of the Manisa Fault Zone (compiled from Bozkurt and Sözbilir, 2006; Özkaymak and Sözbilir, 2008; Özkaymak et al., 2011). See Fig. 1a for location of the map. Abbreviations:GFZ, Gürle Fault Zone; KaF, Karaçay Fault; TuF, Turgutalp Fault; MFZ, Manisa Fault Zone; Kdf, Kayadibi Fault; KiF, Kirazlı Fault.

9

Chapter 2

Some researchers (Bozkurt and Sözbilir, 2006; Özkaymak and Sözbilir, 2008; Özkaymak et al., 2011) documented the fault geometry and segment characteristics of the MFZ. They suggested that the MFZ was divided into separate segments, arranged en échelon in the western part (Fig. 6a), showing a basin-facing step-like structural configuration from the horst block down to the basin floor.
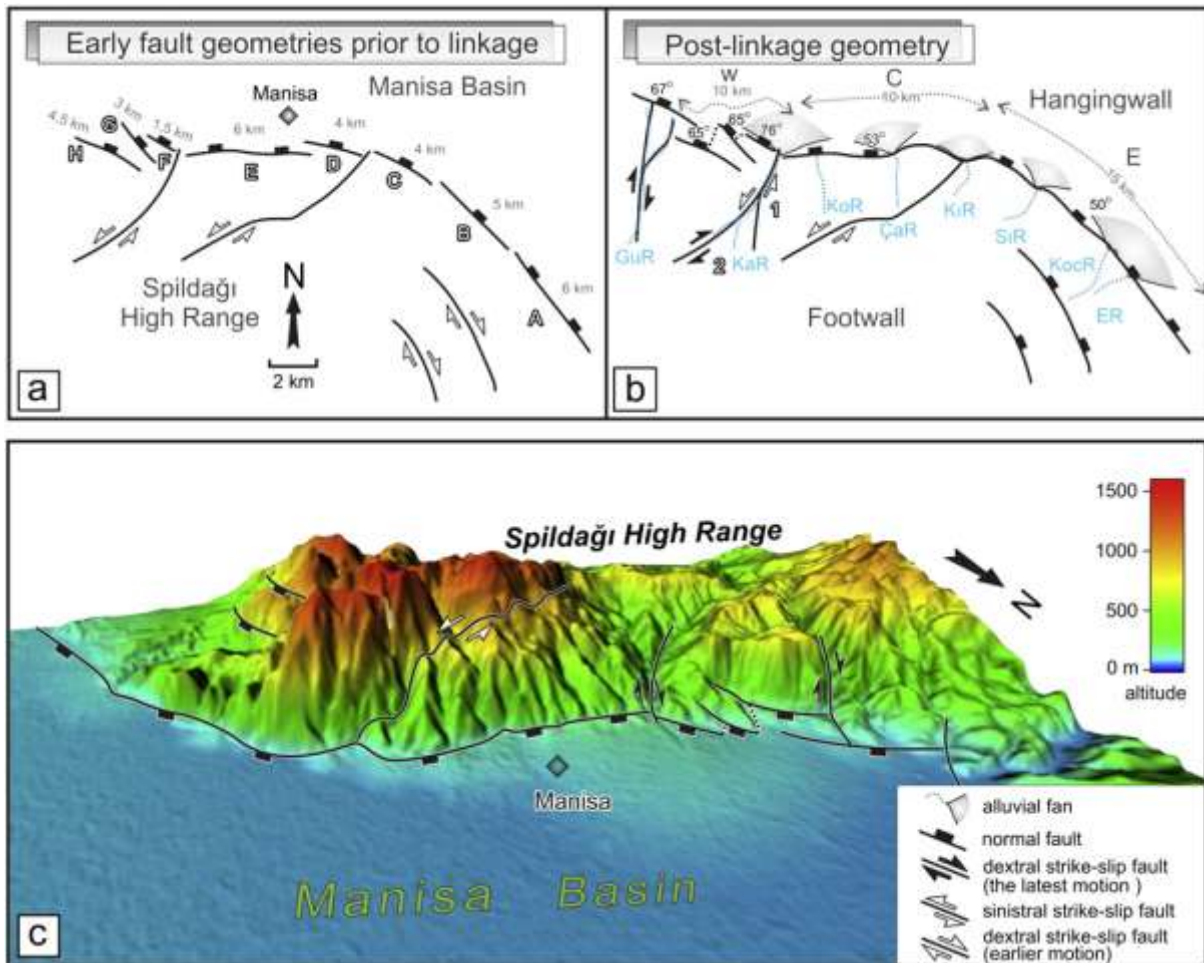
Fig. 6. Fault geometry and segment characteristics of the MFZ (Özkaymak et al. 2011). (a) Early fault geometry prior to linkage; (b) post-linkage geometry of the fault zone; (c) 3D block diagram showing present-day configuration of the study area. Abbreviations: GuR, Gürleçayı River; KaR, Karaçay River; KoR, Kocadere River; ÇaR, Çaybaşı River; KıR, Kırtık River; SıR, Sırtlangöçü River; KocR, Kocakızıl River; ER, Eşref River; W, Western sector; C, Central Sector; E, Eastern Sector.

As the fault grew, the fault segments connected along the strike to form a continuous, 35 km-long northeastward-arched fault trace during the current N–S extensional tectonics. Field observation reveals that interactions between individual segments were accommodated by relay ramp structures, which formed a post linkage geometry (Fig. 6b). The result is an arc-shaped fault zone comprising three distinct sectors, divided by NE-trending strike– slip faults (Fig. 6c). By correlating the base of the Upper Miocene lacustrine limestones (5 Ma; Bozkurt and Sözbilir, 2006) on either side of the fault zone, some researchers (Bozkurt and Sözbilir, 2006;

Özkaymak et al., 2011) estimate a vertical offset (throw) of 1500 m across the central sector and approximately 600 m across the western sector of the MFZ during the Pliocene and Quaternary. Thus, the vertical Plio–Quaternary slip rates, determined from the cumulative displacement across the fault zone, are 0.1 mm/year and 0.3 mm/year for the western and central sectors of the MFZ, respectively (Özkaymak et al., 2011). Bozkurt, 2001; Koçyiğit and Özacar, 2003; Lenk et al., 2003; Sözbilir, 2005; Kaymakcı, 2006). The EW-trending graben faults are laterally terminated by a transversely oriented strike–slip fault zone, namely, The footwall lithology of the MFZ consists of Upper Cretaceous– Palaeogene Bornova Flysch Zone rocks and Upper Miocene lacustrine carbonate and volcanic rocks (Bozkurt and Sözbilir, 2006; Özkaymak and Sözbilir, 2008; Özkaymak et al., 2011). The Bornova Flysch Zone is composed of Mesozoic limestone olistoliths/blocks within a clastic carbonate turbiditic matrix. The unconformably overlying Karadağ formation is a clastic- and carbonate-dominated sequence with dominant greyish-beige lacustrine limestones, marls and claystones (Özkaymak and Sözbilir, 2008). Volcanic rocks cover large areas in the western part of the study area, represented by reddish andesitic lava and greyish-beige tufa with agglomerates of the Early–Middle Miocene (Borsi et al., 1972; Savaşçın, 1978; Ercan et al., 1996). Along the mountain front, the MFZ separates the Late Pleistocene–Early Holocene Emlakdere Formation from the bedrock carbonates of the Bornova Flysch Zone (Özkaymak and Sözbilir, 2008; Özkaymak et al., 2011). The unit is overlain by late Holocene colluvial/alluvial fans. Numerous well-developed alluvial fans of diverse sizes are fed by the basement rocks (Fig. 6b). The recent graben floor is filled with alluvium and axial fluvial sediments. Further, huge polished fault surfaces are exposed along the steep limestone escarpment of the MFZ, thereby testifying to its relatively normal activity. Quaternary colluvia originate from the bedrock carbonates of the Bornova Flysch Zone and accumulate in the immediate hanging wall of the fault. The morphological steps in the topography and their connecting structures interact towards the development of composite large-fault systems; the steps show the tectonic history of the MFZ expressed as steep topographic scarps with a mean slope of 31°.

2.5.2   Manisa manganese mine

In the map (Fig. 7), the manganese mine license is outlined, about 10 km to the west of the village of Sancakliçesmebasi in the region of Manisa, where mining is currently active and produces an ore poorer in Mn than the market demand. Mine is actually working in open pit (Fig. 8 and Fig. 9), but, due to the dipping of the ore bodies and the topographic relief, in the future it will need underground works (Fig. 10). Reserves of Mn ore are relatively high, being estimated to a minimum of 60.000 Mt, but that could exceed 120.000 Mt. Uncertainty is due to the lack of exploration and especially drillings from the mining company. The ore grade is anyway quite low and in general very variable. In some enriched small pockets it can be as high as 57,29% Mn (Tab.1), but the discontinuous character of the ore, together with its complicated structure gives as a result run of mine with an average Mn content of about 16 - 17 wt% Mn. (Tab. 2).
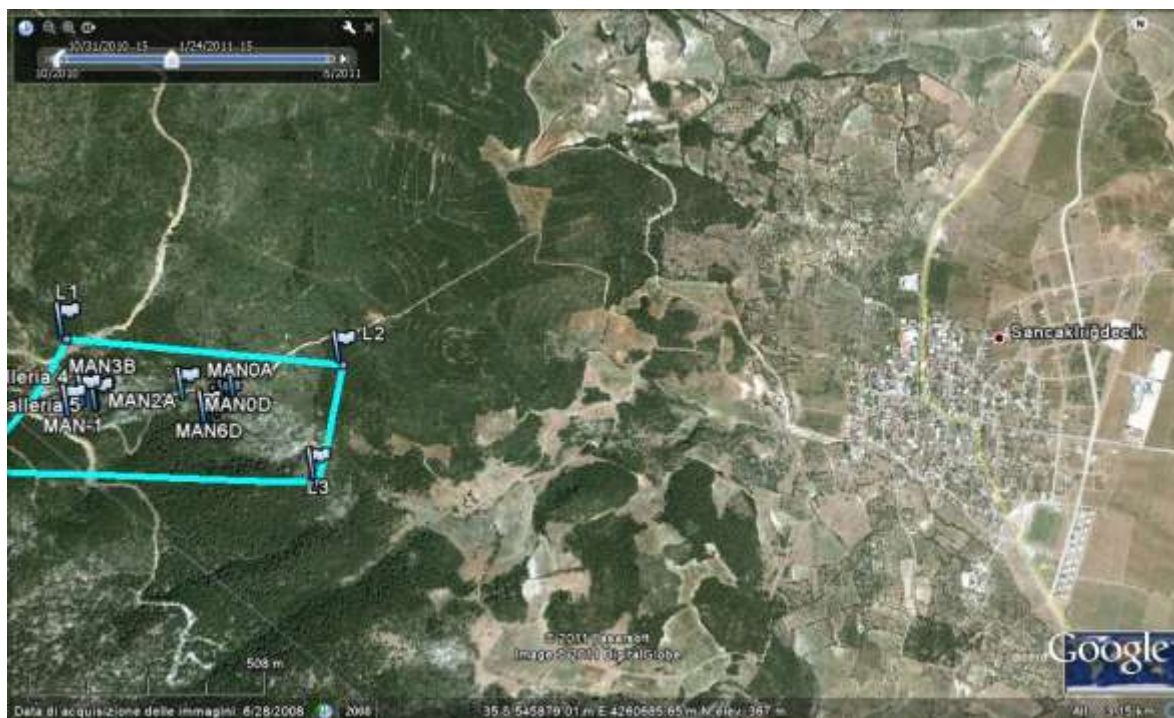
Fig. 7. Satellite image of the the manganese mine license. License borders are outlined in blue.

Fig.8. The manganese mine with some of the sampling points.

Fig. 9. Manganese mine with ore mining front.

Fig. 10. Picture of the the manganese mine.

Fig. 11. Panoramic view of the enrichment plant with shaking tables in the foreground and jig in the background.

The relatively large scale of Mn-rich and Mn-poor domains in this kind of metamorphic deposits, differently from typical fine grained homogeneous Mn deposits within cherts, can allow gravitational enrichment of the ore due to the high liberation that can be attained through comminution. To test the feasibility of such enrichment a stock of 10 Mt of run of mine were taken to a 5 km away enrichment plant, that comprises a jaw crusher, a ball mill, a JIG and two shaking tables. The flowsheet of the plant is shown in Fig. 12. The run of mine is firstly crushed in the jaw crusher then it is sieved at - 20 mm with overflow being recycled in the crusher. In the second stage the material is sent to the mill and then sieved to - 6 mm with the overflow being recycled within the mill. The - 6mm ore is used to feed the jig. As the jig does not work efficiently for griansize - 2mm jig concentrate is sieved within the jig itself with a 2 mm sieve. Portion + 2mm is sent to the concentrate stock and is called jig concentrate. Portion - 2mm is sent to the shaking tables. Table 2 collects - 2mm jig concentrate from the first and the second couple of collectors, table 1 collects - 2mm jig concentrate from the third couple of collectors. Shaking tables concentrates are sent to the concentrate stock while their tailings are sent to discharge together with the jig tailing.

2.5.3 Gravity driven enrichment plant

Jaw Crusher

Sieve 20 mm

JIG

Sieve - 6 mm

Ball Mill

Sieve - 2 mm

Waste

Conc JIG

Table 1

Table 2

Waste tab. 1

Waste Tab.2

Conc Tab. 1

Conc Tab. 2

♦ Final product
Conc Tot Mix Jig +Tab 1 + Tab 2.
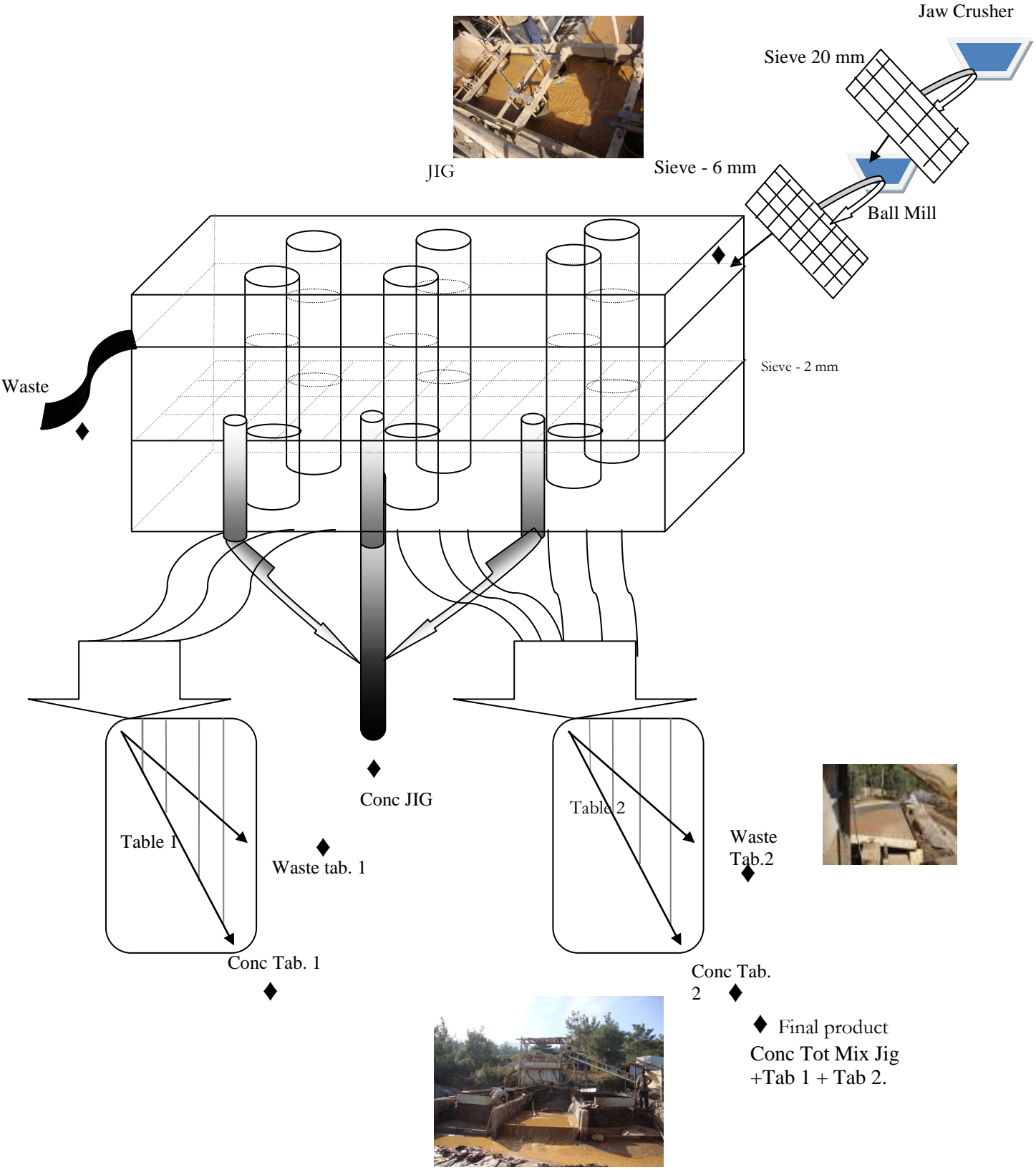
Fig.12. Technical flowsheet of the plant with location of sampling points (♦)

Chapter 2

Samples for the enrichment test were taken from Manisa enrichment plant at different points and are: feed, jig concentrate, jig waste, table1 concentrate, table1 tailing, table2 concentrate, table2 tailing and total concentrate (Fig. 13).

Fig 13. Pictures of manganese enrichment plant: A- comminution devices with jaw crusher, sieves and ball mill, B- Frontal view of enrichment devices with shaking tables and jig, C- View of the jig from the top, D- shaking table 1.

Some samples were collected from the mine (most of them selected as the most Mn-rich) (Tab. 1), and eight samples were collected from the plant (Tab. 2). This phase, consisting of the acquisition and analysis of

data was carried out in the laboratories of the Department of Earth Sciences "A. Desio ", University of Milan, and was initially carried out through a grain size analysis of the samples. Subsequently chemical parameters of samples and in particular the MnO_2 and SiO_2 contents were determined by XRF analysis. Finally the separation efficiency of the plant was determined.

2.5.4   X-ray diffractomer analyses

We carried out the qualitative analysis through X-ray diffractometry (XRD) of the powdered material in order to detect the main mineralogical phases (Figs. 14/a-14/g).

Analyses were done on the rock samples selected from the mine (Tab 1) and sand samples from enrichment plant (Tab. 2): feed, concentrate and tailing from jig and shaking tables, and final product. Along with concentrates a representative amount of rock was crushed and reduced to one sample that was analyzed. XRD results show that by far the most abundant Mn phase in the rock and hence in the concentrates too is pyrolusite (fig. 14/a-g). Gangue has also a very simple mineralogy with quartz as the only detectable gangue silicate in the rock. XRD of concentrates show low amounts of heavy phases (smithsonite, barite) that report to the concentrate during separation. XRD of feed and final concentrate show also a small amount of calcite that is a light phase and hence reports to the tailing during separation.
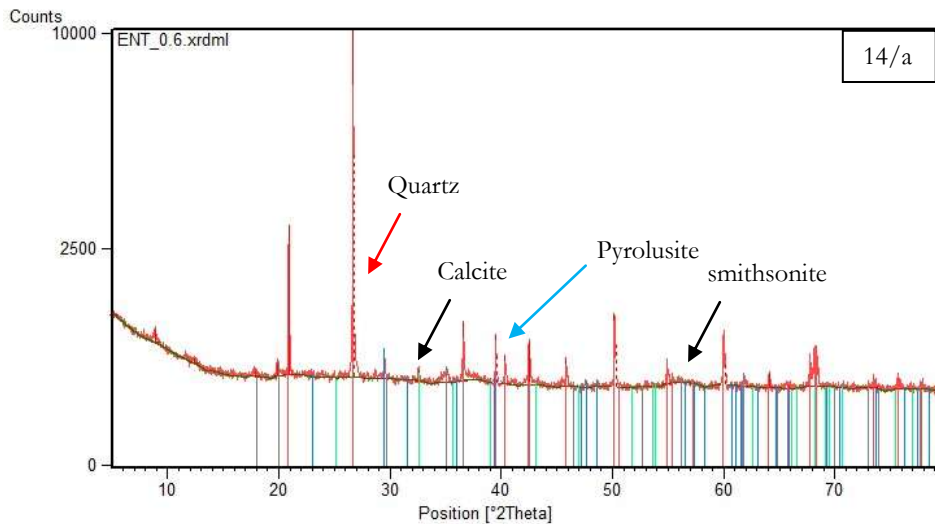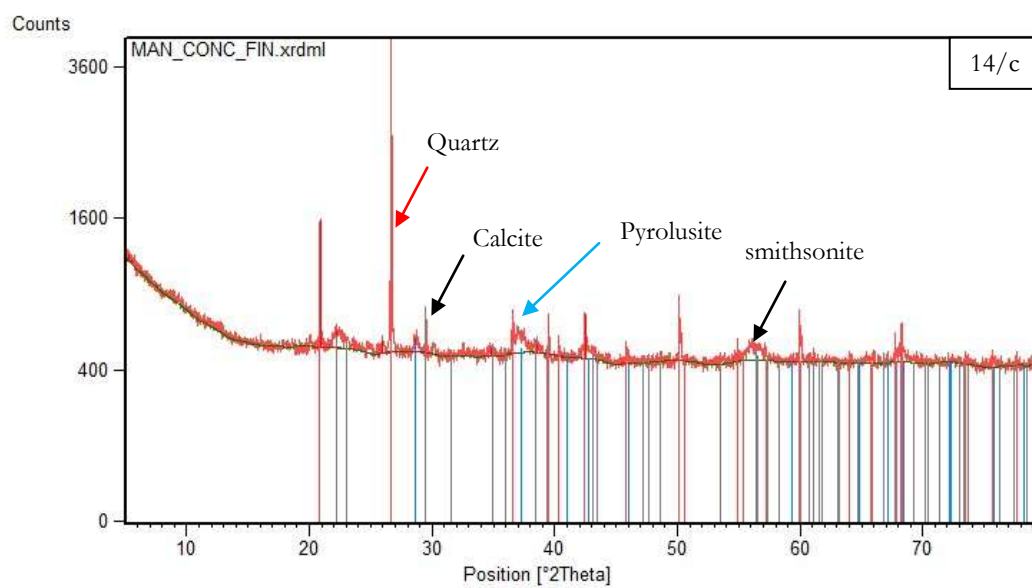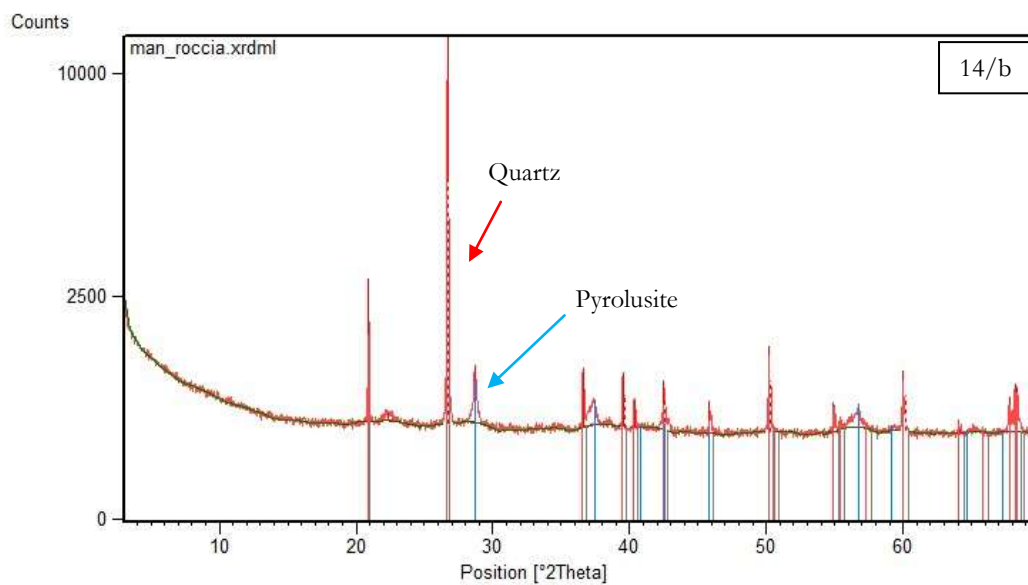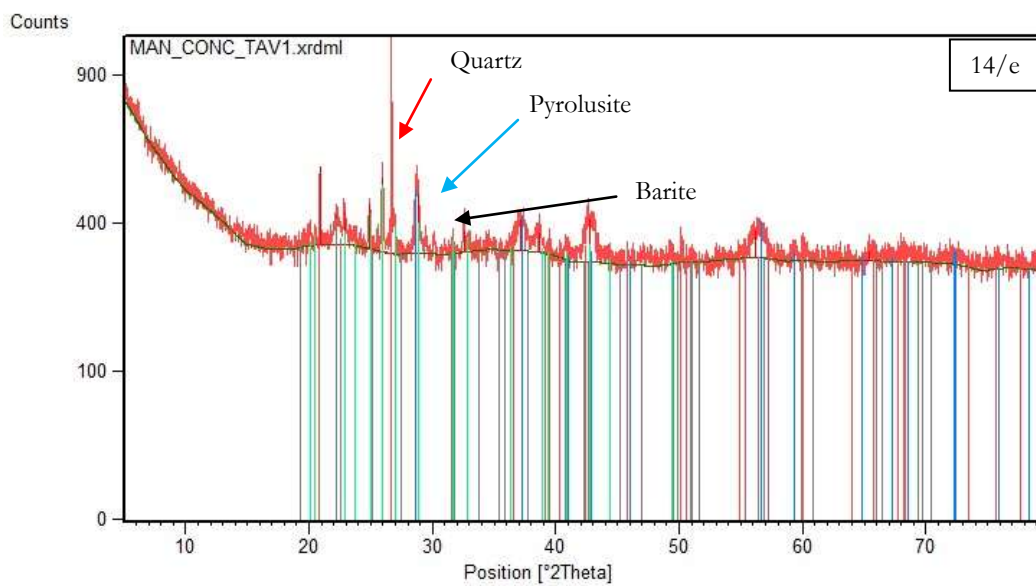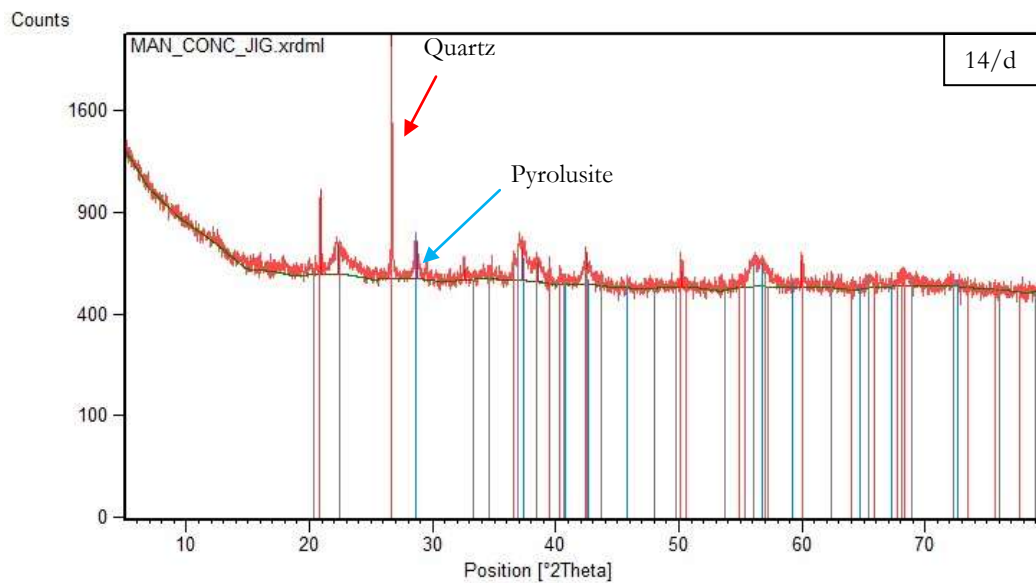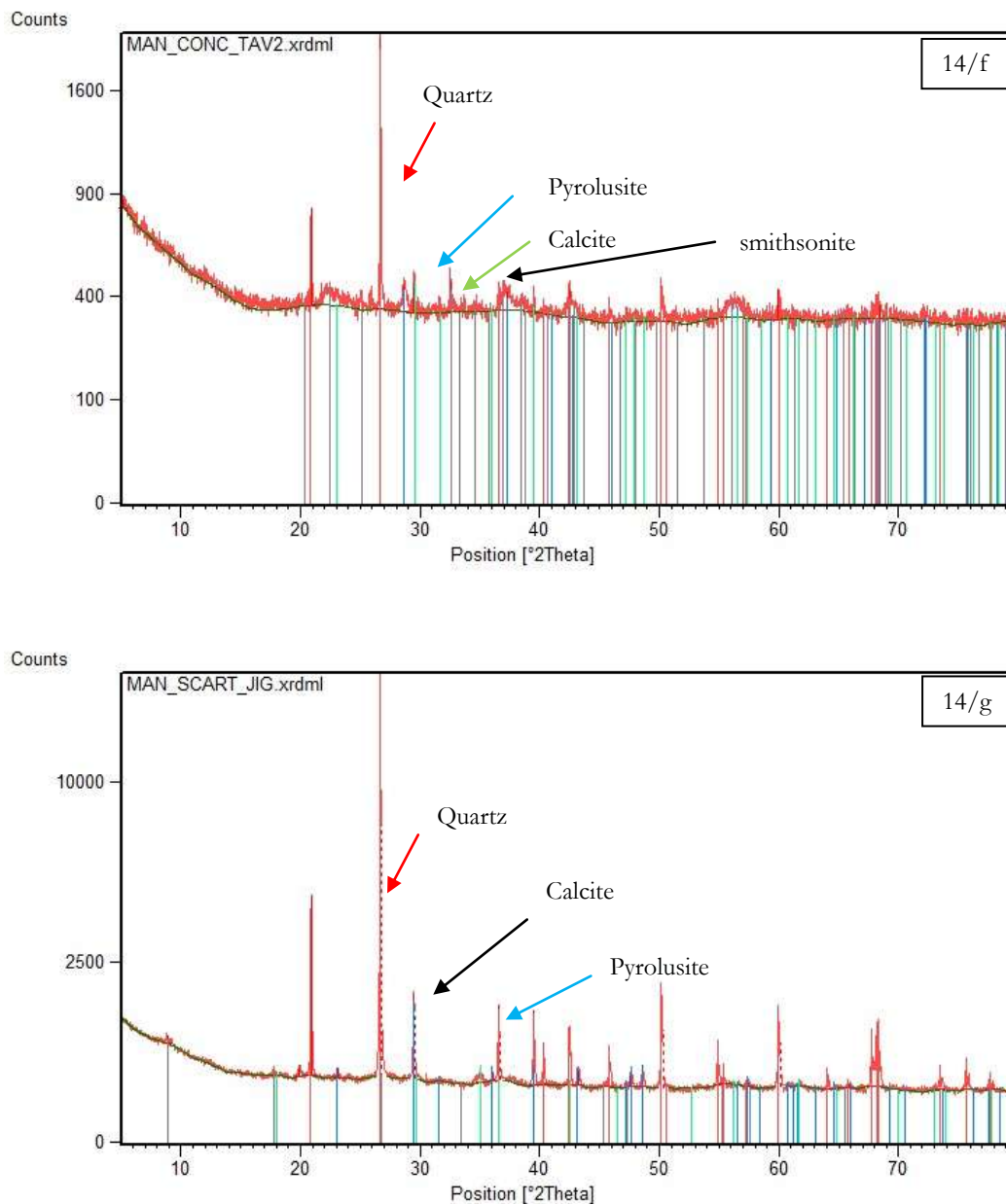
Fig. 14. X-ray diffractions of Mn ore samples from mine (a, b), and enrichment plant (c, d, e, f, g)

2.5.5   Enrichment tests

A fundamental parameter to be considered for the operation of an enrichment plant is the separability of mineralogical species constituting the rock or sand.

It happens in fact that the grinding forms grains, which may consist entirely of manganese, entirely of silicates or can be mixed. The finer the product is grinded the lower is the amount of mixed grains. On the other hand the index of fineness requires for commercial purposes that grain sizes are not too much fine. In addition

Chapter 2

the efficiency of both jig and shaking tables is dramatically reduced if the feed contains high amounts of the silt and especially clay fraction.

For this work chemical analyses were carried out by XRF on powders. The samples were prepared using 4 g of boric acid as a primer and then adding the powdered sample (8 g) and 3 drops of polyvinyl alcohol. Finally it is left in the oven for 24 hours at a temperature of 65° C.

The results obtained from the XRF analysis on the rock samples collected are reported in Table 1.

Sample	Na2O	MgO	Al2O3	SiO2	K2O	Fe2O3	CaO	MnO	Mn (metal)	Sum
M-1 (lumpy)	0,78	0,45	0,28	12,19	0,26	4,56	1,50	72,59	56,22	92,61
M-2 (lumpy)	1,80	0,37	1,10	0,92	0,50	3,00	8,56	70,80	54,83	87,04
M-3 (lumpy)	0,45	0,32	0,31	0,01	0,39	3,72	11,99	63,46	49,15	80,66
Mn-MANISA	0,17	0,36	3,18	8,11	0,85	8,60	1,47	67,98	53,41	164,11
MAN6D	0,09	0,90	1,81	23,01	0,49	7,64	8,00	29,75	23,37	71,68
MAN6C	0,06	0,59	0,18	0,08	0,07	1,38	42,08	24,36	19,14	68,80
MAN3B	0,03	0,31	0,44	65,76	0,14	1,01	1,42	15,27	12,00	84,38
MAN2A	0,05	0,21	0,26	50,19	0,08	0,83	0,39	30,87	24,26	82,89
MAN1	0,05	0,79	1,30	50,18	0,36	2,19	1,65	32,42	25,47	88,94
MAN1STOCK	0,05	0,96	3,48	44,12	0,90	3,75	1,20	29,20	22,94	83,66
MAN0D	0,06	0,64	0,97	5,47	0,18	17,22	29,20	18,43	14,48	72,16
MAN0A	0,01	0,09	0,78	84,34	0,11	1,18	0,66	1,80	**1,41**	88,97
MANISA ROCCIA	0,03	0,14	0,52	57,08	0,16	1,48	0,38	25,53	20,06	85,32
MAN 203	0,12	0,67	0,93	3,59	0,33	4,00	1,56	72,92	**57,29**	84,11
MAN 205	0,08	0,42	0,31	33,55	0,26	1,61	1,07	42,95	33,75	80,26
MAN 202/B	0,08	0,76	0,30	5,21	0,30	3,38	19,81	38,12	29,95	67,94
MAN 202/A	0,07	0,24	0,20	27,74	0,30	3,36	0,40	41,55	32,65	73,86
MAN 201	0,09	0,30	0,72	20,09	0,64	1,13	0,37	53,96	42,40	77,31
MAN 200/B	0,11	0,86	1,48	6,67	0,56	2,33	5,45	60,18	47,28	77,65
MAN 200	0,11	0,38	0,42	2,97	0,15	1,96	1,80	65,99	51,85	73,78
MAN 200/A	0,09	0,74	1,20	8,03	0,48	4,88	12,87	35,13	27,60	63,43

Table.1 XRF analyses of Mn ore samples (wt%) from the mine.

Analyses on rock samples show an extreme variability in SiO_2 and MnO contents that reflects the variability of quartz to pyrolusite ratio. Also CaO content is very variable, reflecting the dishomogeneous distribution of calcite in the rock. In general this extreme variability at the scale of the specimen is due to the coarse texture of the rock derived from metamorphic recrystallization and deformation during metamorphism. In sedimentary Mn ores quartz and Mn minerals are very fine grained and mixed in such a way that they can be liberated only by grinding at a grain size too fine for separation by jig or even by shaking tables. The result is a strongly homogeneous Mn and SiO_2 content that changes only at the deposit scale. At Manisa and possibly in other similar deposits metamorphic recrystallization produced respectively quartz- and pyrolusite- enriched

domains at millimeter to centimeter scale giving as a result an extremely variable MnO and SiO$_2$ content at the outcrop and even at the specimen scale. Such condition can produce a high liberation of Mn phases after grinding at a relatively coarse grain size.

To verify this possibility the enrichment test was planned grinding the ore at a – 6 mm grain size (Tabs. 3, 4).

Sample Mn wt%	Al2O3	CaO	Fe2O3	K2O	MgO	MnO	Mn (metal)	Na2O	SiO2	TOT
Feed 0 - 6 mm	6,44	2,51	5,69	1,89	0,75	20,64	15,99	0,06	51,86	89,84
Feed 4 - 6 mm	4,68	2,95	4,83	1,42	0,62	23,74	18,39	0,07	46,65	84,96
Feed 2 - 4 mm	5,61	2,4	4,73	1,61	0,66	23,47	18,18	0,07	47,09	85,64
Feed 0 - 2 mm	6,31	2,69	5,12	1,79	0,71	17,12	15,26	0,07	53,63	87,44
Feed (average weight)	5,88	2,64	4,96	1,69	0,68	21,79	16,88	0,07	50,34	88,05
Conc JIG	1,56	1,76	3,83	0,5	0,66	60,38	**46,76**	0,13	19,61	88,43
Conc Tab 1	0,19	1,53	4,33	0,27	0,87	50,60	**39,19**	0,05	23,49	81,33
Conc Tab 2	1,09	2,7	4,52	0,44	0,95	49,04	**37,98**	0,05	25,43	84,22
Conc final	2,15	2,04	3,58	0,68	0,61	58,16	**45,04**	0,11	21,84	89,17
Waste JIG	4,18	6,03	3,11	0,75	0,63	6,52	5,05	0	66,95	88,17
Waste Tab 1	3,13	3,61	4,34	0,8	0,79	12,41	9,61	0	60,87	85,95
Waste Tab 2	2,42	4,48	4,27	0,64	0,87	16,05	12,43	0,05	55,2	83,98
Waste Tot	3,60	5,00	3,68	0,75	0,71	9,74	7,54	0,01	63,39	86,88

Table.2 XRF analyses of the samples (wt%) from the enrichment plant.

Sample Mn wt%	+4 mm (%)	4-2 mm (%)	-2 mm (%)	TOT (%)
Feed 0 - 6 mm	13,75	29,58	56,67	100,00
Conc JIG	56,87	39,30	3,83	100,00
Conc Tab 1	0,00	1,00	99,00	100,00
Conc Tab 2	0,00	3,00	97,00	100,00
Conc Final	47,76	31,09	21,14	100,00

Table.3 Distribution wt% of the ore in different grain sizes.

a

	Capacity (wt%)
Conc Jig	78,57
Conc Tav 1	13,57
Conc Tav 2	7,86
Tot	100,00

b

	Capacity wt%
Conc JIG	22
conc tab 1	5,8
conc tab 2	3,2
Waste tab 1+2	35
Waste JIG	34
Tot	100

Table.4 Relative fraction (wt%) of the different concentrates (a). Capacity of the different outflows from the plant (b).

Chapter 2

Given to the variability of Mn wt% in the rock and the fact that ore and host rock are so interfingered that it is impossible to separate them during mining, the feed in average is very poor in Mn (16,88 wt%) (Tab. 2). We also can see a big difference between concentrate from the jig and shaking tables. Jig final concentrate has 46,76 wt% Mn while concentrate from tables is poorer (around 38,6 wt% Mn). That is because on millimeter scale the jig works very well and the grains have a good grade of liberation. There are also differences between the two shaking tables. We have better results from table 1 (39,19 wt% Mn) than from table 2 (37,98 wt% Mn), because the shaking tables work better for the fine grainsizes, and at the table 1 the grain size is finer. The final concentrate, resulting from mixture of jig and table concentrates has a good commercial quality, with 45,04 wt% Mn, where 70,97 wt% of the material comes from the jig and only 29,03 wt% from the tables. The same thing can be seen in the waste where the jig waste has only 5,05 wt% Mn, and the highest concentration of Mn is in the Table 2 (12,43 wt%) and Table 1(9,61 wt%).

Calculation of Separation Efficiency

Using analytical and capacity data collected it is possible to calculate the Separation Efficiency. The aim of beneficiation is to maintain the values of ratio of concentration and recovery as high as possible. This result depends on Separation Efficiency (SE) of the beneficiation technique used, as defined by Schulz (1970):

$$SE = Rm - Rg$$

where Rm is the % recovery of the valuable mineral and Rg is the % recovery of the gangue into the concentrate. In this study the aim of work is to purify the manganese sand from silica in order to use it in steel market. Then previous equation can be used practically in the following form (Wills, 2006):

$$SE = \frac{100Cm(c - f)}{(m - f)f}$$

where C (Capacity) is the fraction of the total feed weight that reports to the concentrate, m is the Mn wt% content of the ore minerals that, for pyrolusite, is 63,19%, c is the Mn wt% of the concentrate and f is the Mn wt% of the feed.

For the whole plant, using data from table 2, and table 4.

$$SE = \frac{100*0.31*63.19*(45.04 - 16.88)}{(63.19 - 16.88)*16.88} = 70.60\%$$

$$SE = 70.60 \%$$

Chapter 2

CONCLUSIONS

According to this test, that was done at Manisa plant for the enrichment of manganese ore, we can say that the experiment works very well at the grain size - 6 mm (Fig 15). We can see a good separation efficiency (70,60 %). Moreover, as we can see from Fig. 15, the Jig works better than the shaking tables, and around 70,97% of final product comes from jig at the grain size 2-6 mm, that is the grainsize and the quality that the market demands.
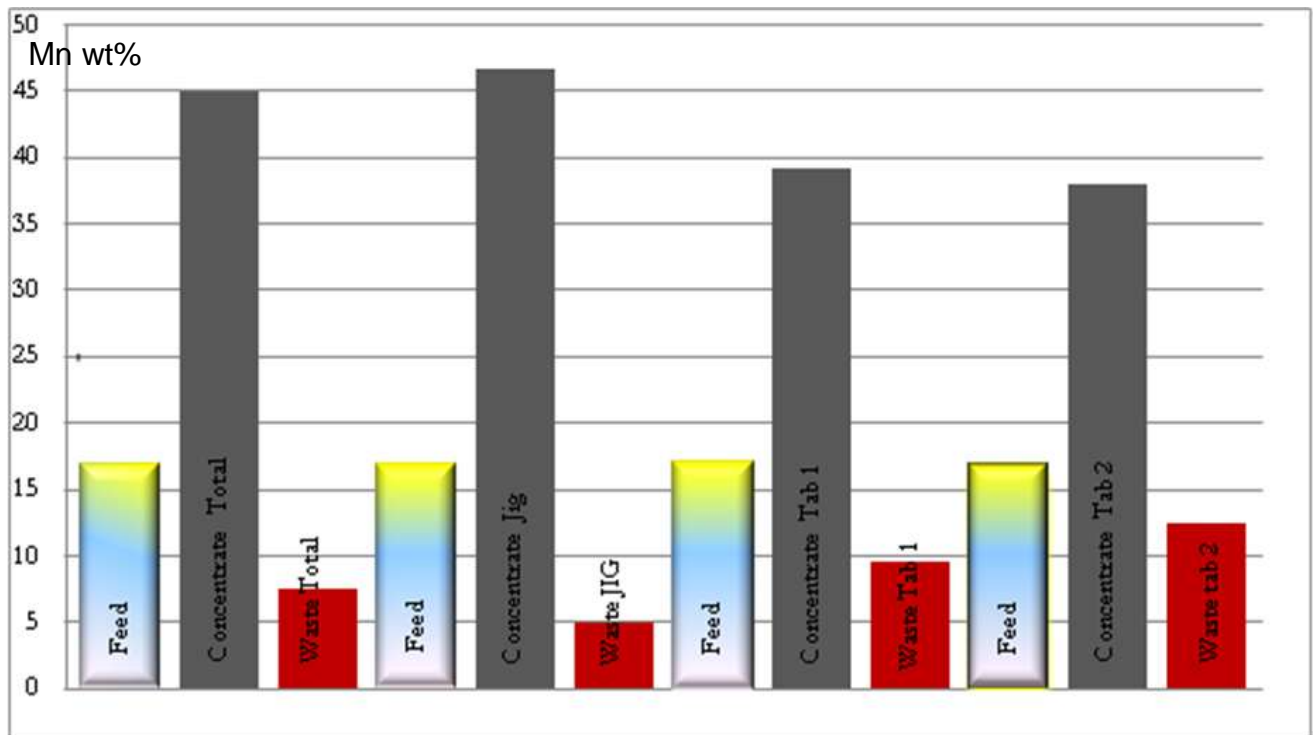
Fig 15. Histogram of feed, concentrate and waste from jig and shaking tables.

2.6 Enrichment test on braunite-rich Eskisehir ophiolite Mn deposit

This work concerns the enrichment tests of braunite-rich Eskisehir Mn deposit, where braunite enrichment allows magnetic separation of the ore.

2.6.1 Geological background

Samples for the enrichment tests were taken from the Taycilar Mn deposit, within the melange zone of the Eskişehir ophiolite complex, Turkey (Fig. 16). The Eskişehir ophiolite is located in the western part of the Izmir-Ankara-Erzincan Suture Zone (IAESZ), that crosses Turkey from the west (Izmir area) to the east (border with Georgia) (Uysal et al., 2009). Manganese deposits within the IAESZ are classified by Ozturk (1997) as radiolarian chert-hosted deposits. They are related to Neo-Tethyan suture and form the epi-ophiolitic sediment succession, together with associated radiolarite, radiolarian chert, siliceous shale and brown claystone.
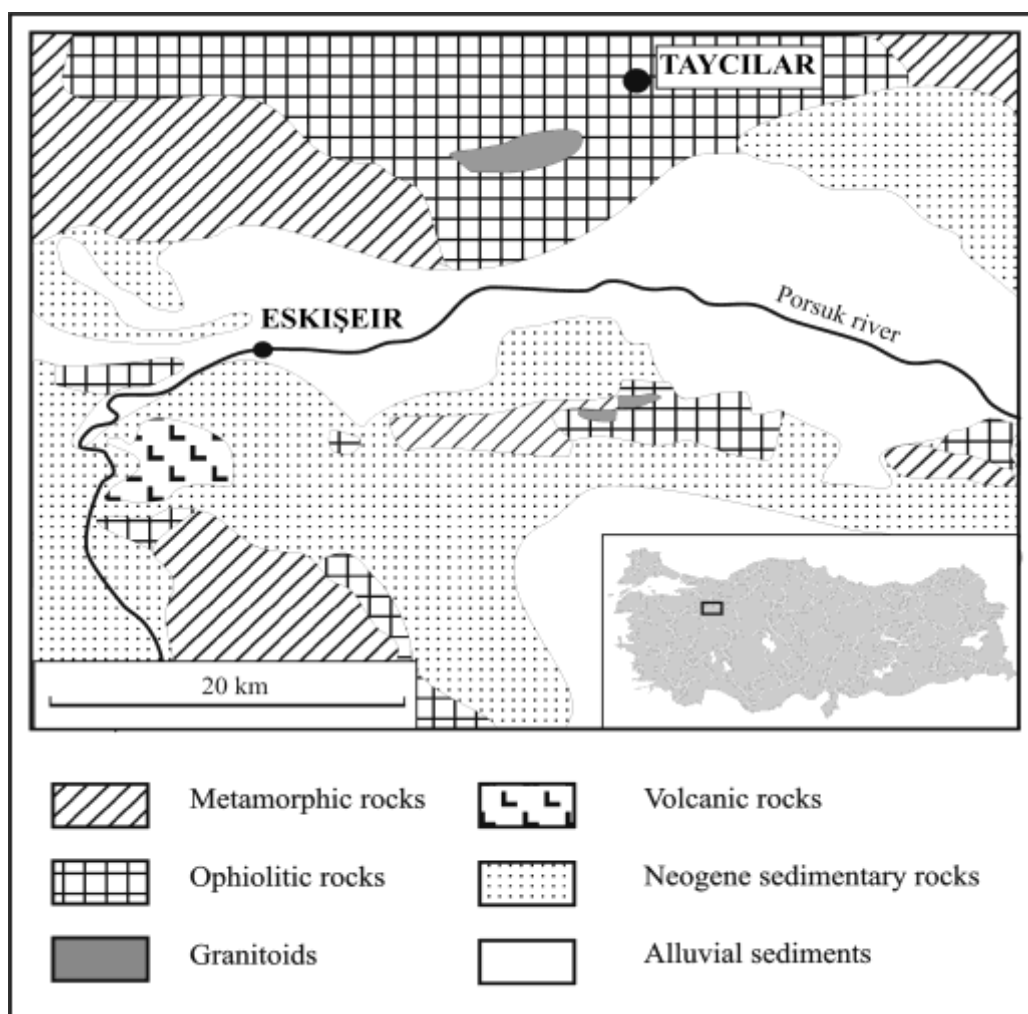
Fig. 16 Geological background of Eskisehir region.

The deposits show high Mn, variable Si and low Al contents. The most important of these deposits is Cayirli, in central Anatolia (Ozturk, 1997). The Taycilar deposit has never been mined and the local geology is not well known due to paucity of outcrops and absence of investigation. Mn-rich rocks are mainly strongly deformed braunite-rich quartzites, with WNW-ESE trend of layering, within quartz-schist and quartzite rocks. These rocks are interlayered with chlorite-bearing schists and are in contact with chromitite-bearing serpentinized peridotites to the south (Fig. 17). About 1.5 km to the southwest of the deposit a small outcrop of gabbro was found. Contacts to the north are not exposed. As a whole the Taycilar deposit belongs to the IAESZ Mn deposits, but it is characterized by a strong metamorphic overprint that changed its mineralogy and texture.
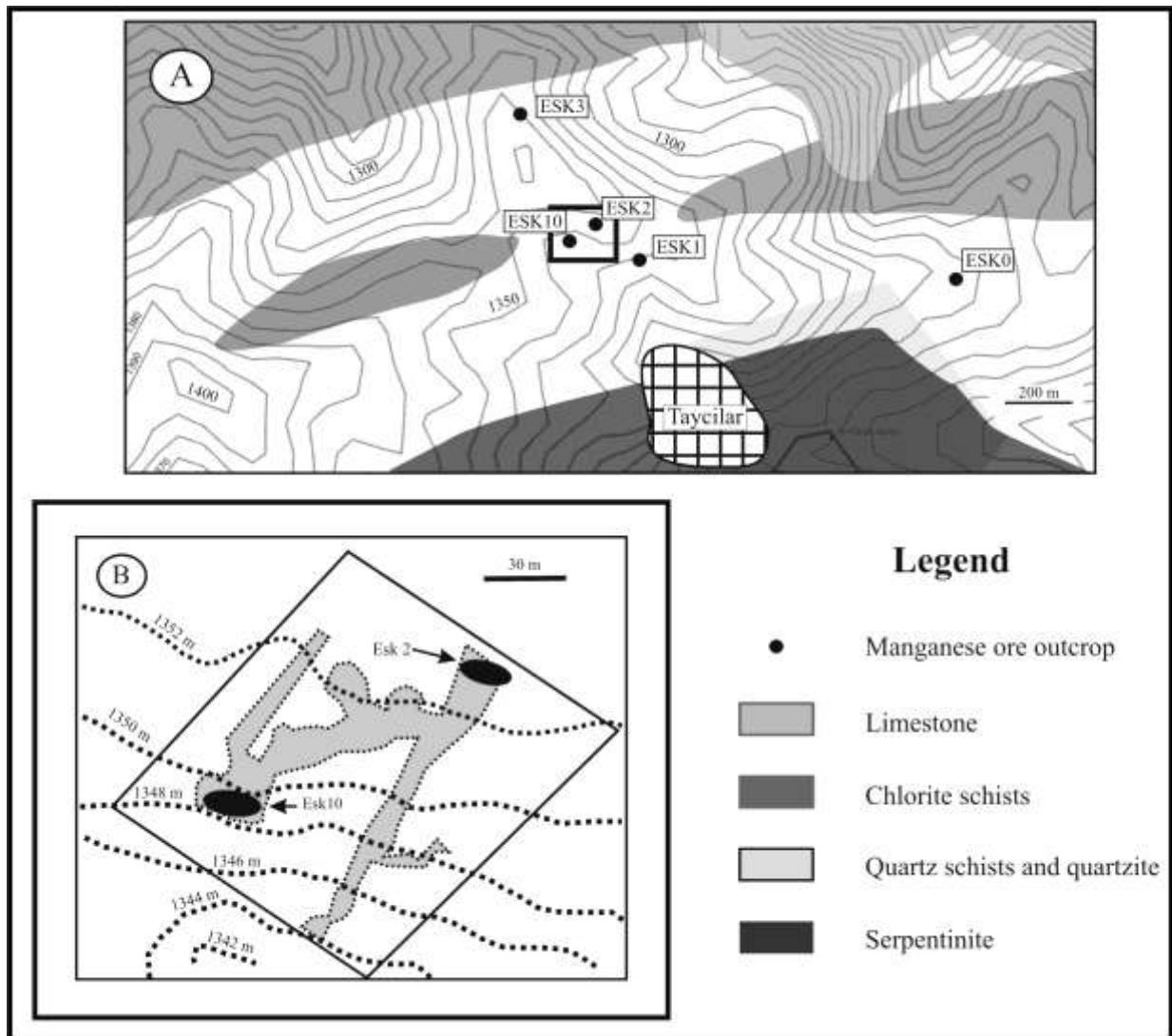
Fig. 17 Geological sketch map of license mine area and surroundings; black line in (B) is the contour of the exploitation licence area.

2.6.2 Field survey

Manganese ore was found during field survey in 5 different outcrops between 0.5 and 1 km N of the village of Taycilar (Fig. 18 a, b). Several ore samples were collected and analyzed in this first phase to determine the average Mn content..

Fig. 18 Photos from the Mn deposit area, manganese ore outcrop (a) and Mn-rich sample (b).

Chapter 2

In a second phase, based on outcrop observations and chemical analyses, a detailed prospection work was performed. This work comprised trenches, drillings and geoelectric survey that provided a preliminary idea of Mn reserves and the direction of the mineral bodies.

2.6.3 Prospection works

2.6.3.1 Geophysical survey

Horizontal and vertical persistance controlling of the investigation site are done with multi-channel (8 channels) and multi-electrode (84 electrodes) R8/IP resistivity monitoring apparatus (Figure 19). Measurements are done at 6 lines with 700 meters length for each line.
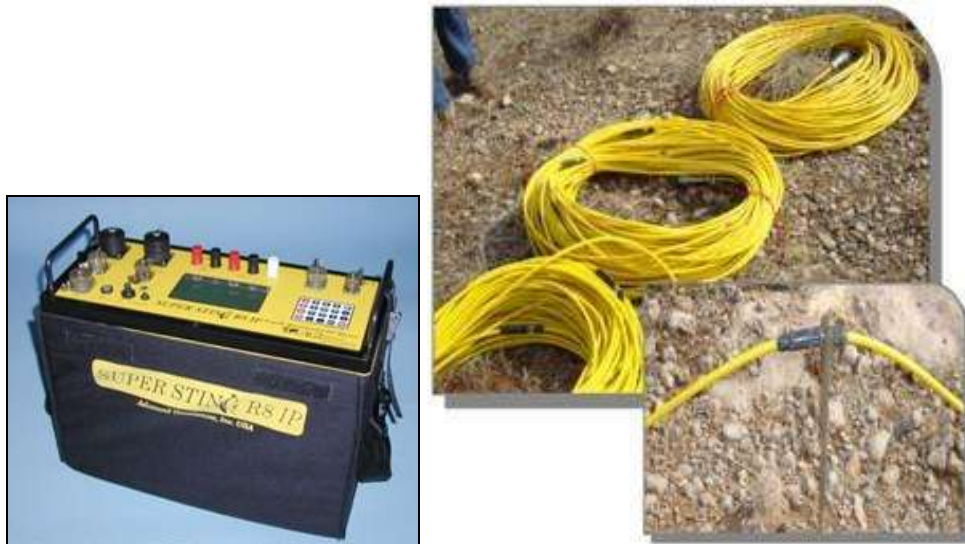
Figure 19. Multi-channel resistivity apparatus for electric resistivity measurements.

The aim of the study is, identifying the potential of the licensed mining field instead of solving the geological structures of the field. For this aim, testing identifications of two outcroped points are done. Distance between electrodes is taken 1 meter for this test measurement. Then real measurement lines are identified. Distance between the electrodes is taken as 3 meters at that line. Map of the geophysical measurement of the line is illustrated in Figure 20 and images of the study is shown in Fig. 21.

After the evaluation of the resistivity imaging measurements, the figures which are Fig. 22, Fig. 23, Fig. 24, Fig. 25, Fig. 26 as electric structural sections are prepared by EarthImager 2D and 3D software program
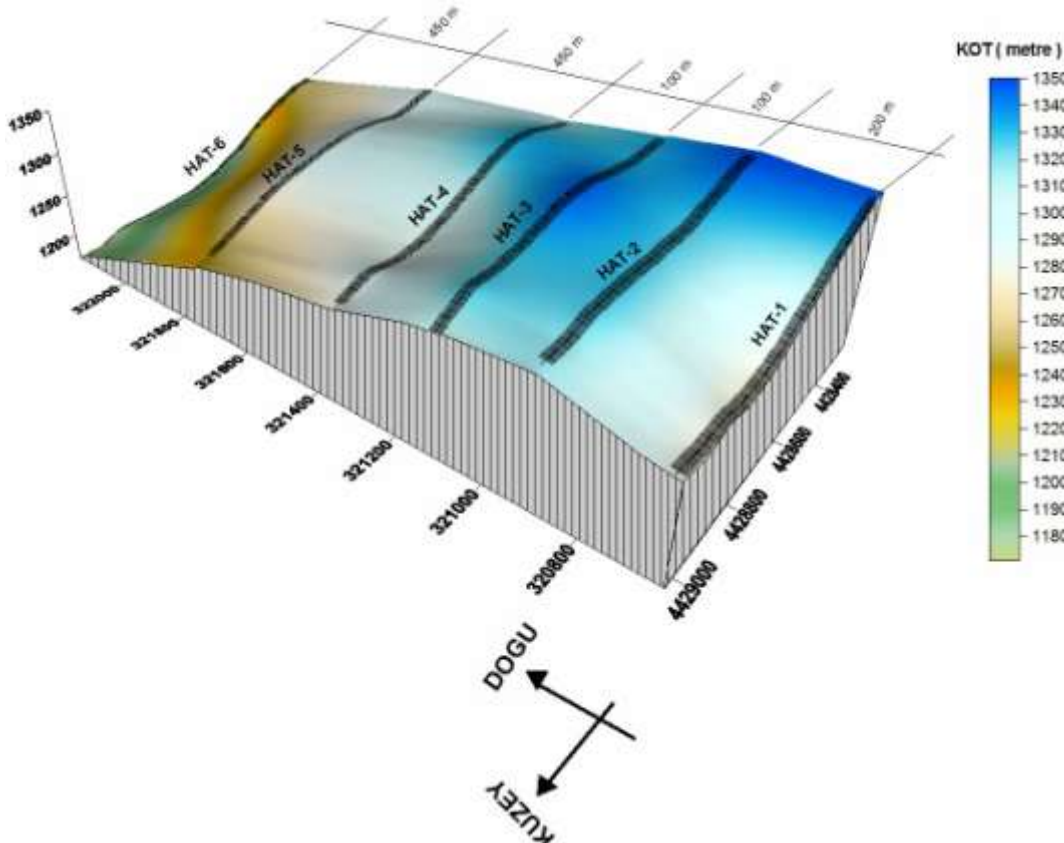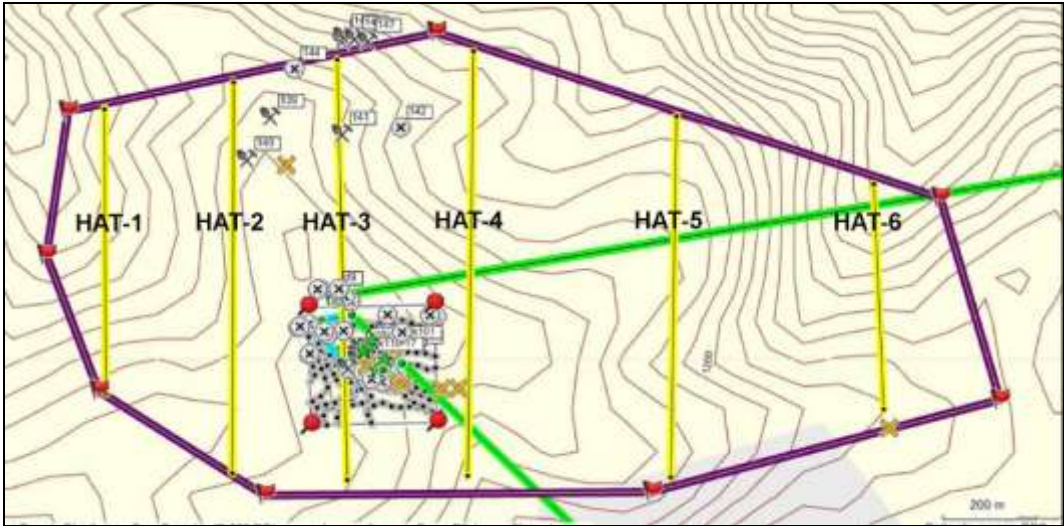
Fig. 20. Geophysical measurement lines showing section and 3D topographic model (**Doğu**:East, **Kuzey**:North, **Hat**:Line).

Fig. 21. The resistivity imaging measurements of Taycılar manganese field.
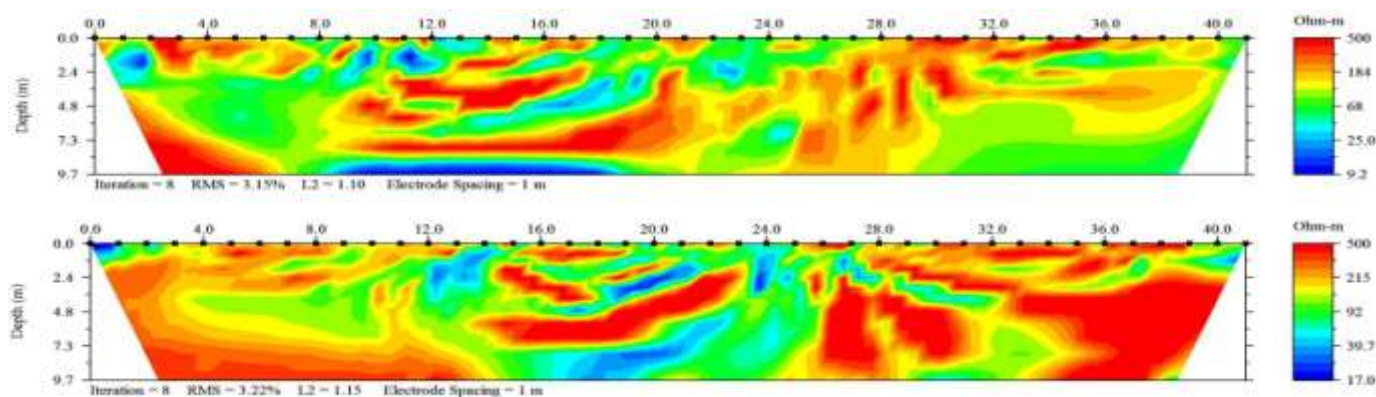
Fig. 22. Ground-electrical section of Taycılar manganese field.

Resistivity value interval of the test measurement is 17-500 ohm.m. High resistivity (<50 ohm.m) host rocks (quartzshist-cloriteshist) located around low resistivity (17-40 ohm.m) manganese.
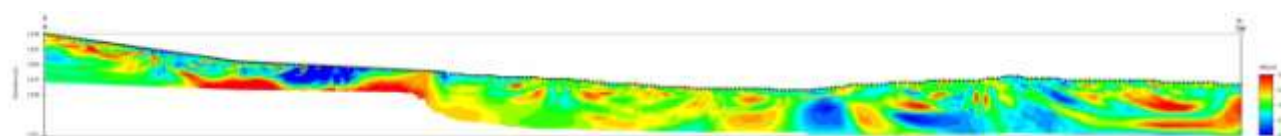
Fig. 23. First line (Line-1) measurement, ground-electric section of Taycılar/Eskişehir manganese field.

Manganese masses have 15-47.4 ohm.m conductivity property between chloriteshist-quartzshist which have more than 100 ohm.m conductivity property.
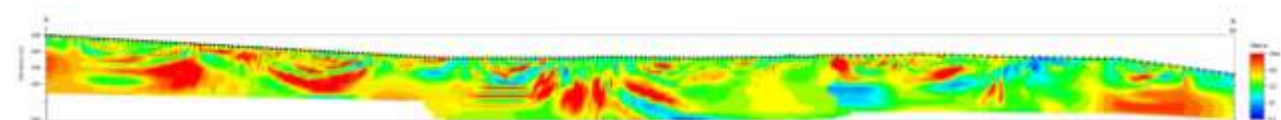
Fig. 24. Second line(Line-2) measurement, ground-electric section of Taycılar/Eskişehir manganese field.

Manganese masses have a value of 8.4-30 ohm.m resistivity between cloriteschist-quartzschist which have 54-1500 ohm.m resistivity
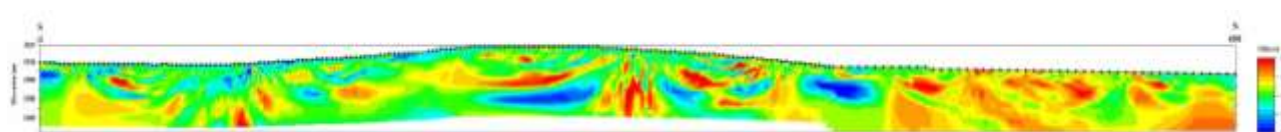
Fig. 25. Third line(Line-3) measurement, ground-electric section of Taycılar/Eskişehir manganese field.

Manganese masses have a value of 8.1-30 ohm.m resistivity between cloriteshist-quartzshist which have 54-1500 ohm.m resistivity. Differences between resistivity values are the result of crystalline orientation intension in manganese and relationship between host rocks.

With the data of 2D geophysical resistivity studies, a 3D model of the field is formed (Fig. 26).
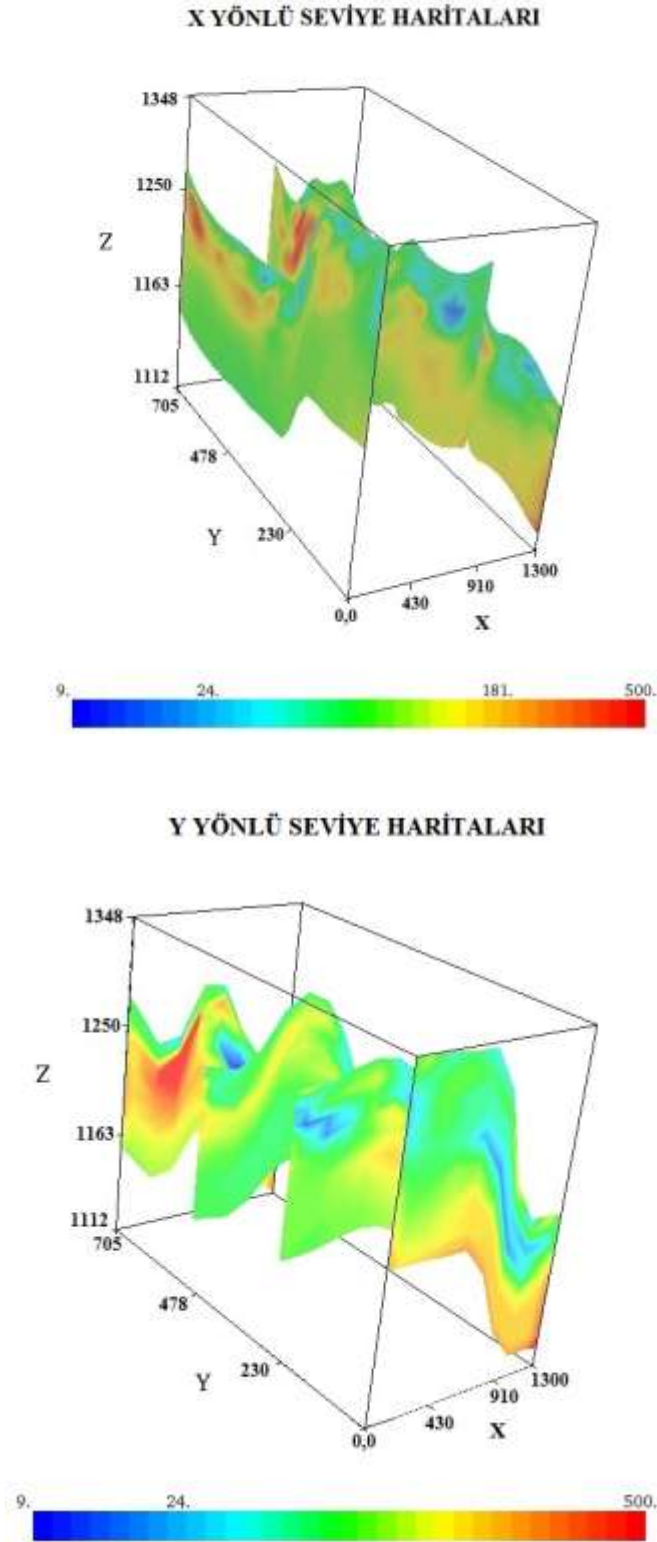
Fig. 26. 3D model of Taycılar/Eskişehir manganese field.

Total manganese volume is calculated as 182,386 m^3 according to 3D models. Unit volume weight of manganese is 7.43 ton/ m^3, total manganese amount is calculated as 1,355,127.98 ton. These calculations are

theorical reserve measurements. The real measurements must be calculated with borehole drilling control. The suggested points coordinates are given by Table 5, for borehole drilling.

2.6.3.2   *Trenches*

A restricted area was chosen, where exploitation permit was obtained, to open some tranches that could make possible to start to extract the first tons of mineral for commercial uses, and to start making some initial tests for enrichment of manganese ore. For this work prospection went on through 3 – 4 m deep trenches (Fig. 27 a,b). After this trenches it is also possible to see if the two bodies, ESK 2 and ESK 10 are connected to each-other. And to see better the orientation of the ore bodies.

Fig. 27. Pictures from the trenches of the Taycilar Mn field.
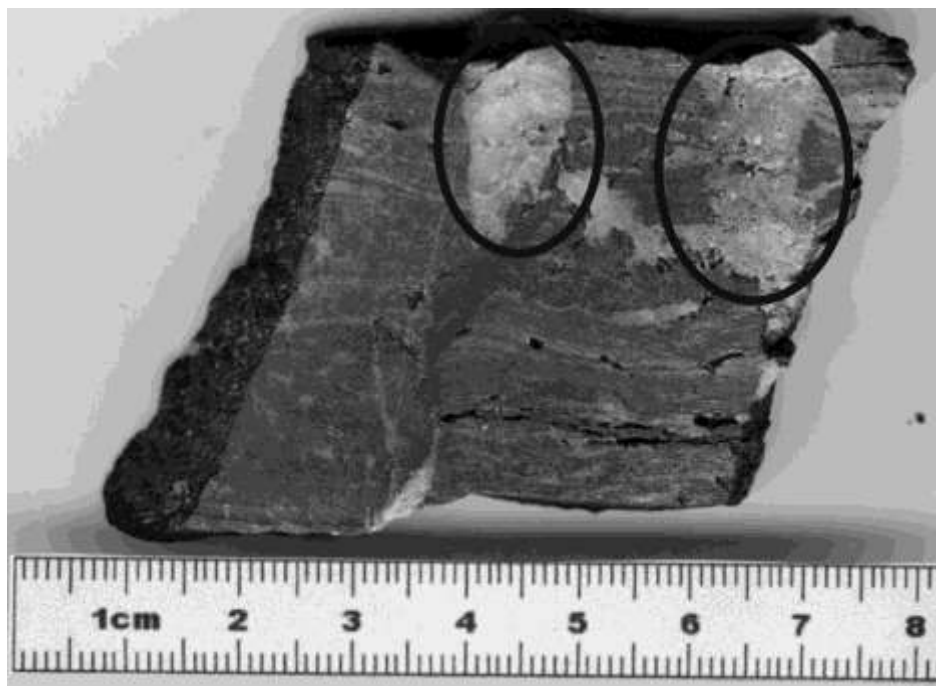
Fig. 28 Picture of polished sample of Mn ore at centimetric scale; quartz-rich domains are encircled.

Results of trench prospection showed that the two ore bodies, corresponding to outcrops ESK2 and ESK10, are not connected underground and are two subparallel discontinuous and deformed lenses with Mn-richer cores. Lens ESK2 is bigger (20x6x0.5 m) and shows a very hard massive Mn-rich core that was located at 1-1.5 m depth. Lens ESK10 is smaller (14x4x0.5 m) and its core, 0.5-1 m from surface, is less hard but with a higher

braunite to quartz ratio. Both cores are made up of centimetric irregular and deformed respectively braunite and quartz domains (Fig. 28) and are surrounded by quartz bodies in a Mn-enriched matrix.

2.6.3.3 Drillings

Geophysical survey indicated favorable conditions to find Mn ore bodies in big amounts. After geophysical survey and trenches the next step was to make some drillings to be sure that geophysical result are atendibile. These drillings were made by a Turkish company. A total of 15 drillings were done from 10 to 25 meters in depth in 6 parallel lines (Figs. 29, 30, 31 and Tab. 5).

Fig. 29 Picture of drillings from Taycilar Mn area.
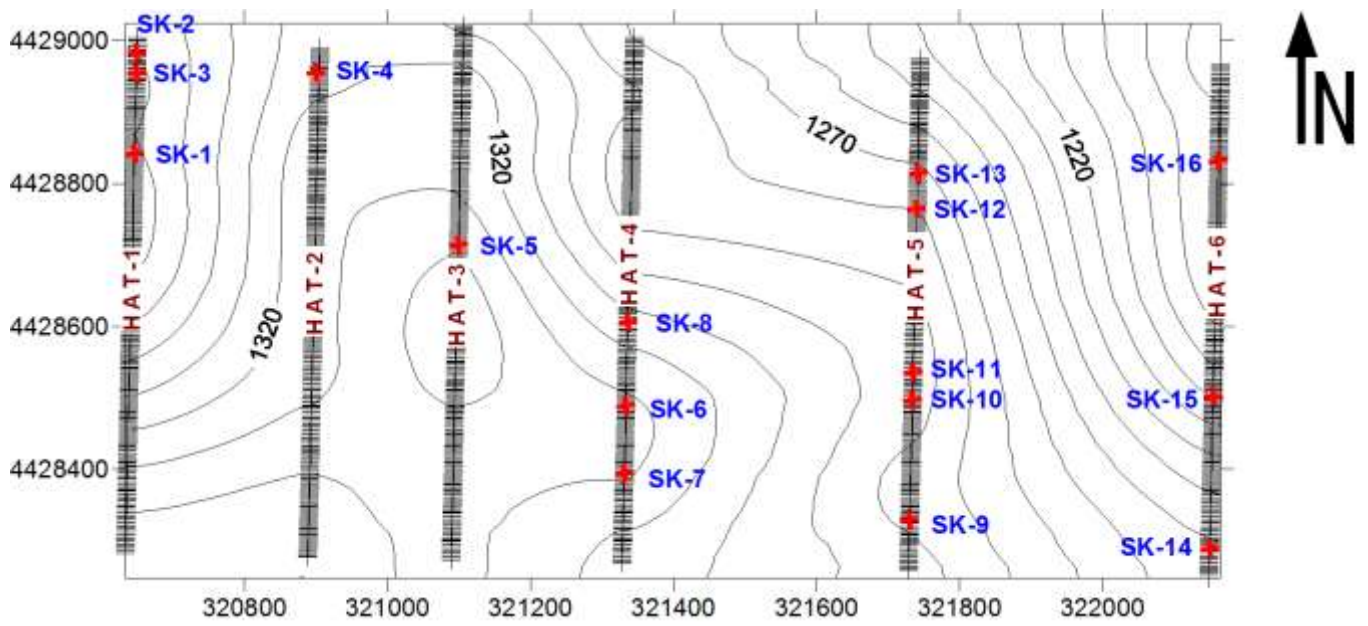
Fig. 30. Map with location of drilling points.
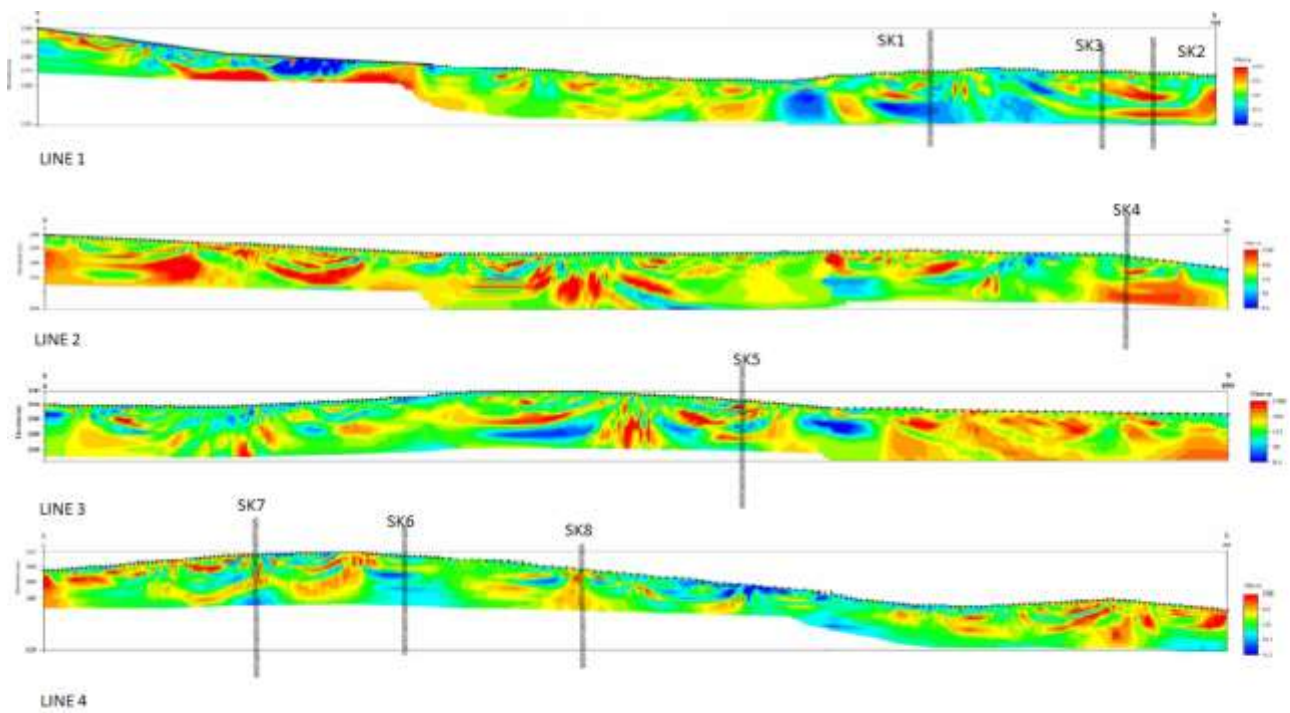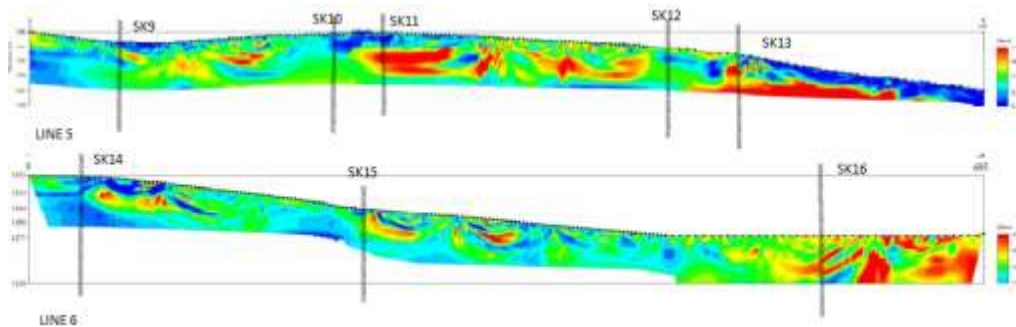
Fig. 31. Geophysical profiles with position of drilling points.

In Fig. 32 we see the report charts of drillings from the Turkish company. The results shows no meaningful bodies of Manganese at depth. The outcrops were only on surface and were not continuous ore bodies. The results show that we found on the depth only quartz, schist, quartzshist, chloroschist and very small amount of manganese on SK 3. Due to the results of the drillings further prospection was stopped.

ADİL ÖZDEMİR
ENGINEERING&DRILLING

SONDAJ LOGU / BORING LOG

Proje İsmi / Project Name		UT GROUP MANGANESE EXPLORATION				Kuyu No / BH No			SK 1
Proje Yeri / Project Location		ESKİŞEHİR/TAYCILAR VILLAGE				Sayfa / Sheet			1
Kot / Ground Elevation (m)			Tarih	Derinlik	YASS	Açıklama	Başlangıç Tarihi / Start Date		18/09/2010
Koordinatlar / Coordinates (m)	X						Bitiş Tarihi / Finish Date		19/09/2010
	Y						Sondaj Yöntemi / Drill Method		ROTARY
İstasyon / Station (km)							Sondaj Makinesi / Drill Rig		TSM 750
Sapma / Offset (m)							Kuyu Derinliği / BH Depth		14,00m

Kuyu Loğing Bit Depth	Örnek No Sample No	Örnek Derinliği Sample Depth	Örnek Türü Sample Type	Matkap Tipi/Çapı Bit Type/Diameter	Muhafaza Borusu Casing	Standart Penetrasyon Deneyi Standard Penetration Test (SPT)		Profil Symbol	Jeolojik Tanımlama Geological Description	Karot Çapı Core Diameter	Örnek Yüzdesi Core Recovery	Kaya Kalitesi RQD	Kırıklar (Ø33 cm) Fractures	Ayrışma Wathering	Dayanım Strength	Yerinde Deneyler In situ Tests
						Darbe Sayısı # of Blows	Grafik Graph									
m		m				15 30 45	10 20 30 40 50			mm	%	%				
1	1		RC						QUARTZSCHIST: Dark brown and grey colored, well altered, weak		10	0		W3 W4	G4	
2																
3	2		RC								50	0		W3 W4	G4	
4																
5	3		RC								70	60		W2	G2	
6				110	Not Used					63,5						
7																
8	4		RC						CHLOROSHIST: White colored, brownish partly altered moderately strong		80	66		W2	G2	
9																
10																
11	5		RC								80	70		W2	G2	
12																

SONDAJ LOGU / BORING LOG

Proje İsmi / Project Name	UT GROUP MANGANESE EXPLORATION	Kuyu No / BH No	SK-1
Proje Yeri / Project Location	ESKİŞEHİR/TAYCILAR VILLAGE	Sayfa / Sheet	2
Kot / Ground Elevation (m)		Başlangıç Tarihi / Start Date	18/09/2010
Koordinatlar / Coordinates (m) X / Y		Bitiş Tarihi / Finish Date	19/09/2010
		Sondaj Yöntemi / Drill Method	ROTARY
İstasyon / Station (km)		Sondaj Makinesi / Drill Rig	TSM-750
Sapma / Offset (m)		Kuyu Derinliği / BH Depth	14,00m

Tarih / Derinlik / YASS / Açıklama

Kuyu Derinliği BH Depth (m)	Örnek No Sample No	Örnek Derinliği Sample Depth (m)	Örnek Türü Sample Type	Matkap Tipi/Çapı Bit Type/Diameter	Muhafaza Borusu Casing	Darbe Sayısı # of Blows 15/30/45	Grafik Graph 10/20/30/40/50	Profil Symbol	Jeolojik Tanımlama Geological Description	Karot Çapı Core Diameter (mm)	Örnek Yüzdesi Core Recovery (%)	Kaya Kalitesi RQD (%)	Kırıklar (#30 cm) Fractures	Ayrışma Weathering	Dayanım Strength	Yerinde Deneyler In-situ Tests
	6		RC	HQ						63,5	65	55		W2	S2	
14									WELL END POINT: 14,00m							
15																

KAYA KALİTESİ / RQD		KIRIKLAR / FRACTURES (# 30 cm)	İNCE DANELİ / FINE GRANIED			İRİ TANELİ / COARSE GRANIED		
0 - 25 % Çok zayıf	/ Very poor		N : 0 - 2	Çok yum.	/ Very soft	N : 0 - 4	Çok gevşek	/ Very loose
25 - 50 % Zayıf	/ Poor	<1 Seyrek / Wide	N : 3 - 4	Yumuşak	/ Soft	N : 5 - 10	Gevşek	/ Loose
50 - 75 % Orta	/ Fair	1 - 2 Orta / Moderate	N : 5 - 8	Orta katı	/ M.stiff	N : 11 - 30	Orta sıkı	/ M.dense
75 - 90 % İyi	/ Good	3 - 10 Sık / Close	N : 9 - 15	Katı	/ Stiff	N : 31 - 50	Sıkı	/ Dense
90 - 100 % Çok iyi	/ Excellent	11 - 19 Çok sık / İntense	N : 16 - 30	Çok katı	/ Very stiff	N : >50	Çok sıkı	/ V. dense
		> 20 Parçalı / Crushed	N : >30	Sert	/ Hard			

AYRIŞMA / WEATHERING		DAYANIKLILIK / STRENGTH		KISALTMALAR / ABBREVIATIONS		NOTLAR / REMARKS
W₁ Taze / Fresh		S₁ Dayanımlı / Strong		UD : Şelbi tüp / Shelby		
W₂ Az ayrışmış / Slighly Weathered		S₂ Orta day. / Mod. Strong		RC : Karot numune / Core sam		
W₃ Orta derecede ay. / Mod. Weathered		S₃ Orta zayıf / Mod. Weak		PD : Paker deneyi / Packer		
W₄ Çok ayrışmış / Highly Weathered		S₄ Zayıf / Weak		GD : Geçirgenlik / Permeabi.		
W₅ Tamamen ayrışmış / Completely Weat.		S₅ Çok zayıf / Very weak		Pr : Presiyometre / Packer T.		

Sondör / Driller	Cemil ÖZKAN	Mühendis / Engineer	Geo. Eng. Özkan ÖZTÜRK

ADİL ÖZDEMİR
ENGINEERING&DRILLING

SONDAJ LOGU / BORING LOG

Proje İsmi / Project Name	UT GROUP MANGANESE EXPLORATION					Kuyu No / BH No		SK-2
Proje Yeri / Project Location	ESKİŞEHİR/TAYCILAR VILLAGE					Sayfa / Sheet		1
Kot / Ground Elevation (m)		Tarih	Derinlik	YASS	Açıklama	Başlangıç Tarihi / Start Date		20/09/2010
Koordinatlar / Coordinates (m) X						Bitiş Tarihi / Finish Date		20/09/2010
Y						Sondaj Yöntemi / Drill Method		ROTARY
İstasyon / Station (km)						Sondaj Makinesi / Drill Rig		TSM-750
Sapma / Offset (m)						Kuyu Derinliği / BH Depth		13,00m

Kuyu Derinliği BH Depth (m)	Örnek No Sample No	Örnek Derinliği Sample Depth (m)	Örnek Türü Sample Type	Matkap Tipi/Çapı Bit Type/Diameter	Muhafaza Borusu Casing	Standart Penetrasyon Deneyi / Standard Penetration Test (SPT) Darbe Sayısı # of Blows 15 30 45	Grafik Graph 10 20 30 40 50	Profil Symbol	Jeolojik Tanımlama Geological Description	Karot Çapı Core Diameter (mm)	Örnek Yüzdesi Core Recovery (%)	Kaya Kalitesi RQD (%)	Kırıklar (#30 cm) Fractures	Ayrışma Weathering	Dayanım Strength	Yerinde Deneyler In-situ Tests
1	1		RC		Used						0	0		W3	S3 S4	
2																
3	2		RC								40	20		W2	S2 S1	
4																
5	3		RC								90	70		W2	S2 S1	
6	4		RC	HQ					QUARTZSCHIST; White, grey and ligth green colored, quartz vines contents, poorly weathered, moderately strong and strong	63,5	100	100		W2	S2 S1	
7																
8	5		RC		Not Used						85	70		W2	S2 S1	
9	6		RC								75	75		W2	S2 S1	
10																
11	7		RC								75	66		W2	S2 S1	
12																

KAYA KALİTESİ / RQD		KIRIKLAR / FRACTURES (# 30 cm)		İNCE TANELİ / FINE GRANIED			İRİ TANELİ / COARSE GRANIED		
0 - 25 % Çok zayıf	/ Very poor			N : 0 - 2	Çok yum.	/ Very soft	N : 0 - 4	Çok gevşek	/ Very loose
25 - 50 % Zayıf	/ Poor	<1 Seyrek	/ Wide	N : 3 - 4	Yumuşak	/ Soft	N : 5 - 10	Gevşek	/ Loose
50 - 75 % Orta	/ Fair	1 - 2 Orta	/ Moderate	N : 5 - 8	Orta katı	/ M.stiff	N : 11 - 30	Orta sıkı	/ M.dense
75 - 90 % İyi	/ Good	3 - 10 Sık	/ Close	N : 9 - 15	Katı	/ Stiff	N : 31 - 50	Sıkı	/ Dense
90 - 100 % Çok iyi	/ Excellent	11 - 19 Çok sık	/ Intense	N : 16 - 30	Çok katı	/ Very stiff	N : >50	Çok sıkı	/ V. dense
		> 20 Parçalı	/ Crushed	N : >30	Sert	/ Hard			

AYRIŞMA / WEATHERING			DAYANIKLILIK / STRENGTH			KISALTMALAR / ABBREVIATIONS		NOTLAR / REMARKS
W1	Taze	/ Fresh	S1	Dayanımlı	/ Strong	UD : Şelbi tüp	/ Shelby	
W2	Az ayrışmış	/ Slightly Weathered	S2	Orta day.	/ Mod. Strong	RC : Karot numune	/ Core sam	
W3	Orta derecede ay.	/ Mod. Weathered	S3	Orta zayıf	/ Mod. Weak	PD : Paker deneyi	/ Packer	
W4	Çok ayrışmış	/ Highly Weathered	S4	Zayıf	/ Weak	GD : Geçirgenlik	/ Permeabi.	
W5	Tamamen ayrışmış	/ Completely Weat.	S5	Çok zayıf	/ Very weak	Pr : Presiyometre	/ Packer T.	
Sondör / Driller		Cemil ÖZKAN			Mühendis / Engineer		Geo. Eng. Özkan ÖZTÜRK	

ADİL ÖZDEMİR
ENGINEERING&DRILLING

SONDAJ LOGU / BORING LOG

Proje İsmi / Project Name	UT GROUP MANGANESE EXPLORATION					Kuyu No / BH No	SK-3
Proje Yeri / Project Location	ESKİŞEHİR/TAYCILAR VILLAGE					Sayfa / Sheet	1
Kot / Ground Elevation (m)		Tarih	Derinlik	YASS	Açıklama	Başlangıç Tarihi / Start Date	21/09/2010
Koordinatlar / Coordinates (m) X	4428447					Bitiş Tarihi / Finish Date	22/09/2010
Y	36322212					Sondaj Yöntemi / Drill Method	ROTARY
İstasyon / Station (km)						Sondaj Makinesi / Drill Rig	TSM-750
Sapma / Offset (m)						Kuyu Derinliği / BH Depth	13,00 m

Kuyu Derinliği BH Depth	Örnek No Sample No	Örnek Derinliği Sample Depth	Örnek Türü Sample Type	Matkap Tipi/Çapı Bit Type/Diameter	Muhafaza Bonsu Casing	Standart Penetrasyon Deneyi Standard Penetration Test (SPT)		Profil Symbol	Jeolojik Tanımlama Geological Description	Karot Çapı Core Diameter	Örnek Yüzdesi Core Recovery	Kaya Kalitesi RQD	Kırıklar (#30 cm) Fractures	Ayrışma Weathering	Dayanım Strength	Yerinde Deneyler In-situ Tests
						Darbe Sayısı # of Blows 15 30 45	Grafik Graph 10 20 30 40 50									
m		m								mm	%	%				
1	1		RC	Used							0	0		W4	S4	
2																
3	2		RC						MANGANESE; Brown-Black colored, from place to place quartz bands contents, poorly weathered, moderately strong		30	0		W2	S2	
4																
5	3		RC							63,5	25	0		W2	S2	
6			HQ													
7	4		RC								40	0		W2	S2	
8																
9	5		RC	Not Used							0	0		W4	S5	
10									CHOLOROSCHIST-QUARTZSCHIST; ligth grey and green, well weathered, low cemented, very weak							
11																
12	6		RC								10	0		W4	S5	

KAYA KALİTESİ / RQD		KIRIKLAR / FRACTURES		İNCE DANELİ / FINE GRANIED			İRİ TANELİ / COARSE GRANIED		
0 - 25 % Çok zayıf	/ Very poor	(# 30 cm)		N : 0 - 2	Çok yum.	/ Very soft	N : 0 - 4	Çok gevşek	/ Very loose
25 - 50 % Zayıf	/ Poor	<1 Seyrek	/ Wide	N : 3 - 4	Yumuşak	/ Soft	N : 5 - 10	Gevşek	/ Loose
50 - 75 % Orta	/ Fair	1 - 2 Orta	/ Moderate	N : 5 - 8	Orta katı	/ M.stiff	N : 11 - 30	Orta sıkı	/ M.dense
75 - 90 % İyi	/ Good	3 - 10 Sık	/ Close	N : 9 - 15	Katı	/ Stiff	N : 31 - 50	Sıkı	/ Dense
90 - 100 % Çok iyi	/ Excellent	11 - 19 Çok sık	/ İntense	N : 16 - 30	Çok katı	/ Very stiff	N : >50	Çok sıkı	/ V. dense
		> 20 Parçalı	/ Crushed	N : >30	Sert	/ Hard			

AYRIŞMA / WEATHERING			DAYANIKLILIK / STRENGTH			KISALTMALAR / ABBREVIATIONS		NOTLAR / REMARKS
W₁	Taze	/ Fresh	S₁	Dayanımlı	/ Strong	UD : Şelbi tüp	/ Shelby	
W₂	Az ayrışmış	/ Slighly Weathered	S₂	Orta day.	/ Mod. Strong	RC : Karot numune	/ Core sam	
W₃	Orta derecede ay.	/ Mod. Weathered	S₃	Orta zayıf	/ Mod. Weak	PD : Paker deneyi	/ Packer	
W₄	Çok ayrışmış	/ Highly Weathered	S₄	Zayıf	/ Weak	GD : Geçirgenlik	/ Permeabi.	
W₅	Tamamen ayrışmış	/ Completely Weat.	S₅	Çok zayıf	/ Very weak	Pr : Presiyometre	/ Packer T.	

Sondör / Driller	Cemil ÖZKAN	Mühendis / Engineer	Geo. Eng. Özkan ÖZTÜRK

ADİL ÖZDEMİR
ENGINEERING&DRILLING

SONDAJ LOGU / BORING LOG

Proje İsmi / Project Name	UT GROUP MANGANESE EXPLORATION					Kuyu No / BH No		SK-4
Proje Yeri / Project Location	ESKİŞEHİR/TAYCILAR VILLAGE					Sayfa / Sheet		1
Kot / Ground Elevation (m)			Tarih	Derinlik	YASS	Açıklama	Başlangıç Tarihi / Start Date	23/09/2010
Koordinatlar / Coordinates (m) X	4428449						Bitiş Tarihi / Finish Date	24/09/2010
Y	36322209						Sondaj Yöntemi / Drill Method	ROTARY
İstasyon / Station (km)							Sondaj Makinesi / Drill Rig	TSM-750
Sapma / Offset (m)							Kuyu Derinliği / BH Depth	9,00 m

Kuyu Derinliği BH Depth (m)	Örnek No Sample No	Örnek Derinliği Sample Depth (m)	Örnek Türü Sample Type	Matkap Tipi/Çapı Bit Type/Diameter	Muhafaza Borusu Casing	Standart Penetrasyon Deneyi SPT Darbe Sayısı # of Blows 15 30 45	Grafik Graph 10 20 30 40 50	Profil Symbol	Jeolojik Tanımlama Geological Description	Karot Çapı Core Diameter (mm)	Örnek Yüzdesi Core Recovery (%)	Kaya Kalitesi RQD (%)	Kırıklar (#30 cm) Fractures	Ayrışma Weathering	Dayanım Strength	Yerinde Deneyler In-situ Tests
1	1		RC		Used						0	0		W3	S4	
2																
3	2		RC								75	0		W3	S4	
4				HQ					CHLOROSCHIST; Ligth grey and very ligth green colored, moderately weathered, weak	63,5						
5	3		RC								20	0		W3	S4	
6					Not Used											
7																
8	4		RC								15	0		W3	S4	
9									WELL END POINT: 9,00 m							
10																
11																
12																

KAYA KALİTESİ / RQD		KIRIKLAR / FRACTURES		İNCE DANELİ / FINE GRANIED			İRİ TANELİ / COARSE GRANIED		
0 - 25 % Çok zayıf	/ Very poor	(# 30 cm)		N : 0 - 2	Çok yum.	/ Very soft	N : 0 - 4	Çok gevşek	/ Very loose
25 - 50 % Zayıf	/ Poor	<1 Seyrek	/ Wide	N : 3 - 4	Yumuşak	/ Soft	N : 5 - 10	Gevşek	/ Loose
50 - 75 % Orta	/ Fair	1 - 2 Orta	/ Moderate	N : 5 - 8	Orta katı	/ M.stiff	N : 11 - 30	Orta sıkı	/ M.dense
75 - 90 % İyi	/ Good	3 - 10 Sık	/ Close	N : 9 - 15	Katı	/ Stiff	N : 31 - 50	Sıkı	/ Dense
90 - 100 % Çok iyi	/ Excellent	11 - 19 Çok sık	/ İntense	N : 16 - 30	Çok katı	/ Very stiff	N : >50	Çok sıkı	/ V. dense
		> 20 Parçalı	/ Crushed	N : >30	Sert	/ Hard			

AYRIŞMA / WEATHERING		DAYANIKLILIK / STRENGTH		KISALTMALAR / ABBREVIATIONS		NOTLAR / REMARKS
W₁ Taze	/ Fresh	S₁ Dayanımlı	/ Strong	UD : Şelbi tüp	/ Shelby	
W₂ Az ayrışmış	/ Slighly Weathered	S₂ Orta day.	/ Mod. Strong	RC : Karot numune	/ Core sam.	
W₃ Orta derecede ay.	/ Mod. Weathered	S₃ Orta zayıf	/ Mod. Weak	PD : Paker deneyi	/ Packer	
W₄ Çok ayrışmış	/ Highly Weathered	S₄ Zayıf	/ Weak	GD : Geçirgenlik	/ Permeabi.	
W₅ Tamamen ayrışmış	/ Completely Weat.	S₅ Çok zayıf	/ Very weak	Pr : Presiyometre	/ Packer T.	

Sondör / Driller	Cemil ÖZKAN	Mühendis / Engineer	Geo. Eng. Özkan ÖZTÜRK

ADİL ÖZDEMİR
ENGINEERING&DRILLING

SONDAJ LOGU / BORING LOG

Proje İsmi	/ Project Name		UT GROUP MANGANESE EXPLORATION					Kuyu No	/ BH No		SK-5
Proje Yeri	/ Project Location		ESKİŞEHİR/TAYCILAR VILLAGE					Sayfa	/ Sheet		1
Kot	/ Ground Elevation (m)			Tarih	Derinlik	YASS	Açıklama	Başlangıç Tarihi / Start Date			24/09/2010
Koordinatlar / Coordinates (m)		X	4428440					Bitiş Tarihi / Finish Date			26/09/2010
		Y	36322190					Sondaj Yöntemi / Drill Method			ROTARY
İstasyon	/ Station	(km)						Sondaj Makinesi / Drill Rig			TSM-750
Sapma	/ Offset	(m)						Kuyu Derinliği / BH Depth			25,00 m

Kuyu Derinliği BH Depth	Örnek No Sample No	Örnek Derinliği Sample Depth	Örnek Türü Sample Type	Matkap Tipi/Çapı Bit Type/Diameter	Muhafaza Bonusu Casing	Standart Penetrasyon Deneyi Standard Penetration Test (SPT) Darbe Sayısı # of Blows	Grafik Graph	Profil Symbol	Jeolojik Tanımlama Geological Description	Karot Çapı Core Diameter	Örnek Yüzdesi Core Recovery	Kaya Kalitesi RQD	Kırıklar (#30 cm) Fractures	Ayrışma Weathering	Dayanım Strength	Yerinde Deneyler In-situ Tests
m		m				15 30 45	10 20 30 40 50			mm	%	%				
1–4	1		RC		Used				QUARTZSCHIST; Grey and dark brown, moderately-highly weathered, moderately-highly weak		0	0		W3 W4	S3	
5	2		RC						CLAY; Dark brown and reddish colored		15	0		W3	S3	
6–7	3		RC	NQ						47,6	0	0		W2	S2	
9	4		RC		Not Used				QUARTZSCHIST; Ligth grey and ligth green colored, partly , slightly weathered, moderately strong		10	0		W2	S2	
11–12	5		RC								10	5		W2	S2	

SONDAJ LOGU / BORING LOG

Proje İsmi	/ Project Name	UT GROUP MANGANESE EXPLORATION					Kuyu No	/ BH No	SK-5
Proje Yeri	/ Project Location	ESKİŞEHİR/TAYCILAR VILLAGE					Sayfa	/ Sheet	2
Kot	/ Ground Elevation (m)		Tarih	Derinlik	YASS	Açıklama	Başlangıç Tarihi / Start Date		24/09/2010
Koordinatlar / Coordinates (m)	X	4428440					Bitiş Tarihi / Finish Date		26/09/2010
	Y	36322190					Sondaj Yöntemi / Drill Method		ROTARY
İstasyon	/ Station (km)						Sondaj Makinesi / Drill Rig		TSM-750
Sapma	/ Offset (m)						Kuyu Derinliği / BH Depth		25,00 m

Kuyu Derinliği BH Depth (m)	Örnek No Sample No	Örnek Derinliği Sample Depth (m)	Örnek Türü Sample Type	Matkap Tipi/Çapı Bit Type/Diameter	Muhafaza Bonusu Casing	Darbe Sayısı # of Blows	Grafik Graph	Profil Symbol	Jeolojik Tanımlama Geological Description	Karot Çapı Core Diameter (mm)	Örnek Yüzdesi Core Recovery (%)	Kaya Kalitesi RQD (%)	Kırıklar (#30 cm) Fractures	Ayrışma Wathering	Dayanım Strength	Yerinde Deneyler In-situ Tests
14	6		RC								15	0		W2	S2	
15																
16																
17	7		RC								5	0		W2	S2	
18									QUARTZSCHIST; Ligth grey and ligth green colored, from place to place big quartz, sligthly weathered, moderately strong	47,6						
19	8		RC	NQ	Not used						15	0		W2	S2	
20	9		RC								5	0		W2	S2	
21	10		RC								8	0		W2	S2	
22																
23	11		RC								10	0		W2	S2	
24																
25									WELL END POINT: 25,00 m							

KAYA KALİTESİ / RQD		KIRIKLAR / FRACTURES		İNCE DANELİ / FINE GRANIED			İRİ TANELİ / COARSE GRANIED		
0 - 25 % Çok zayıf	/ Very poor	(# 30 cm)		N : 0 - 2	Çok yum.	/ Very soft	N : 0 - 4	Çok gevşek	/ Very loose
25 - 50 % Zayıf	/ Poor	<1 Seyrek	/ Wide	N : 3 - 4	Yumuşak	/ Soft	N : 5 - 10	Gevşek	/ Loose
50 - 75 % Orta	/ Fair	1 - 2 Orta	/ Moderate	N : 5 - 8	Orta katı	/ M.stiff	N : 11 - 30	Orta sıkı	/ M.dense
75 - 90 % İyi	/ Good	3 - 10 Sık	/ Close	N : 9 - 15	Katı	/ Stiff	N : 31 - 50	Sıkı	/ Dense
90 - 100 % Çok iyi	/ Excellent	11 - 19 Çok sık	/ İntense	N : 16 - 30	Çok katı	/ Very stiff	N : >50	Çok sıkı	/ V. dense
		> 20 Parçalı	/ Crushed	N : >30	Sert	/ Hard			

AYRIŞMA / WEATHERING			DAYANIKLILIK / STRENGTH			KISALTMALAR / ABBREVIATIONS		NOTLAR / REMARKS
W₁	Taze	/ Fresh	S₁	Dayanımlı	/ Strong	UD : Şelbi tüp	/ Shelby	
W₂	Az ayrışmış	/ Slighly Weathered	S₂	Orta day.	/ Mod. Strong	RC : Karot numune	/ Core sam.	
W₃	Orta derecede ay.	/ Mod. Weathered	S₃	Orta zayıf	/ Mod. Weak	PD : Paker deneyi	/ Packer	
W₄	Çok ayrışmış	/ Highly Weathered	S₄	Zayıf	/ Weak	GD : Geçirgenlik	/ Permeabi.	
W₅	Tamamen ayrışmış	/ Completely Weat.	S₅	Çok zayıf	/ Very weak	Pr : Presiyometre	/ Packer T.	

Sondör / Driller	Cemil ÖZKAN	Mühendis / Engineer	Geo. Eng. Özkan ÖZTÜRK

ADİL ÖZDEMİR
ENGINEERING&DRILLING

SONDAJ LOGU / BORING LOG

Proje İsmi / Project Name	UT GROUP MANGANESE EXPLORATION		Kuyu No / BH No	**SK-6**
Proje Yeri / Project Location	ESKİŞEHİR/TAYCILAR VILLAGE		Sayfa / Sheet	1
Kot / Ground Elevation (m)	Tarih / Derinlik / YASS / Açıklama		Başlangıç Tarihi / Start Date	27/09/2010
Koordinatlar / Coordinates (m) X 4428461			Bitiş Tarihi / Finish Date	27/09/2010
Y 36322209			Sondaj Yöntemi / Drill Method	ROTARY
İstasyon / Station (km)			Sondaj Makinesi / Drill Rig	TSM-750
Sapma / Offset (m)			Kuyu Derinliği / BH Depth	10,00 m

Standart Penetrasyon Deneyi / Standard Penetration Test (SPT)

Darbe Sayısı / # of Blows: 15 30 45
Grafik / Graph: 10 20 30 40 50

Profil / Symbol

Jeolojik Tanımlama / Geological Description

Karot Çapı / Core Diameter (mm), Örnek Yüzdesi / Core Recovery (%), Kaya Kalitesi / RQD (%), Kırıklar (#30 cm) / Fractures, Ayrışma / Weathering, Dayanım / Strength, Yerinde Deneyler / In-situ Tests

Matkap Tipi/Çapı / Bit Type/Diameter — Used / NQ / Not Used

Örnek No / Sample No: 1 (RC), 2 (RC), 3 (RC)

QUARTZSCHIST; Dark brown, white and grey colored, between 7,00-8,50 m white colored calcoschists, moderatly weathered, moderately strong-weak

Core Diameter: 47,6

Sample	Core Recovery	RQD	Weathering	Strength
1	0	0	W3	S3
2	20	0	W3	S3
3	50	18	W3	S4

CHLOROSCHIST; Ligth green and ligth brown, moderately weathered, weak

WELL END POINT: 10,00 m

KAYA KALİTESİ / RQD

0 - 25 % Çok zayıf	/ Very poor
25 - 50 % Zayıf	/ Poor
50 - 75 % Orta	/ Fair
75 - 90 % İyi	/ Good
90 - 100 % Çok iyi	/ Excellent

KIRIKLAR / FRACTURES (# 30 cm)

<1 Seyrek	/ Wide
1 - 2 Orta	/ Moderate
3 - 10 Sık	/ Close
11 - 19 Çok sık	/ Intense
> 20 Parçalı	/ Crushed

İNCE DANELİ / FINE GRANIED

N : 0 - 2	Çok yum.	/ Very soft
N : 3 - 4	Yumuşak	/ Soft
N : 5 - 8	Orta katı	/ M.stiff
N : 9 - 15	Katı	/ Stiff
N : 16 - 30	Çok katı	/ Very stiff
N : >30	Sert	/ Hard

İRİ TANELİ / COARSE GRANIED

N : 0 - 4	Çok gevşek	/ Very loose
N : 5 - 10	Gevşek	/ Loose
N : 11 - 30	Orta sıkı	/ M.dense
N : 31 - 50	Sıkı	/ Dense
N : >50	Çok sıkı	/ V. dense

AYRIŞMA / WEATHERING

W1	Taze	/ Fresh
W2	Az ayrışmış	/ Slighly Weathered
W3	Orta derecede ay.	/ Mod. Weathered
W4	Çok ayrışmış	/ Highly Weathered
W5	Tamamen ayrışmış	/ Completely Weat.

DAYANIKLILIK / STRENGTH

S1	Dayanımlı	/ Strong
S2	Orta day.	/ Mod. Strong
S3	Orta zayıf	/ Mod. Weak
S4	Zayıf	/ Weak
S5	Çok zayıf	/ Very weak

KISALTMALAR / ABBREVIATIONS

UD : Şelbi tüp	/ Shelby
RC : Karot numune	/ Core sam
PD : Paker deneyi	/ Packer
GD : Geçirgenlik	/ Permeabi.
Pr : Presiyometre	/ Packer T.

NOTLAR / REMARKS

Sondör / Driller	Cemil ÖZKAN	Mühendis / Engineer — Geo. Eng. Özkan ÖZTÜRK

ADİL ÖZDEMİR
ENGINEERING&DRILLING

SONDAJ LOGU / BORING LOG

Proje İsmi / Project Name	UT GROUP MANGANESE EXPLORATION					Kuyu No / BH No	SK-7
Proje Yeri / Project Location	ESKİŞEHİR/TAYCILAR VILLAGE					Sayfa / Sheet	1
Kot / Ground Elevation (m)		Tarih	Derinlik	YASS	Açıklama	Başlangıç Tarihi / Start Date	28/09/2010
Koordinatlar / Coordinates (m) X	4428470					Bitiş Tarihi / Finish Date	28/09/2010
Y	36322178					Sondaj Yöntemi / Drill Method	ROTARY
İstasyon / Station (km)						Sondaj Makinesi / Drill Rig	TSM-750
Sapma / Offset (m)						Kuyu Derinliği / BH Depth	20,00 m

Standard Penetration Test (SPT). Core Diameter 47,6 mm. NQ.

QUARTZSCHIST; Brown, grey and white colored, between 7,50-10,00 m white colored calcoschists, moderately weathered, moderately strong-weak

QUARTZSCHIST; Brown, grey and white, moderately weathered, moderately strong-weak

CHLOROSCHIST; Grey and green, moderately weathered, moderately strong-weak

Sample values (Core Recovery / RQD / Weathering / Strength):
- Sample 1 (RC): 0 / 0 / W3 / S3
- Sample 2 (RC): 10 / 0 / W3 / S3
- Sample 3 (RC): 15 / 0 / W3 / S3
- Sample 4 (RC): 15 / 8 / W3 / S3
- Sample 5 (RC): 15 / 0 / W3 / S3
- Sample 6 (RC): 0 / 0 / W3 / S3

SONDAJ LOGU / BORING LOG

Proje İsmi / Project Name	UT GROUP MANGANEZ ARAŞTIRMASI				Kuyu No	/ BH No	SK-7

| Proje Yeri / Project Location | ESKİŞEHİR/TAYCILAR KÖYÜ | | | | Sayfa / Sheet | 2 |

Kot / Ground Elevation (m)		Tarih	Derinlik	YASS	Açıklama	Başlangıç Tarihi / Start Date	28/09/2010
Koordinatlar / Coordinates (m) X	4428470					Bitiş Tarihi / Finish Date	28/09/2010
Y	36322178					Sondaj Yöntemi / Drill Method	ROTARY
İstasyon / Station (km)						Sondaj Makinesi / Drill Rig	TSM-750
Sapma / Offset (m)						Kuyu Derinliği / BH Depth	20,00 m

Standart Penetrasyon Deneyi

Kuyu Derinliği BH Depth (m)	Örnek No Sample No	Örnek Derinliği Sample Depth (m)	Örnek Türü Sample Type	Matkap Tipi/Çapı Bit Type/Diameter	Muhafaza Borusu Casing	Darbe Sayısı # of Blows (15 30 45)	Grafik Graph (10 20 30 40 50)	Profil Symbol	Jeolojik Tanımlama Geological Description	Karot Çapı Core Diameter (mm)	Örnek Yüzdesi Core Recovery (%)	Kaya Kalitesi RQD (%)	Kırıklar (#30 cm) Fractures	Ayrışma Weathering	Dayanım Strength	Yerinde Deneyler In-situ Tests
14–15	7		RC						CHLOROSCHIST; Grey and ligth green coloredi, moderately weathered, moderately-highly weak			10	0	W3	S3	
16–18	8		NQ / RC	Not Used					CLAY; Dark brown and reddish colored	47,6		20	0	W3	S3	
18–20									CHLOROSCHIST; Grey and dark green colored, moderately weathered, moderately-highly weak							
20									WELL END POINT: 20,00 m							

KAYA KALİTESİ / RQD		KIRIKLAR / FRACTURES		İNCE DANELİ / FINE GRANIED			İRİ TANELİ / COARSE GRANIED		
0 - 25 % Çok zayıf	/ Very poor	(# 30 cm)		N : 0 - 2	Çok yum.	/ Very soft	N : 0 - 4	Çok gevşek	/ Very loose
25 - 50 % Zayıf	/ Poor	<1 Seyrek	/ Wide	N : 3 - 4	Yumuşak	/ Soft	N : 5 - 10	Gevşek	/ Loose
50 - 75 % Orta	/ Fair	1 - 2 Orta	/ Moderate	N : 5 - 8	Orta katı	/ M.stiff	N : 11 - 30	Orta sıkı	/ M.dense
75 - 90 % İyi	/ Good	3 - 10 Sık	/ Close	N : 9 - 15	Katı	/ Stiff	N : 31 - 50	Sıkı	/ Dense
90 - 100 % Çok iyi	/ Excellent	11 - 19 Çok sık	/ İntense	N : 16 - 30	Çok katı	/ Very stiff	N : >50	Çok sıkı	/ V. dense
		> 20 Parçalı	/ Crushed	N : >30	Sert	/ Hard			

AYRIŞMA / WEATHERING		DAYANIKLILIK / STRENGTH		KISALTMALAR / ABBREVIATIONS		NOTLAR / REMARKS
W₁ Taze	/ Fresh	S₁ Dayanımlı	/ Strong	UD : Şelbi tüp	/ Shelby	
W₂ Az ayrışmış	/ Slighly Weathered	S₂ Orta day.	/ Mod. Strong	RC : Karot numune	/ Core sam	
W₃ Orta derecede ay.	/ Mod. Weathered	S₃ Orta zayıf	/ Mod. Weak	PD : Paker deneyi	/ Packer	
W₄ Çok ayrışmış	/ Highly Weathered	S₄ Zayıf	/ Weak	GD : Geçirgenlik	/ Permeabi.	
W₅ Tamamen ayrışmış	/ Completely Weat.	S₅ Çok zayıf	/ Very weak	Pr : Presiyometre	/ Packer T.	

Sondör / Driller	Cemil ÖZKAN	Mühendis / Engineer	Geo. Eng. Özkan ÖZTÜRK

ADİL ÖZDEMİR
ENGINEERING&DRILLING

SONDAJ LOGU / BORING LOG

Proje İsmi / Project Name	UT GROUP MANGANESE EXPLORATION				Kuyu No / BH No	SK-8
Proje Yeri / Project Location	ESKİŞEHİR/TAYCILAR VILLAGE				Sayfa / Sheet	1

Kot / Ground Elevation (m)			Tarih	Derinlik	YASS	Açıklama	Başlangıç Tarihi / Start Date	29/09/2010
Koordinatlar / Coordinates (m)	X	4428524					Bitiş Tarihi / Finish Date	29/09/2010
	Y	36321766					Sondaj Yöntemi / Drill Method	ROTARY
İstasyon / Station (km)							Sondaj Makinesi / Drill Rig	TSM-750
Sapma / Offset (m)							Kuyu Derinliği / BH Depth	20,00 m

Kuyu Derinliği BH Depth	Örnek No Sample No	Örnek Derinliği Sample Depth	Örnek Türü Sample Type	Matkap Tipi/Çapı Bit Type/Diameter	Muhafaza Borusu Casing	Standart Penetrasyon Deneyi Standard Penetration Test (SPT)		Profil Symbol	Jeolojik Tanımlama Geological Description	Karot Çapı Core Diameter	Örnek Yüzdesi Core Recovery	Kaya Kalitesi RQD	Kırıklar (#30 cm) Fractures	Ayrışma Weathering	Dayanım Strength	Yerinde Deneyler In-situ Tests
						Darbe Sayısı # of Blows	Grafik Graph									
m		m				15 30 45	10 20 30 40 50			mm	%	%				
	1		RC						QUARTZSCHIST; Ligth brown and white colored, slightly weathered, moderately strong		0	0		W2	S2	
	2		RC								3	0		W2	S2	
	3		RC								80	47		W2	S1 S2	
	4		RC						CHLOROSCHIST; Ligth grey, white, brown, partly black, slightly weathered, moderately strong-strong		75	48		W2	S1 S2	
	5		RC								90	80		W2	S1 S2	

SONDAJ LOGU / BORING LOG

Proje İsmi / Project Name	UT GROUP MANGANESE EXPLORATION					Kuyu No / BH No		SK-8
Proje Yeri / Project Location	ESKİŞEHİR/TAYCILAR VILLAGE					Sayfa / Sheet		2
Kot / Ground Elevation (m)		Tarih	Derinlik	YASS	Açıklama	Başlangıç Tarihi / Start Date		29/09/2010
Koordinatlar / Coordinates (m) X	4428524					Bitiş Tarihi / Finish Date		29/09/2010
Y	36321766					Sondaj Yöntemi / Drill Method		ROTARY
İstasyon / Station (km)						Sondaj Makinesi / Drill Rig		TSM-750
Sapma / Offset (m)						Kuyu Derinliği / BH Depth		20,00 m

Kuyu Derinliği BH Depth (m)	Örnek No Sample No	Örnek Derinliği Sample Depth (m)	Örnek Türü Sample Type	Matkap Tipi/Çapı Bit Type/Diameter	Muhafaza Borusu Casing	Standart Penetrasyon Deneyi — Darbe Sayısı # of Blows 15 30 45	Standart Penetrasyon Deneyi — Grafik Graph 10 20 30 40 50	Profil Symbol	Jeolojik Tanımlama Geological Description	Karot Çapı Core Diameter mm	Örnek Yüzdesi Core Recovery %	Kaya Kalitesi RQD %	Kırıklar (#30 cm) Fractures	Ayrışma Wathering	Dayanım Strength	Yerinde Deneyler In-situ Tests
14	6		RC								85	73		W2	S1 S2	
16	7		RC						CHLOROSCHIST; Dark colors dominated, slightly ligth grey and dark green seen, 5-10 cm calsite infilling, slightly weathered, moderately strong-weak		100	93		W2	S1 S2	
18 / 19	8		RC								100	67		W2	S1 S2	
20									WELL END POINT: 20,00 m							

KAYA KALİTESİ / RQD		KIRIKLAR / FRACTURES		İNCE DANELİ / FINE GRANIED			İRİ TANELİ / COARSE GRANIED	
0 - 25 % Çok zayıf	/ Very poor	(# 30 cm)		N : 0 - 2	Çok yum.	/ Very soft	N : 0 - 4 Çok gevşek	/ Very loose
25 - 50 % Zayıf	/ Poor	<1 Seyrek	/ Wide	N : 3 - 4	Yumuşak	/ Soft	N : 5 - 10 Gevşek	/ Loose
50 - 75 % Orta	/ Fair	1 - 2 Orta	/ Moderate	N : 5 - 8	Orta katı	/ M.stiff	N : 11 - 30 Orta sıkı	/ M.dense
75 - 90 % İyi	/ Good	3 - 10 Sık	/ Close	N : 9 - 15	Katı	/ Stiff	N : 31 - 50 Sıkı	/ Dense
90 - 100 % Çok iyi	/ Excellent	11 - 19 Çok sık	/ İntense	N : 16 - 30	Çok katı	/ Very stiff	N : >50 Çok sıkı	/ V. dense
		> 20 Parçalı	/ Crushed	N : >30	Sert	/ Hard		

AYRIŞMA / WEATHERING			DAYANIKLILIK / STRENGTH			KISALTMALAR / ABBREVIATIONS		NOTLAR / REMARKS
W₁	Taze	/ Fresh	S₁	Dayanımlı	/ Strong	UD : Şelbi tüp	/ Shelby	
W₂	Az ayrışmış	/ Slighly Weathered	S₂	Orta day.	/ Mod. Strong	RC : Karot numune	/ Core sam	
W₃	Orta derecede ay.	/ Mod. Weathered	S₃	Orta zayıf	/ Mod. Weak	PD : Paker deneyi	/ Packer	
W₄	Çok ayrışmış	/ Highly Weathered	S₄	Zayıf	/ Weak	GD : Geçirgenlik	/ Permeabi.	
W₅	Tamamen ayrışmış	/ Completely Weat.	S₅	Çok zayıf	/ Very weak	Pr : Presiyometre	/ Packer T.	
Sondör / Driller			Cemil ÖZKAN			Mühendis / Engineer		Geo. Eng. Özkan ÖZTÜRK

Fig. 32 Report charts of all the cores that were drilled in Taycilar Mn area.

	Drilling	Coordinates		Core diameter
	No	X	Y	(mm)
Line 1	SK-1	36S 320646	4428843	27
	SK-2	320649	4428983	28
	SK-3	320649	4428955	28
Line 2	SK-4	320900	4428955	31
Line 3	SK-5	321099	4428714	47
Line 4	SK-6	321333	4428489	30
	SK-7	321331	4428394	65
	SK-8	321336	4428606	20
Line 5	SK-9	321730	4428329	20
	SK-10	321734	4428497	20
	SK-11	321735	4428536	15
	SK-12	321740	4428765	28
	SK-13	321742	4428815	20
Line 6	SK-14	322150	4428289	20
	SK-15	322155	4428502	15

Table. 5 Borehole drilling points in Taycılar/Eskişehir manganese field

2.6.3.4   Texture and mineralogy

Due to the coarse texture of the braunite-rich quartzite XRD data were collected from a partition of the original sample of about 500 g, representative of the whole rock, that was powdered with a ball mill. Samples were analysed with a Philips X'Pert Pro X-ray powder diffractometer at the Dipartimento di Scienze della Terra, University of Milan, Italy.

XRD analyses (XRD pattern from sample ESK10 is shown as an example in Fig. 33) show that a similar mineralogical association was identified in all samples. It comprises braunite and quartz as main phases, with minor pyrolusite and cryptomelane as Mn phases and plagioclase as gangue phase. Some phases, present in small amount only in some samples, are hematite, rutile, minnesotatite and jianshuiite.
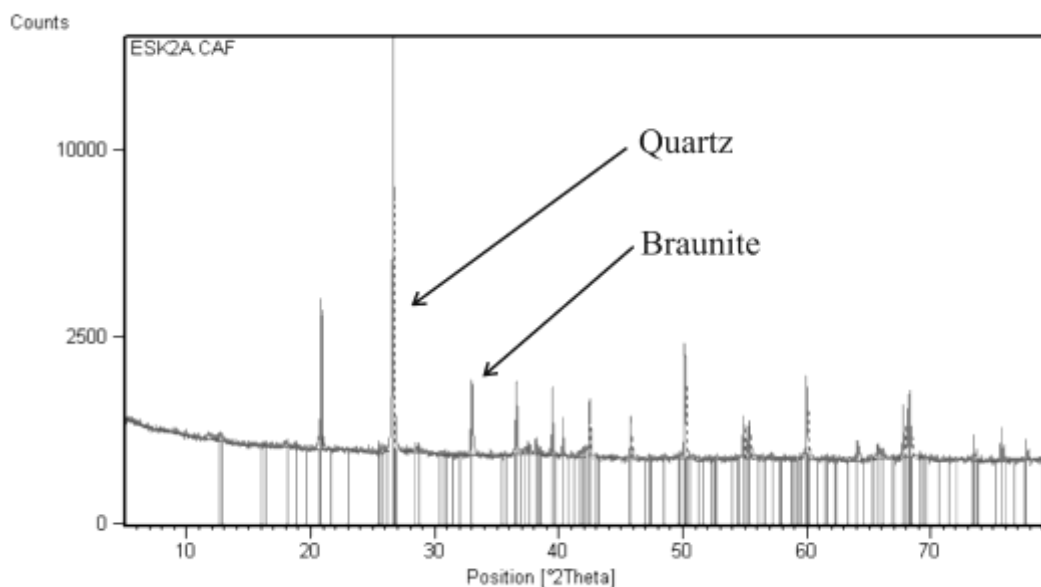
Fig. 33 X-ray diffraction pattern of braunite-rich Eskisehir Mn ore.

2.6.3.5   Whole rock chemistry

Whole rock analyses were carried out on samples with X-Ray fluorescence (XRF) at Dipartimento di Scienze della Terra, University of Milan, Italy.

Results on analysed elements (MnO, SiO_2, Fe_2O_3, Al_2O_3, CaO), as oxides, are shown in Table 6. Even in such a small set of data samples show a wide range of MnO content, between 5 and 67 wt% (Table 3).

wt%	Fe_2O_3	MnO	SiO_2	Al_2O_3	CaO
ESK0A	3.76	18.20	60.96	4.62	0.88
ESK0B	4.80	4.72	75.94	2.48	0.45
ESK1	1.72	36.58	48.14	1.08	0.55
ESK2A	3.02	40.89	36.41	2.61	1.39
ESK2B	3.02	58.76	33.26	5.71	3.37
ESK2C	5.69	23.24	50.10	9.28	1.11
ESK3	0.99	44.12	51.49	0.36	0.38
ESK10A	0.18	66.97	29.35	0.63	0.74
ESK10B	4.14	6.02	73.82	6.72	0.54
ESK10C	1.88	4.73	87.00	1.99	0.43
ESK10D	3.03	16.52	67.13	3.85	0.85

Table 6 XRF analyses of outcrop samples.

SiO_2 content is reversely correlated to MnO content, on the other hand Fe_2O_3, Al_2O_3 and CaO are low and not variable. Data suggest that, where the metamorphic overprint is stronger, the original assemblage is transformed in an almost bimineralic association, comprising only braunite and quartz, where all oxides except MnO and SiO_2 are below 1 wt%.

2.7 Mineralogical characteristics of braunite

Braunite is a relatively rare manganese ore, which is not found only in deposits of manganese usually known and exploited, where the useful minerals are usually oxides of manganese, iron and manganese oxides and hydroxides of manganese.

There are, however, althought rare, cultivated fields of Manganese of braunite, including one of the most significant is to kajilidongri, Mahyda Pradesh, India, which presents lithologies similar to those of the deposits of Eskisehir.

The braunite is classifiable as a silicate of manganese divalent and trivalent, of general formula Mn (II) Mn (III) $6SiO_{12}$. The distribution of the elements inside is as follows: Mn = 63.60%, Si = 4.64% O = 31.75%. Expressed as oxides distribution, is as follows: MnO = 11.73%, Mn_2O_3 = 78.33%, SiO_2 = 9.94%. The braunite therefore, thanks to the low degree of oxidation (manganese trivalent) compared to the oxides of manganese (manganese tetravalent), although it is a silicate, presents high content of manganese in compared with other useful minerals of manganese, even slightly higher than those of the pyrolusite (MnO_2, Mn = 63.19%) and the manganite [MnO (OH)], Mn = 62.47%) and much higher than the psilomelano [(Ba $H_2O)_2$ Mn_5O_{10}], Mn = 46.56%).

Among the characteristic properties of braunite there is its ferromagnetic character, bound to the presence of substitutions with the magnetite. It has even been used in oil fields in the Kodur manganese Manganese Belt, India, to perform magnetic prospecting of the mineralization.

The ferromagnetic character of the mineralization makes it possible in theory, where the grain of the mineralization is sufficiently coarse, a concentration of the ore through magnetic separation. In the case of Eskisehir field, the metamorphic transformation of the original deposit has generated a general increase of the grain, with the formation of domains enriched in manganese and silica in centimeter size, a condition which allows to hypothesize the possibility to enrich successfully the braunite mineralization

2.7.1 Braunite enrichment tests

Mineralogy and texture of the Taycilar deposit show conditions that can favour magnetic enrichment of ore at relatively coarse grainsize, providing the opportunity to produce a high grade gravel and sand final product.

Even if most of the mined Mn deposits host Mn mainly as oxides, braunite-dominated ores are known, like the Waziristan ores, Pakistan (Tahir Shah, 2007), or the Kalahari manganese field, South Africa (Gutzmer and

Beukes, 1996), and mined, like at Kajlidongri mine, India (Ostwald and Nayak, 1993). Magnetic enrichment of a braunite-rich manganese ore is reported by Rao et al (1998) for the Chikla manganese ore, Maharastra, India. They performed high intensity wet magnetic separation on a 44 wt% Mn ore grinded to -0.1 mm, obtaining a 51 wt% Mn product at a 95% Mn recovery, compared with a 47 wt% Mn product obtained via jigging.

Most steel industry applications of manganese require a millimetric to centimetric grainsize of ore and hence fine grained chert-hosted manganese ores usually are not enriched. In our experiments we aimed at studying the possibility of magnetically enriching braunite-rich manganese ore at much coarser grainsize than those used by Rao et al. (1998), and having a gravel and sand final product as a result.

Magnetic properties of Mn ore have been assessed in magnetic prospecting (Bhimasankaram and Rao, 1957). Braunite shows a paramagnetic behaviour that is strongly affected by incorporation of elements, like Mg and Fe, substituting Mn (Abs-Wurmbach et al, 2002). In addition the Taycilar deposit shows a metamorphic texture that allows significative separation of Mn-rich phases and quartz at relatively fine grainsize of crushed ore.

Enrichment tests were done in two different phases. Firstly we checked the possibility to enrich a high grade Mn ore from cores of lenses ESK2 and ESK10 (samples ESK2C and ESK10C), where recrystallization during metamorphism produced pluricentimetric quartz domains within a massive braunite groundmass. The second phase consisted in enrichment tests of mixed low and high grade ore (sample ESK2B, representative of the whole ESK2 lens), where braunite is disseminated in millimetric crystal clusters within quartzite.

2.7.1.1 *High grade Mn Ore*

Magnetic separation tests were carried out with a 1.5 m wide one step permanent roll magnetic separator, working at 9000 gauss power, used in a closeby magnesite ore enrichment plant. Feed was supplied with a vibrating feeder suiting the width of the separator.

For the test samples ESK2C and ESK10C, taken from the prospecting trenches and about 25 kg each, were used. Ore was hand crushed to 95 wt% +4 mm and 100% -20 mm. Anyway, due to the different hardness of the samples, ESK10 is coarser after crushing, with only 25% -10 mm against 60% of ESK2C. Results of separation tests are shown in Table 3 together with the recovery rates.

Mn enrichment is respectively 6.55 wt% and 4.86 wt% for ESK2C and ESK10C (Table 8), that corresponds to 8.46 wt% and 6.28 wt% on a MnO basis, respectively. Mn recovery is very high for ESK2C, 93.7 %, and much lower for ESK10C, 77.7 %.

2.7.1.2   Low grade Mn Ore

Magnetic separation experiments were carried out with a Permroll® 50 mm wide one step laboratory permanent roll magnetic separator at University of Eskisehir. Roll speed, roll vibration and position of blades separating concentrate, mix and waste were kept constant during the two experiments.

About 20 kg of sample ESK2D, taken from low grade Mn ore portion of ESK2 lens, within the prospecting trench, were crushed to 100% -4 mm and passed through magnetic separator. Later a second test was done to check effect of grain size on separation. For this second test another batch of 20 kg of sample (ESK2E) from the same place was collected, crushed to -4 mm and sieved to three different grain sizes (-1, -2+1, and -4+2 mm) before enrichment.

2.7.1.2.1   Test Nr. 1

Feed, crushed to -4 mm, was passed through magnetic separator, that gave, as output, a concentrate a mix and a waste. The three output materials where then sieved to three grain sizes: +2-4 mm, +1-2 mm and -1 mm, and analyzed (Table 7). MnO enrichment is 13.05 wt% that corresponds to 10.11 wt% in terms of Mn.

wt%	SiO_2	Al_2O_3	Fe_2O_3	MnO	CaO	MgO	K_2O	Total recovery	Mn recovery	SE
Esk 2C Feed	36.41	2.61	3.02	40.89	1.39	0.81	0.55			
Esk 2C Conc	22.74	3.00	2.70	49.35	2.71	1.22	0.77	77.6	93.7	32.0
Esk 10C Feed	35.30	0.68	1.97	50.81	0.83	0.41	0.52			
Esk10C Conc	37.33	0.70	1.37	57.09	0.80	0.73	0.38	69.2	77.2	22.4

Table 7 XRF analyses, recoveries and Separation Efficiency for high manganese ore test.

2.7.1.2.2   Test Nr. 2

Feed, crushed to -4 mm, was sieved and divided into three grain sizes: +2-4 mm, +1-2 mm and 0-1 mm. The three new feeds were then passed through the magnetic separator, that gave, as output, three concentrates, three mixes and three wastes. The analyses of all the products are reported in Table 8.

MnO enrichment is respectively 17.57 wt% for the total and about 13 wt% for the three different grain sizes. MnO enrichment ranges between 11.33 and 13.23 wt% for the different grain sizes (8.78 and 10.25 wt% in terms of Mn) with a decrease from coarser to finer portions.

wt%	SiO$_2$	Al$_2$O$_3$	Fe$_2$O$_3$	MnO	CaO	MgO	K$_2$O	Total recovery	Mn recovery	SE
Esk2D feed	71.17	1.54	1.15	19.77	0.62	0.57	0.32			
Esk2D conc	55.82	1.75	1.45	32.82	0.77	0.76	0.33	54.16	89.07	43.5
Esk2D mix	79.14	1.40	0.80	8.30	0.57	0.34	0.30			
Esk2D tail	88.03	0.64	0.22	1.76	0.28	0.22	0.10			
Esk2D conc +2	55.81	1.26	1.30	35.25	0.67	0.42	0.22	47.18	78.32	48.7
Esk2D mix +2	73.75	1.37	0.93	15.71	0.64	0.41	0.24			
Esk2D tail +2	85.24	0.70	0.31	2.04	0.30	0.45	0.16			
Esk2D conc +1-2	58.07	1.46	1.26	31.73	0.70	0.62	0.30	56.28	93.82	44.8
Esk2D mix +1-2	80.10	2.04	0.99	4.28	0.76	0.48	0.44			
Esk2D tail +1-2	86.05	0.96	0.55	3.40	0.46	0.33	0.20			
Esk2D conc -1	56.94	2.26	1.97	29.42	0.86	0.93	0.45	63.64	96.23	40.9
Esk2D mix -1	80.29	1.60	0.48	2.31	0.58	0.30	0.27			
Esk2D tail -1	88.00	0.57	0.29	1.99	0.26	0.33	0.13			
Esk2E feed +2	71.67	1.17	0.83	20.20	0.59	0.32	0.22			
Esk2E conc +2	59.14	1.11	0.83	33.43	0.70	0.42	0.17	46.15	77.36	45.9
Esk2E mix +2	71.30	1.52	1.35	17.22	0.67	0.45	0.36			
Esk2E tail +2	82.44	1.12	0.63	4.93	0.48	0.31	0.24			
Esk2E feed +1-2	73.16	1.42	0.95	15.62	0.60	0.47	0.29			
Esk2E conc +1-2	60.78	1.44	1.24	31.96	0.67	0.56	0.29	50.70	92.57	45.3
Esk2E mix +1-2	78.82	2.36	1.24	4.41	0.86	0.56	0.55			
Esk2E tail +1-2	86.18	0.74	0.36	2.29	0.38	0.39	0.15			
Esk2E feed -1	68.57	1.84	1.41	18.90	0.75	0.70	0.35			
Esk2E conc -1	56.10	2.45	2.05	31.53	0.93	1.02	0.46	58.75	95.44	50.8
Esk2E mix -1	79.92	1.92	0.59	2.88	0.70	0.40	0.31			
Esk2E tail -1	86.35	0.85	0.24	1.98	0.44	0.27	0.12			
Esk2E feed tot	70.56	1.50	1.10	18.93	0.66	0.51	0.29			
Esk2E conc tot	57.91	1.81	1.48	32.29	0.81	0.73	0.33	52.29	87.50	47.9
Esk2E mix tot	74.83	1.74	1.10	11.32	0.70	0.45	0.37			
Esk2E tail tot	84.62	0.95	0.43	3.32	0.45	0.31	0.18			

Table 8 XRF analyses, recoveries and Separation Efficiency for low manganese ore test 1. ESK2E tot values are calculated as weighed averages of each product.

Chapter 2

Discussion

Mineralogy and texture of the Taycilar deposit show conditions that can allow magnetic enrichment of ore at relatively coarse grain size, providing the opportunity to produce a commercial grade gravel and sand final product.

Even if most of the mined Mn deposits host Mn mainly as oxides, braunite-dominated ores are known, like the Waziristan ores, Pakistan (Tahir Shah, 2007), or the Kalahari manganese field, South Africa (Gutzmer and Beukes, 1996), and mined, like at Kajlidongri mine, India (Ostwald and Nayak, 1993). Magnetic enrichment of a braunite-rich manganese ore is reported by Rao et al (1998) for the Chikla manganese ore, Maharastra, India. They performed high intensity wet magnetic separation on a 44 wt% Mn ore grinded to -0.1 mm, obtaining a 51 wt% Mn product at a 95% Mn recovery, compared with a 47 wt% Mn product obtained via jigging.

Most steel industry applications of manganese require a millimetric to centimetric grain size of ore and hence fine grained chert-hosted manganese ores can not be usually enriched. In our experiments we aimed at studying the possibility of magnetically enriching braunite-rich manganese ore at a much coarser grain size than those used by Rao et al. (1998), and having a gravel and sand final product as a result.

Magnetic properties of Mn ore have been assessed in magnetic prospecting (Bhimasankaram and Rao, 1957). Braunite shows a paramagnetic behaviour that is strongly affected by incorporation of elements, like Mg and Fe, substituting Mn (Abs-Wurmbach et al, 2002).

Mineralogical study of Taycilar manganese ore confirmed that the only important manganese phase is braunite, with only traces of manganese oxides. Gangue is, by far, dominated by quartz, whose behaviour is diamagnetic (Hrouda and Kapicka, 1986). In addition the Taycilar deposit shows a metamorphic texture that allows good separation of Mn-rich phases and quartz at relatively coarse grain size of crushed ore.

Both high and low grade manganese ore enrichment tests produced an increase of MnO content in concentrate at different recoveries. Parameters used to describe results of enrichment tests are MnO increase, total recovery, Mn recovery and Separation Efficiency (SE). MnO increase is simply defined as the difference between MnO content of concentrate and feed and was chosen as MnO content is more often used as a commercial parameter than simple Mn content. Total recovery is the fraction of the total feed weight that reports to the concentrate and provides information on the amount of valuable product that can be produced. Mn recovery is the fraction of Mn in the feed the reports to the concentrate and provides information on the efficiency of the valuable metal extraction from the ore. Finally SE was defined by Schulz (1970) as:

$$SE = Rm - Rg$$

where Rm is the % recovery of the valuable mineral and Rg is the % recovery of the gangue into the concentrate and provides information on the efficiency of separation between the valuable metal and the other elements during enrichment.

Previous equation can be used practically in the following form (Wills, 2006):

$$SE = \frac{100 Cm(c-f)}{(m-f)f}$$

where C is the total recovery, m is the Mn wt% content of the valuable mineral, c is the Mn wt% of the concentrate and f is the Mn wt% content of the feed. This formula is valid only assuming that all the valuable metal is contained in the same mineral (Wills, 1979), that is the case of Taycilar ore where other Mn phases are present only in traces.

High grade Mn ore test was designed more like a depuration than an enrichment test as the main purpose was to get a high total recovery in order to lose a low amount of Mn and hence to get a relatively high Mn recovery. On the other hand low grade Mn ore tests were designed to emphasize MnO increase in concentrate, as the MnO content of the feed was very low and hence they were planned for a lower total recovery. Results are summarized in Figures 34 and 35.
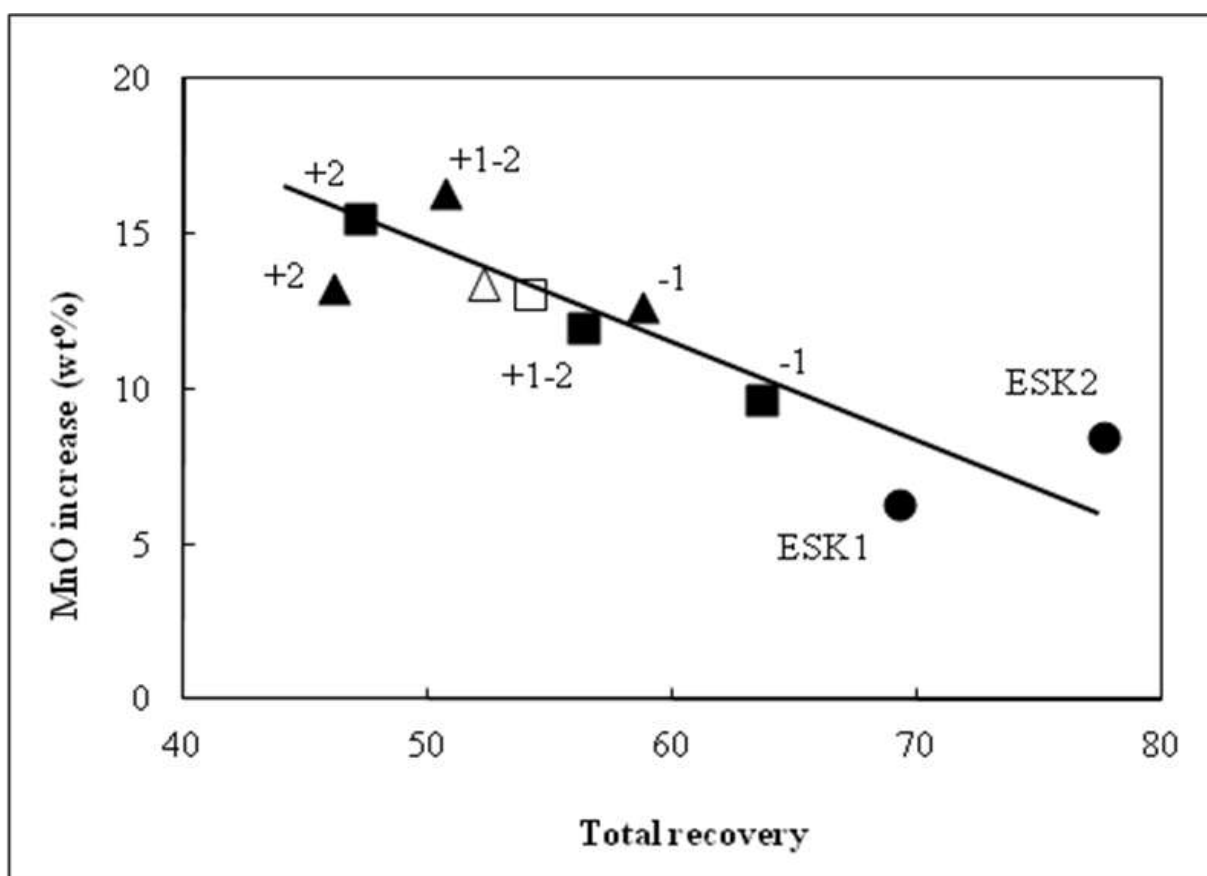
Fig. 34 Variation of Mn ore wt% and total recovery.
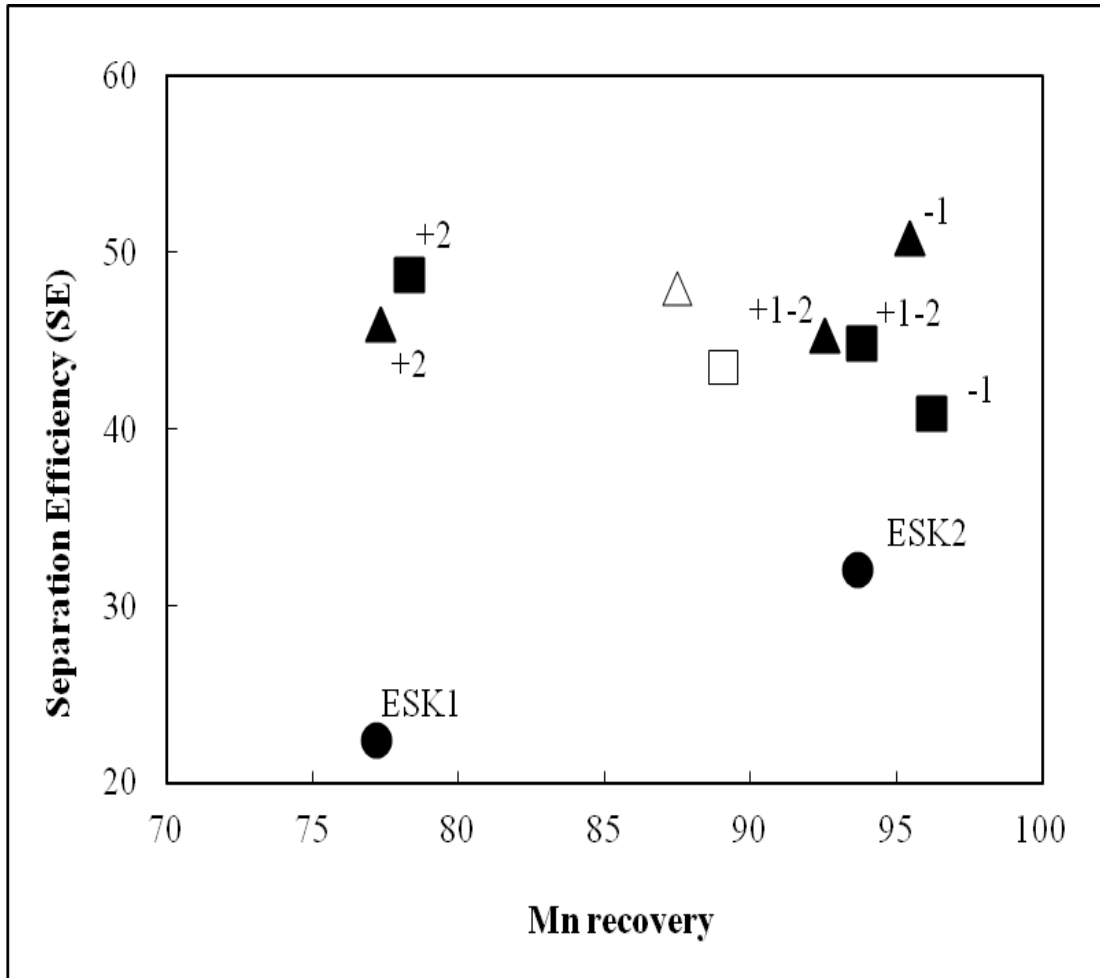
Fig. 35 Variation between Mn recovery and Separation Efficiency.

Two main parameters affect separation during tests: degree of liberation of the valuable mineral (i.e. braunite) and the deviation from gravity driven paths of particles due to the effect of magnetic field on braunite-rich particles. Coarse grain size of high grade Mn ore test was chosen because texture of the rock shows the presence of centimetric quartz lenses within a massive braunite ore. Results on ESK2 sample are very good with an MnO increase of more than 8 wt% at a high total recovery and a very high Mn recovery (Table 8). This means that almost only quartz reported to the tailing. The MnO increase when compared to total recovery is even better than that of low grade Mn ore tests at finer griainsize as in the chart it falls well above the regression line of the low grade Mn ore tests (Fig. 34). The low value of SE (Fig. 35), is due to the high proportion of quartz the reports to the concentrate and is the to the will to maximize Mn recovery. Results of ESK10 test are much worse: MnO increase is about 2% lower than ESK2 and, what is worse, Mn recovery dramatically decreases of 17.5 %. A strong decrease of liberation degree cannot justify these results as the texture of the sample is similar to that of ESK2. On the other +10 mm clasts make up 80 % of the sample and it was observed that coarsest clasts can easily rebound on the roll when they impact it after a 50 cm fall from the feeder. The dramatic decrease in the performance for ESK10 is due to its coarser grain size and we suggest that 10 mm can be an upper limit for particle size to avoid an important effect particle rebounding.

Low grade Mn ore tests needed an higher MnO increase in order to produce a valuable concentrate. Total enrichment gave good results with an MnO increase around 13 wt% (Fig. 34), an Mn recovery around 87 % and an SE around 47 (Fig. 35).

The small difference between results of test 1 without grain size pre-sorting of feed and test 2 where three feeds, with restricted grain size ranges, were tested separately indicates that separation of feed in different grain sizes, a money and time consuming operation, is not convenient.

Pre-sorting does not affect +2 class while a bigger MnO increase is compensated by a lower total recovery for +1-2 and -1 classes (Fig. 34)

The effect is better seen in Fig. 35 that shows how -1 class, at the same Mn recovery, has a higher SE for the pre-sorted sample that is compensated by a lower SE at slightly lower Mn recovery for +2 class.

While SE changes only slightly for both tests and for all grain sizes there is an abrupt fall of Mn recovery for +2 class in both tests. This cannot be due to a rebound effect as the flow of magnetic and non magnetic sands from the feeder is very smooth (Fig. 35) and can be attributed to a much higher proportion of middlings in this class and the consequent decrease in degree of liberation, that brings much Mn to the tailings.

Fig. 36 Picture of magnetic drum separator from university of Eskisehir, with ellipsed encircling concentrate (left) and waste (right) products.

In low Mn ore there is no separation of braunite-rich and gangue-rich domains and enrichment gives the best results at +1-2 grain size, due to the decrease of middlings content of the feed with decrease of grain size. In high Mn ore the separation of centimetric braunite- and quartz-rich-domains cannot be successfully used for efficient separation at centimetric grain size, due to the rebound effect on the magnetic roll. The best solution for the studied ore seems to be the magnetic separation (Fig.36) of low grade ore at +1-2 grain size and its mixing with not enriched high grade ore.

In general braunite-rich deposits can be successfully enriched via magnetic separation to produce a sand or sand-gravel concentrate, suitable for the manganese market, but a study of the texture of the rock is pivotal to set up the best separation conditions.

7. Conclusions

Magnetic enrichment tests on braunite-rich metamorphic Mn ore show that this technique can be advantageously applied to this kind of deposits at grain size +1 mm. Optimal grain size for enrichment depends on the texture of the rock that, in turn, depends on the degree of the metamorphic overprint. Hence a detailed study of the texture of all portions of the deposits is necessary to set up the best conditions for magnetic separation of braunite. In the range +1-25 mm low-grade deposits can be more efficiently enriched at lower grain size due to the decreasing amount of middlings. At these conditions it is possible to get high Mn recovery together with important increase of Mn content in the concentrate. On the other hand the formation of eye-texture with quartz lenses within high Mn ore, or, more in general, any separation of centimetric Mn-rich and Mn- poor domains during metamorphism cannot be efficiently exploited for magnetic separation at centimetric grain size as 10 mm is an upper grain size limit for this technique.

Finally pre-sorting of low-grade feed in different grain size classes does not significantly improve separation efficiency and, as it is a time and money consuming operation, it is not advised.

Chapter 2

3 WORK IN PROGRESS– Projects for the extraction of pyrite in Albania and Kosovo

3.1 Pyrite uses and pyrite market

Pyrite, iron disulfide, is one of the most ubiquitous minerals of earth's crust. It is found in igneous, metamorphic and sedimentary rocks and crystallizes at both high and low temperatures.

General formula: AX_2 where A = Au, Co, Cu, Fe, Mn, Ni, Os, Pd, Pt, Ru, and X = As, Bi, S, Sb, Se, Te.

Iron disulfide, FeS_2

Fe = 46,5

S = 53,45%

It is used for the production of sulfuric acid, but because of environmental pollution nowadays this use is still working only in China.

The main uses in the world today are :

1.	Stainless steel production	60%
2.	Abrasives production	15%
3.	Dyes, pigments for glasses	20%
4.	Brakes	3%
5.	Rechargeable batteries industry	2%

Quantity:

- Western countries: 20 000 ton/year
- Asia: 15 000 ton/year

The pyrite market for these new industrial uses is expected to increase rapidly in the next years.

3.2 Geological background of studied pyrite sites

The present work deals with projects for the extraction of pyrite in Albania and Kosovo (Fig. 37) for these new industrial applications.

For the projects three different ways to recover pyrite were considered:

a) as a by-product of pyrite-bearing active mines (Trepca, Kosovo; Fusharrez, Albania);

b) re-opening of abandoned pyrite mines used in past for sulfuric acid production (Spaç, Albania);

c) exploitation of a new pyrite deposit (Lunik, Albania).

Fig. 37. Map of pyrite-bearing sites considered for this study in Albania and Kosovo.

The map of the places where prospections to extract the pyrite ore are possible is shown in Fig. 37. Hereafter these places will be described following the classification mentioned above, beginning with the Trepca mine in Kosovo and the Fusharrez mine in Albania, taking into account that they are active mines where it is probably easier and less costly to extract pyrite.

Trepca Mine

The war-torn region of Kosovo in the Balkans has a long and involved history of mining. Over the years the world-famous Trepca mine (Fig. 38) has yielded millions of tons of lead and zinc as well as thousands of tons of silver and bismuth. More than 60 mineral species have been identified from the deposit. Minerals that have reached the specimen market include countless thousands of fine specimens of sulfides such as pyrite, pyrrhotite, arsenopyrite, sphalerite and galena, associated with well-crystallized quartz, dolomite, vivianite, ludlamite, calcite and rhodochrosite. From 1930-1940 the mine yielded 5,7 millions of tons of ore, and the on-site flotation plant produced 625,000 tons of lead concentrates, 685,000 tons of zinc concentrates, and 444,000 tons of a mixed concentrate of lead, copper and pyrite. The decline started in 1975 and accelerated after 1990 when Belgrade revoked the autonomy of Kosovo. The mine was closed in august 2000 after the war in Kosovo. Trepca Stan Terg Mine was reopened thanks to the efforts of the mine management and workers in 2005 with a production, in its first year, of 15.000 ton of lead-zinc ore. Since then, production has increased each year, reaching 128.000 tons in 2010.

Resources are still huge and could be enlarged by further exploration as the ore bodies have not yet been bounded.

Trepca legal status is Trepca Mine under UNMIK (United Nations Interim Administration Mission in Kosovo) rules and regulations, and on may 2013 will be under administration of KPA (Kosovo Privatisation Agency).

The biggest mines belonging to Trepca Mine are Stari Terg mine close to Mitrovica, and Artana Mine, close to Pristina, both sampled for this study.
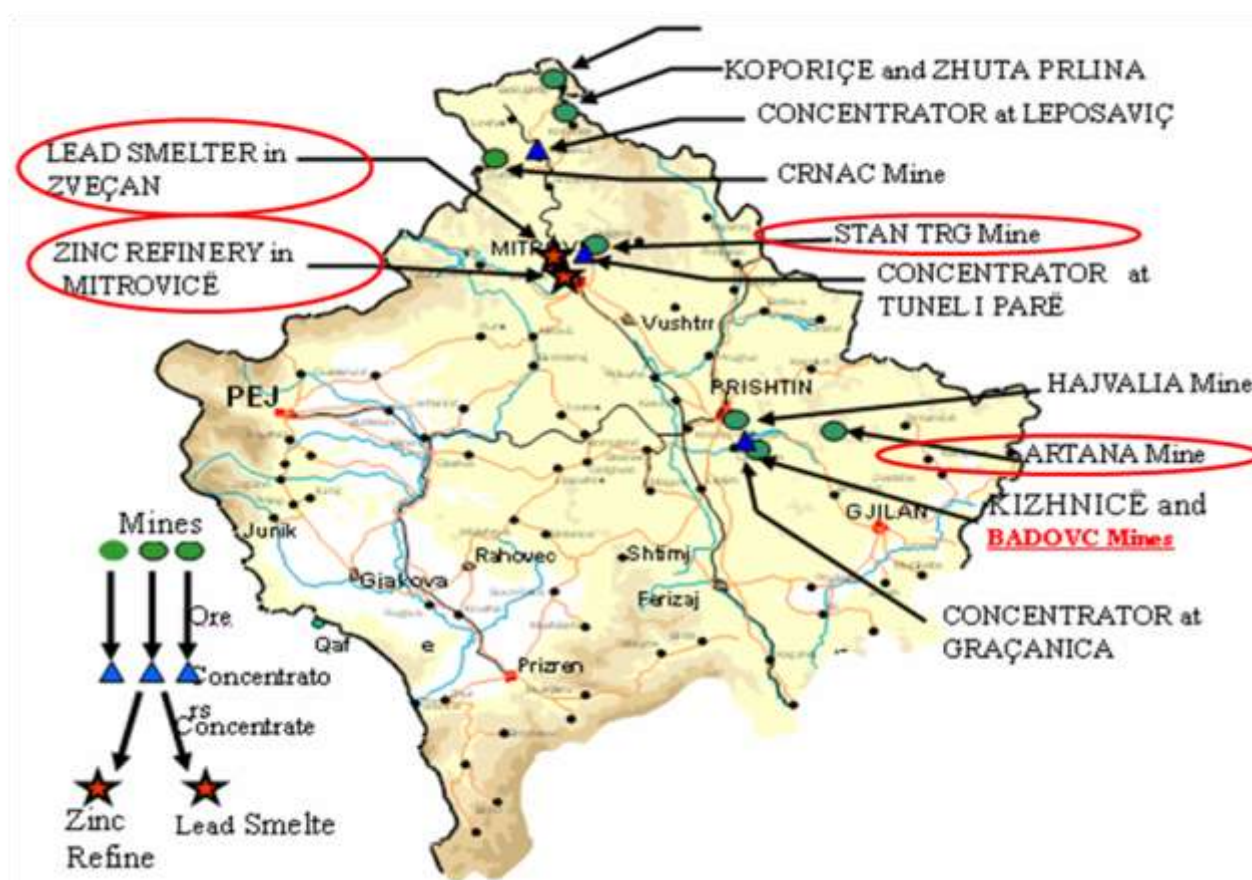
Fig. 38. Map of Kosovo and different mines of Trepça Mine.

The linear Trepça "Belt" of lead-zinc mineralization extends for over 80 km in northern Kosovo (Fig 39), and includes numerous mines and occurrences. It lies within the NNW-SSE trending Vardar tectonic zone. The regional structure marks the fundamental suture between the Serbo-Kosovaro-Macedonian Massif, which is underlain by late Proterozoic metamorphic successions, and the Dinarides (Fig.40), which comprise Mesozoic zones with typical Alpine deformation. The Vardar Zone contains fragments of Paleozoic crystalline schist and phyllite, with unconformable overlying Triassic clastics, phyllites, volcanoclastic rocks and Upper Triassic carbonates. Serpentinized ultrabasic rocks, gabbros, diabases and sediments of the ophiolite association characterize the Jurassic. The Cretaceous sequence consists of a complex series (sometimes described as

mélange) of clastics, serpentinites, mafic volcanics and volcanoclastic rocks, and carbonates. The Tertiary (Oligocene-Miocene) andesite, trachyte and latite sub-volcanic intrusives, volcanics and pyroclastic rocks occur at several centres within the Trepça Belt, covering large areas. They are particularly well developed in the eastern sector (the so-called Inner Vardar sub-zone) of the Vardar zone. Miocene and Pliocene shallow water sediments fill the Kosovo Basin, which borders the central and southern sectors of the Trepça Belt to the west (Hyseni et al., 2010).
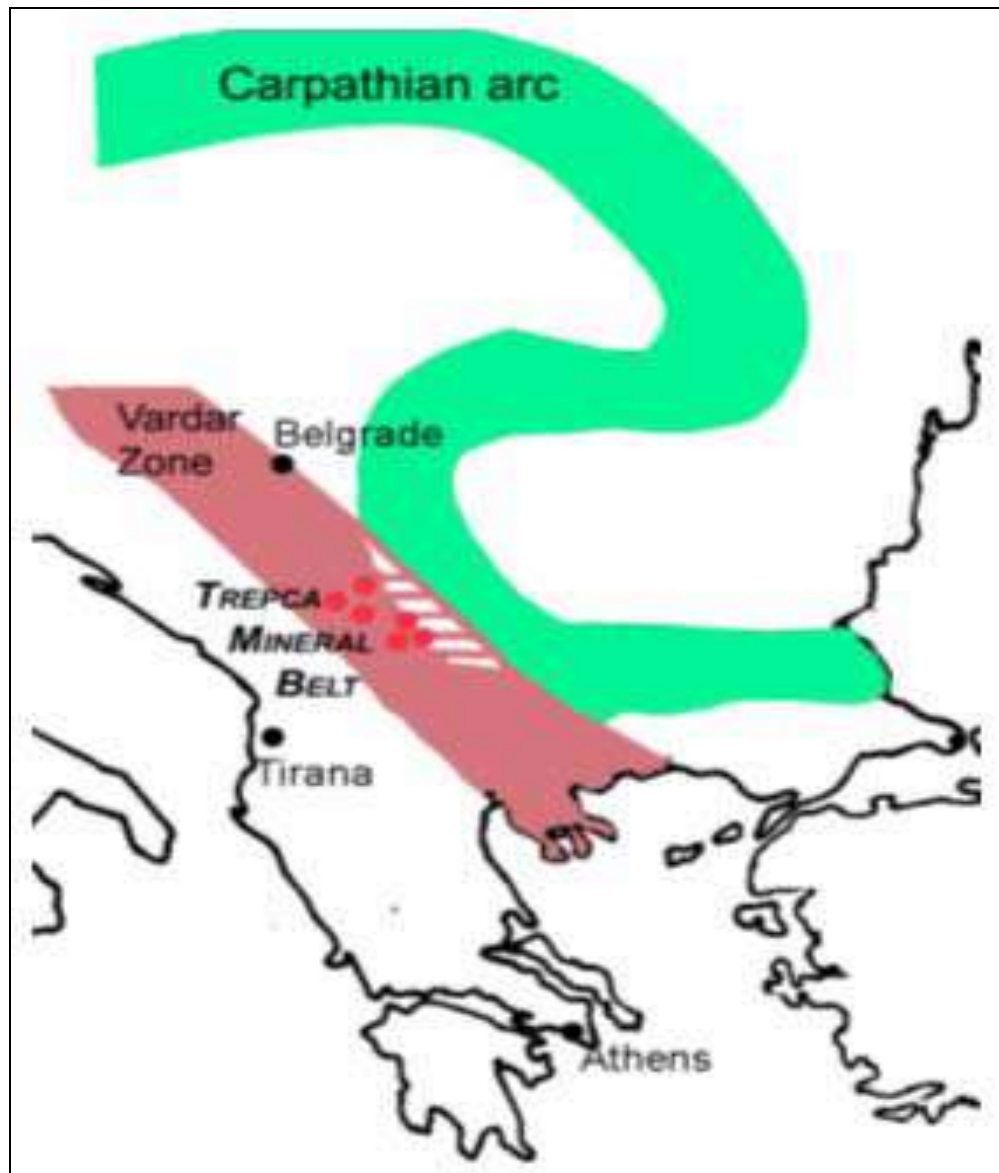
Fig 39. Geological location of Trepça mineral belt.
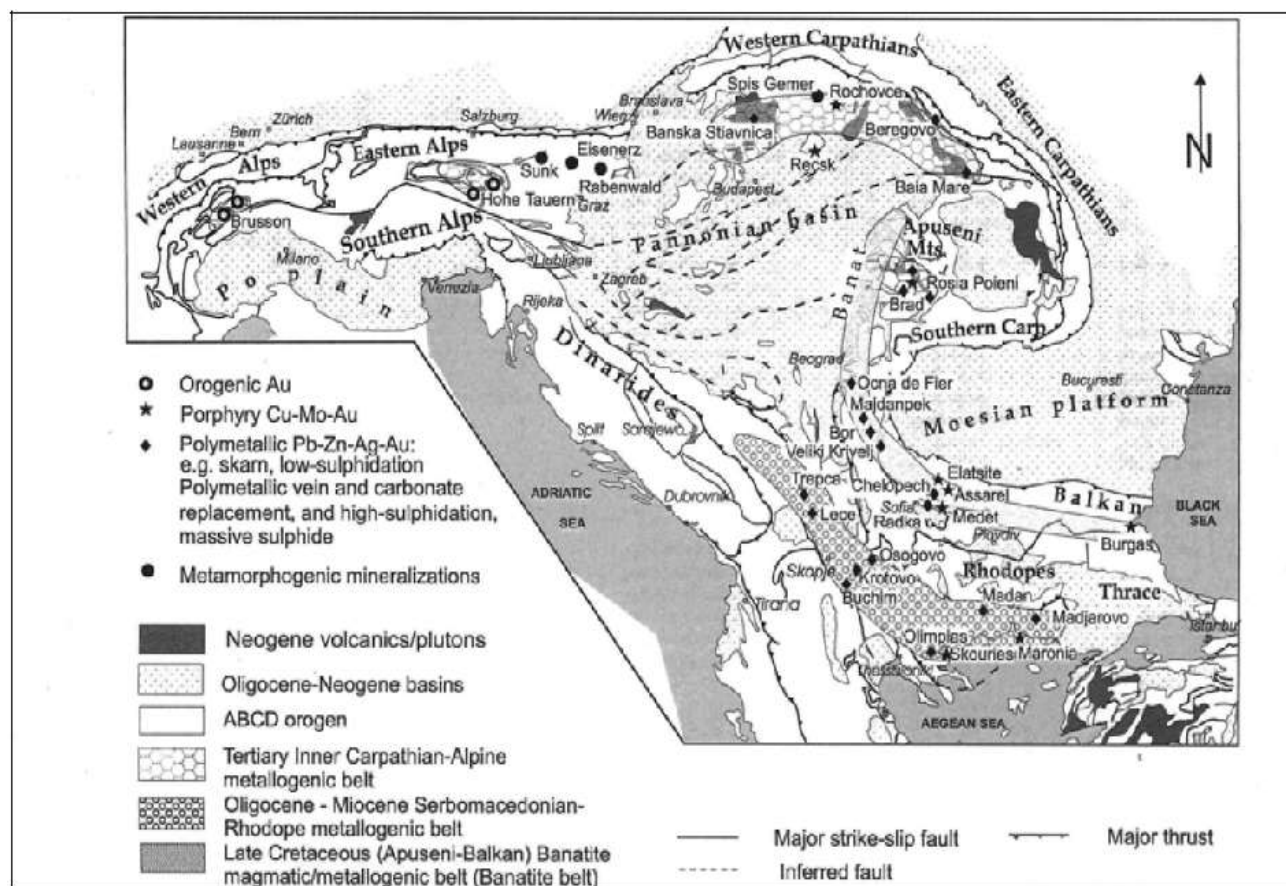
Fig 40. Simplified tectonic map of Neubauer et. Al. (2005) dispaying the distribution of major tectonic units and ore deposits in the ABCD (Alpine-Balkan-Carpathian-Dinaride belt) region.

As mentioned by Dimitrijevic (2000) and Sudar et al. (2006), "Vardar Zone" internal organization in three parallel subzones (internal, central and external) (Fig 41) is differently conceived by the geodynamicians, according to the position they devote to an important unit of this zone, the "Kopaonik Block and Ridge area", which outcrops in Kopaonik Mt, north of Trepca and includes several Pb – Zn – (Ag) ore deposits like Belo Brdo (Veselinovic – Williams et al., 2007). Nontheless, this block narrows in the South in the direction of Mitrovica, and in the Trepca area its deposits are covered by younger sediments and pyroclastites, which has led to locate Trepca mine (Fig. 42) without ambiguity as in the External Vardar Subzone (EVSZ).
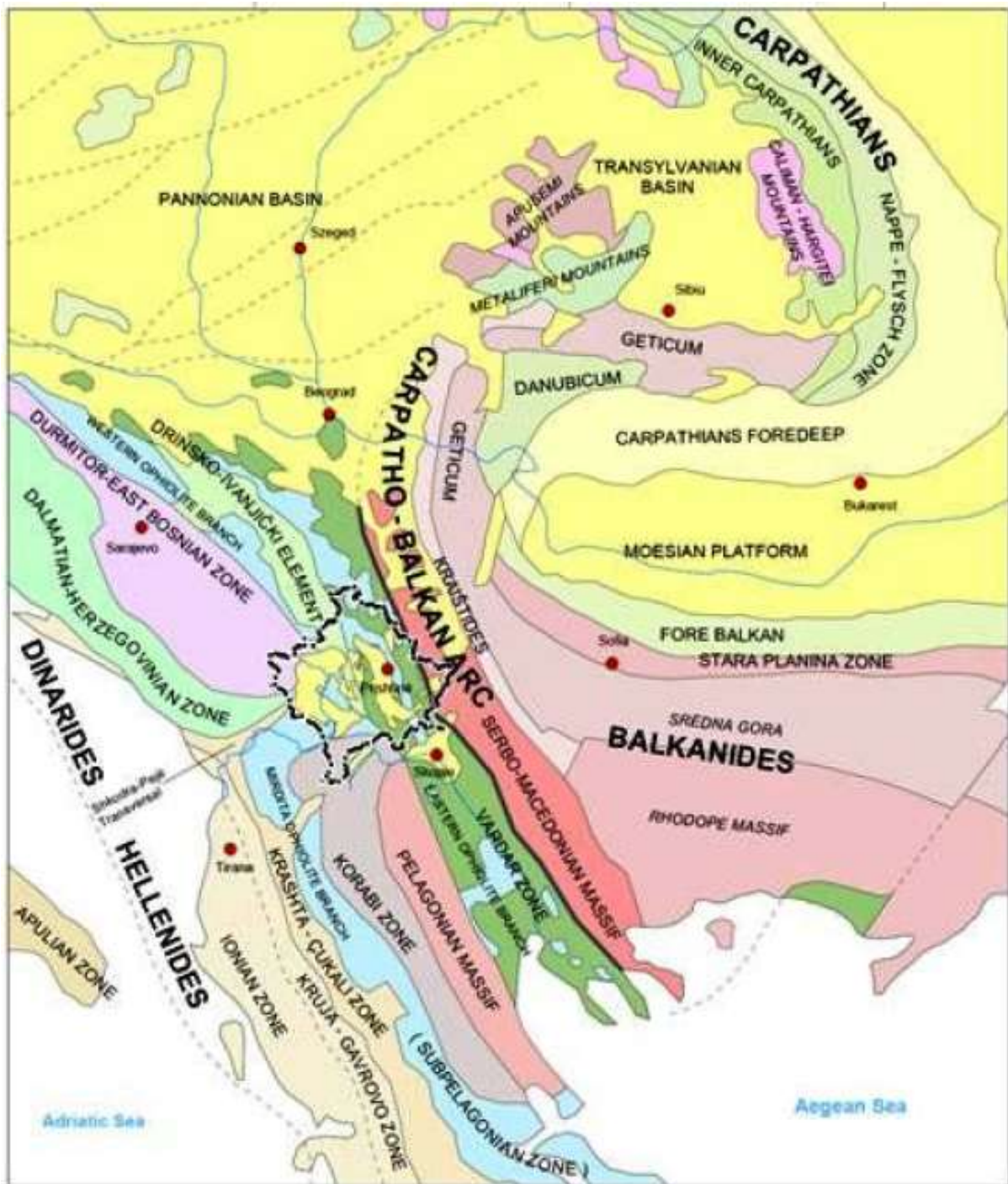
**Fig.41** Geotectonic setting of Kosovo (Dimitrijevic 2001)
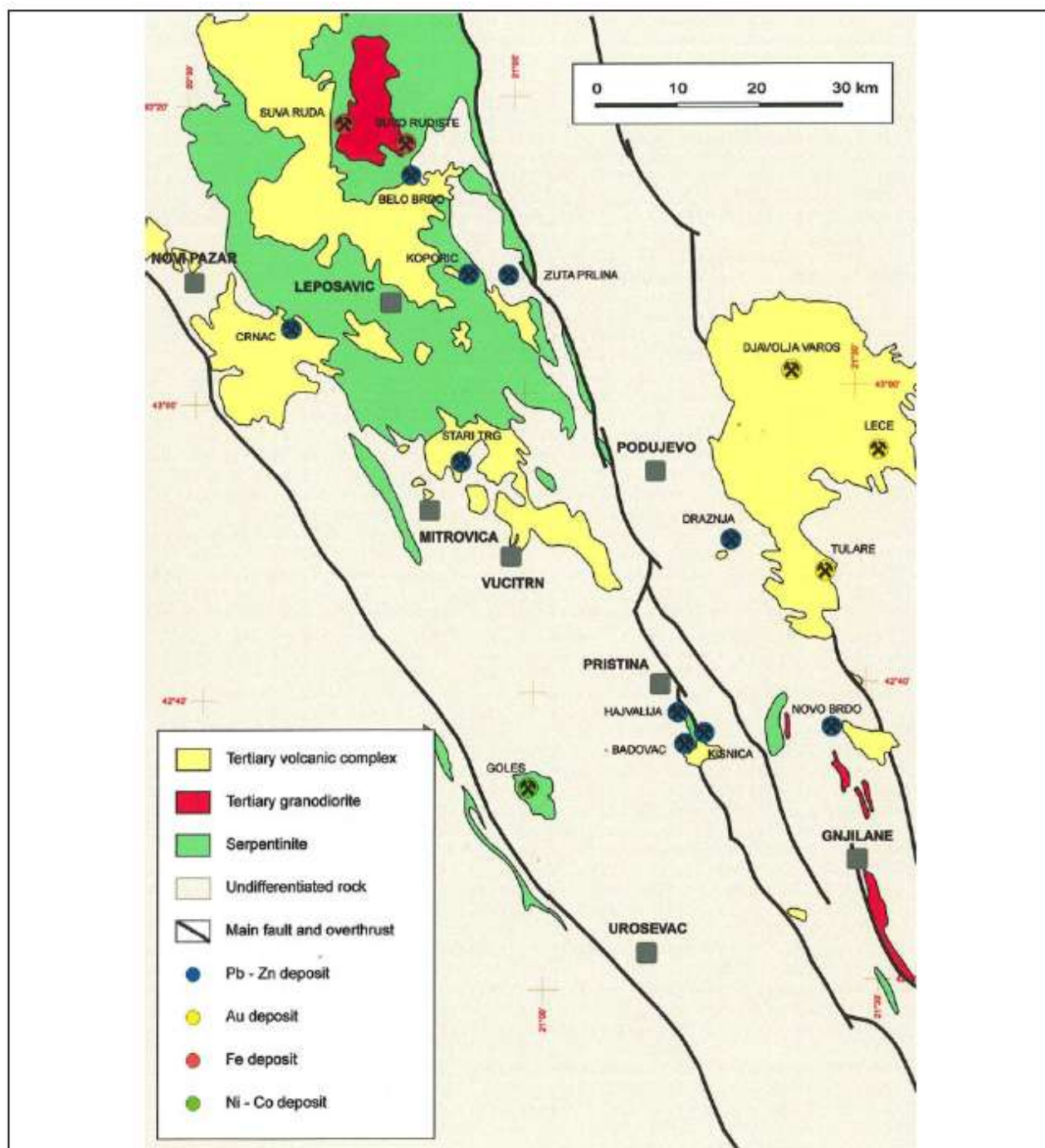
Fig.42 Geological sketch map of Trepca mine area (Monthel et al., 2001).

Chapter 3

At Stanterg, massive sulfide ore of economic importance forms continuous, columnar shaped ore bodies of carbonate replacement type (skarn) related to the emplacement of tertiary magmas (granodiorite and dacite-andesite) (Fig.43). These are located along the carbonate-schist contact and dip parallel to the plunge of the anticline and structural fabric and the dip of the flanks. The ore bodies extend along a strike length of 1,200 m (Figs. 43, 44, 45), and have been explored to a depth of 925 m below the surface (11 levels) (Fig. 46).

The Trepca mine ore deposits consist (Forgan 1950 ; Schumacher 1950) of a series of 11 manto orebodies that are intercalated between thick marmorised limestones at the footwall (Mazhiq limestones, at least 300 m thick) and thick sericite schists at the hanging wall (Figs. 43, 44, 45). In some places along the stratigraphic conctact there is an intercalated layer of quartzite and quartz – micaschists, from 5 up to 100 m thick, that Strucl (1981) interpreted as metamorphosed sandstones corresponding to the base of the jurassic transgression over the paleozoic schists. The contact between limestones and schists is folded in an asymmetric anticline, the northwest – southeast axis of which plunges 40° towards the northwest. The southern limb of the anticline dips 65° SW whereas the northen dips 35° N.
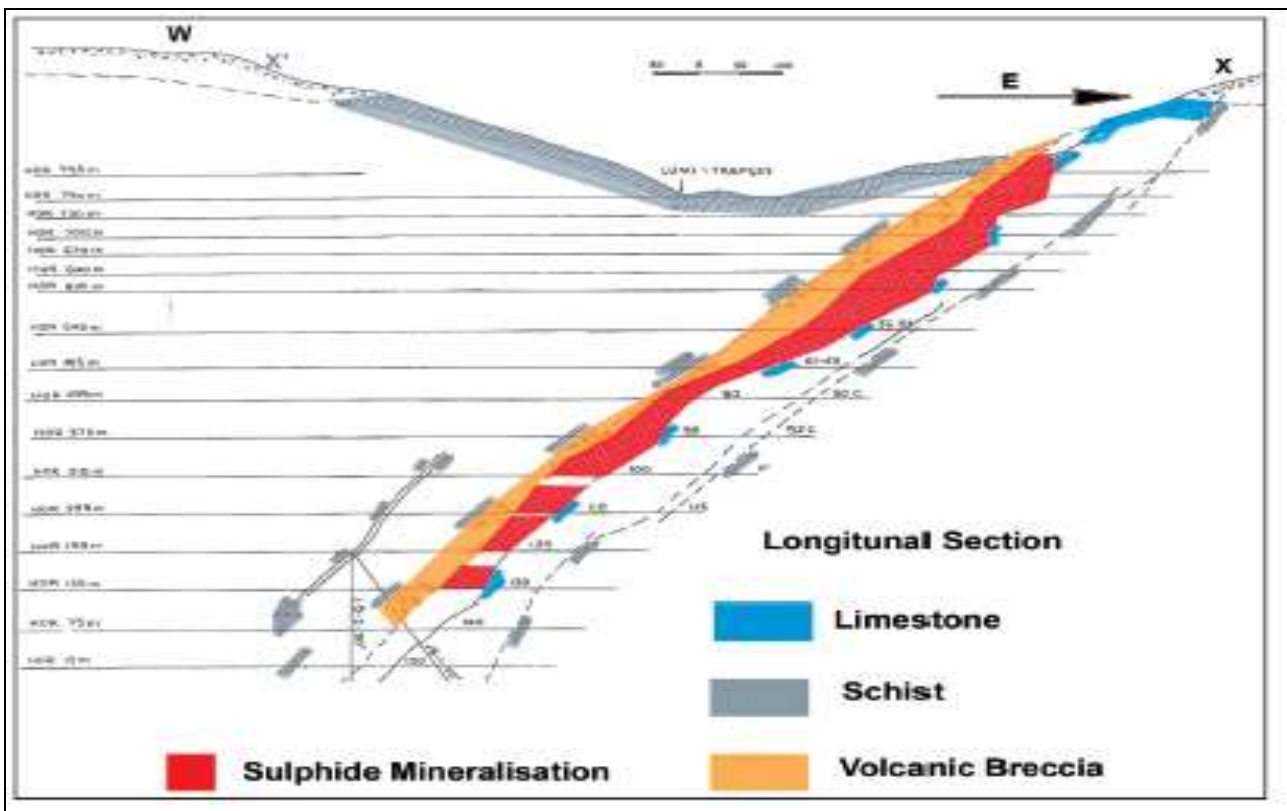

Fig. 43 Transverse cross- section along the Trepca antiform hinge axis, showing the mineralized skarn at the contact between the volcanic breccia and the limestones (initiated by Titcomb and Forgan 1936 and completed by the geologist of the mine till Maliqi 2001).
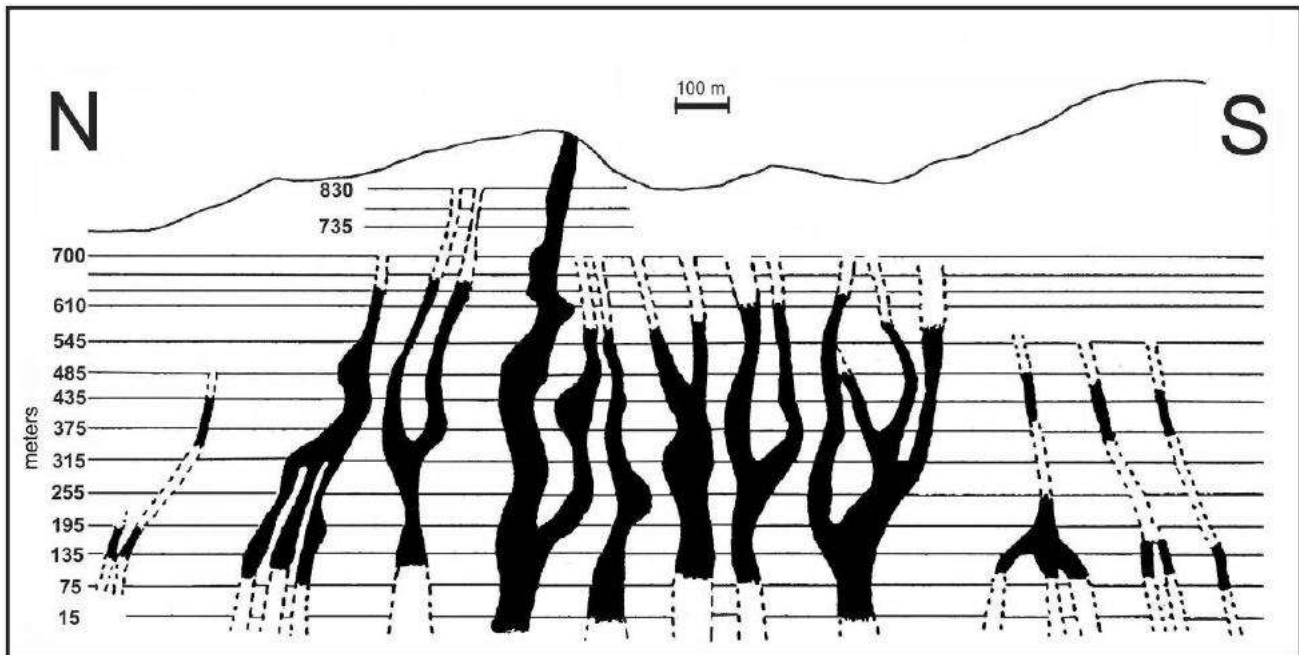
Fig. 44 Map of the unfolded contact between schists and limestones in Trepca, showing the elevations of each mining level and the 11 columnar – shaped orebodies (in black) coalescing downdip (modified from Kurtanovic, 1985).
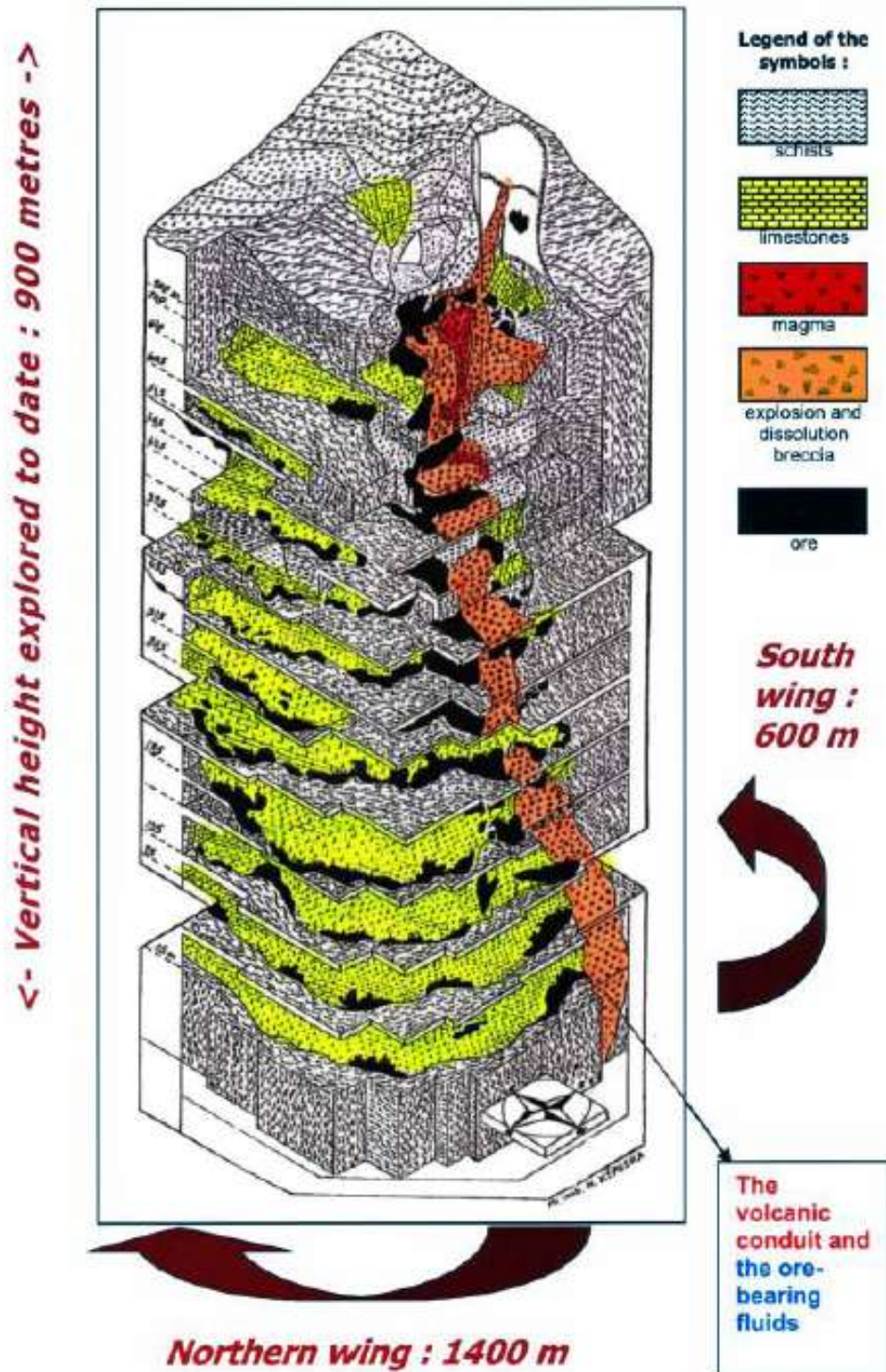
Fig.45 Geological block diagram of the Trepca ore deposit, from Kepuska. H (1998, modified). The projection used
increases the apparent pitch of the volcanic conduit and the axis of the mineralized anticlinal hinge.

Fig 46. Exploitation front from 11th level of Stanterg mine, Mitrovica, Kosovo.

The other important place that we sampled for the present study is the tailing of Artana Mine (Fig. 47, 48), that is a lead, zinc, silver and gold mine.This mine, exploited since Roman times, is reported to contain an in-situ resource of 2,670,000 t of ore at 4.40 wt% Pb, 4.90 wt% Zn, 137 g/t Ag and 1 g/t Au. The sampled tailing dumps are located at the embankments of the Krivareka river (Fig. 47 and 48).

The rocks in the surroundings of Artana mine belong to the series of Veles (Serbian-Kosovo-Macedonian) massif, mainly granite-gneisses, serpentinites, gabbroic rocks and granitoids as well as cretaceous and tertiary rocks, dominantly sediments, andesites and volcaniclastic rocks (Durmishaj et al., 2012).

Fig 47. Picture of waste dump of Artana mine.

Fig 48. Picture of waste dump of Artana mine.

Fusharrez and Spac mines.

Fusharrez active mine and Spac abandoned mine are here shown together because of their similar geologic setting. They are both located in the northern part of Mirdita ophiolite.

The Mirdita ophiolite is located in the Jurassic age Mirdita-Pindos ophiolite belt of Albania and Greece (Figs. 48, 49) that ranges from ultrabasic to mafic rocks with a number of andesitic and felsic volcanic domes in the central portion. The volcanic rocks are overlain by a sedimentary melange.
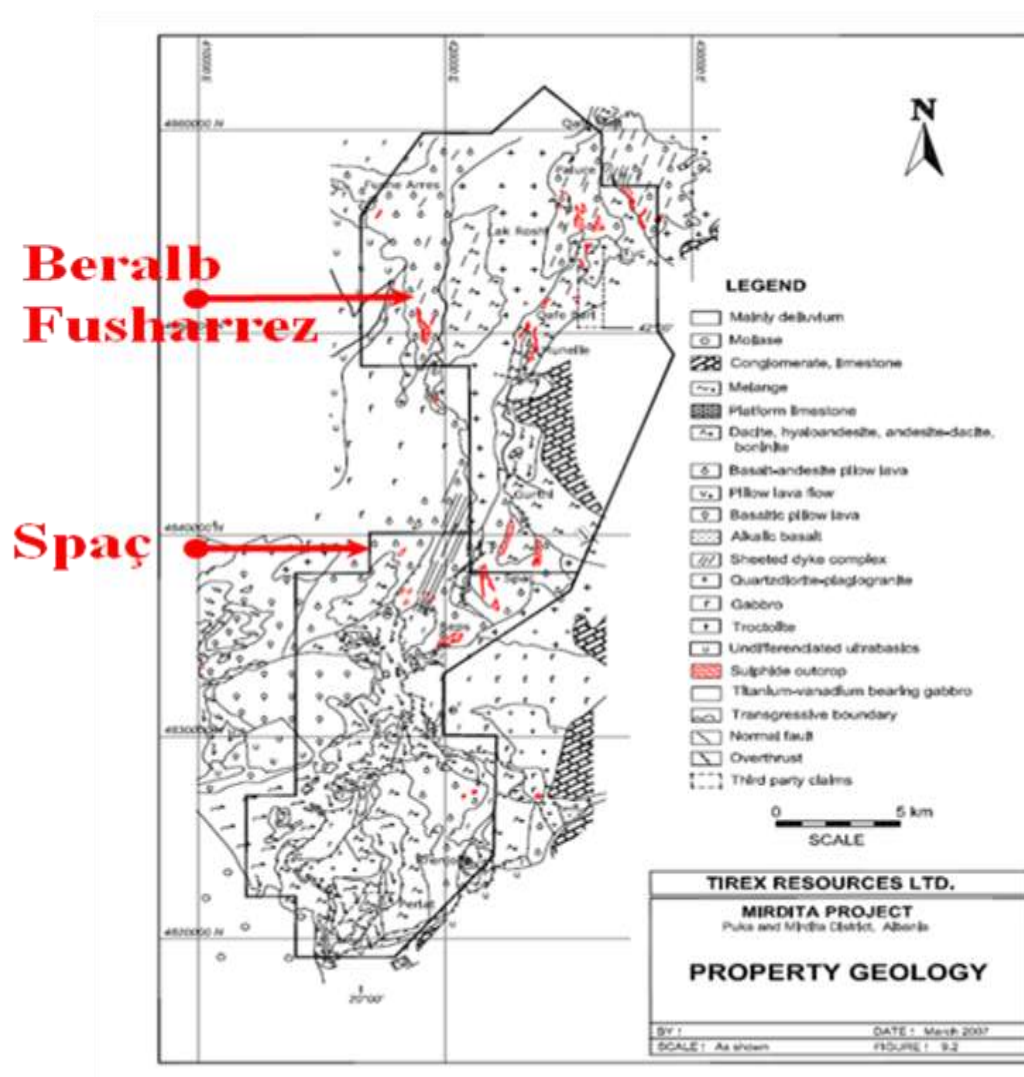

Fig. 49. Geologic map of Mirdita project mining licence area that includes both Fusharrez and Spac mines.
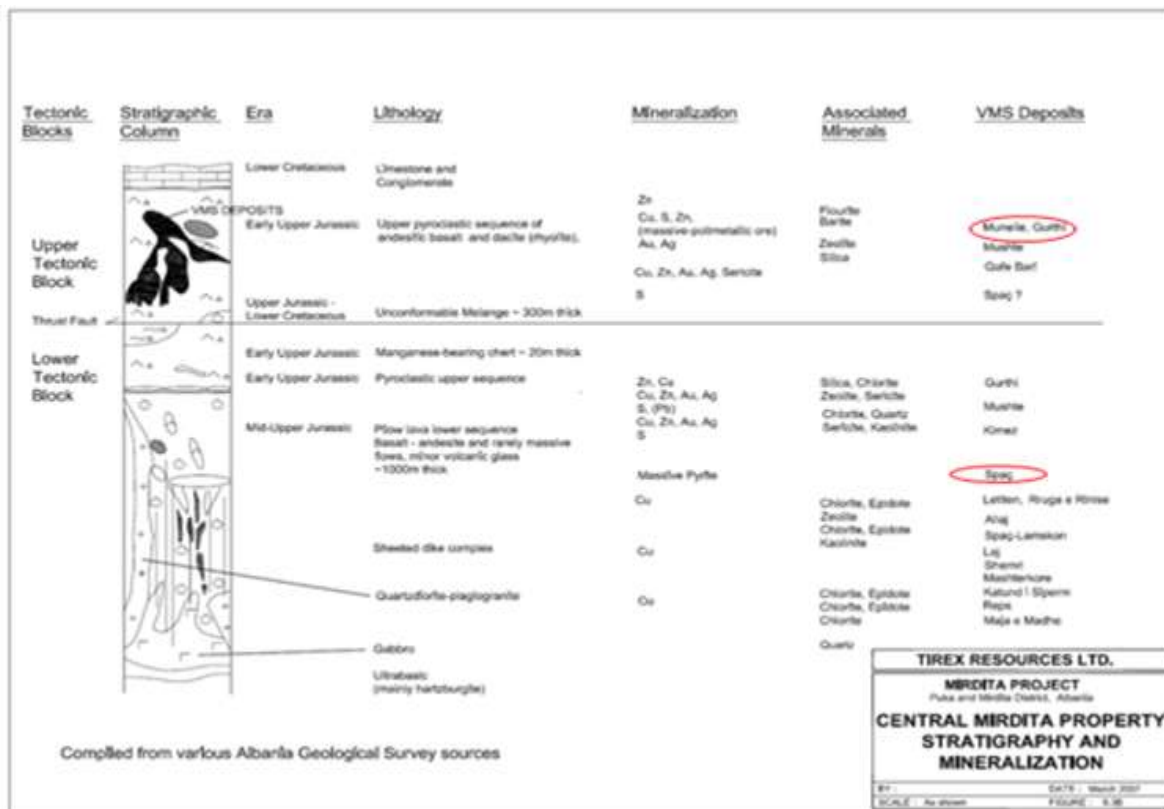
Fig. 50 Stratigraphy and mineralization of central Mirdita property, Mirdita project.

Fusharrez is a copper mine under the administration of Turkish Beralb mining company (Figs. 49, 50). Copper ore at about 2.3 wt% Cu is enriched at a plant located in Fusharrez by flotating cells that produce 12 to 22 wt% copper concentrate (Figs. 51, 52), whose tailings are strongly enriched in pyrite. Some preliminary studies were performed on selected samples and, at the moment, we are in negotiations for further collaboration.

Fig. 51 View of tailing dump after copper ore enrichment.

Fig.52 Picture of a flotation enrichment cell of copper ore, Fusharrez.

Chapter 3

Spac is an abandonated pyrite mine closed in 1985 (Figs. 53, 54). It was the biggest pyrite mine in Albania and has still around 70 000 tons of pyrite ore reserves not exploited yet. Due to the high quality of the ore mine did not require any enrichment plant and ore was stocked as it is and then sent to the sulfuric acid production plant. Several inspection trips at the mine led to the discovery of a stock of 1000 tons of pyrite. All the mine is nowadays under the jurisdiction of a governamental agency of Albania.

Fig 53. One of the adits of Spac mine, Albania.

Fig 54. Pyrite stock at Spac mine, Albania.

Lunik, Librazhd, Albania

The never exploited pyrite "Lunik" deposit is close to the rural Lunik village, about 15 km to the north of the small town of Libazhd. It is in outcrop a 1.5 m thick dike within volcanic rocks (Figs.55, 56, 57). It probably represent an hydrothermal conduit that was formed in underwater conditions inside with pillow basalts and at low temperature hydrothermal conditions.
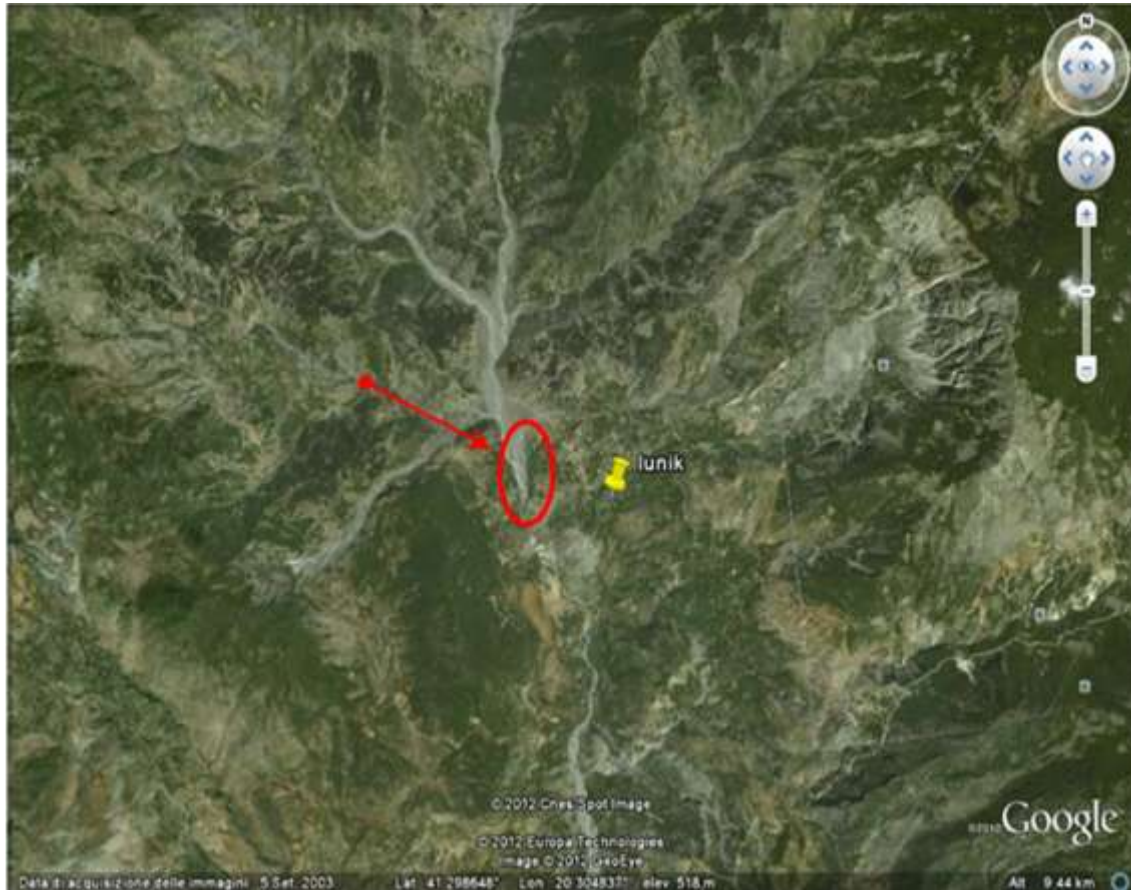
Fig. 55. Location of Lunik pyrite field.

Basaltic rocks of Lunik are placed over the gabbro through gabbrodiabase or over the ultramafic sequence of the western ophiolites through ocean metamorphic rocks (metabasalt), and covered normally by the upper-medium Jurassic siliceous radiolarite, or transgressively by heterogeneous ophiolitic melange of upper Jurassic (Titonian).

Vulcanites of this series in many sectors underwent low grade metamorphism in zeolite to greenschist facies and are affected by low temperature hydrothermal alteration that was responsible for the precipitation of pyrite.

Fig. 56 Pyrite ore outcrop.

Fig. 57 Detail of the pyrite ore outcrop in Fig. 56.

Chapter 3

3.3   Preliminary evaluation of pyrite fields

Several inspections to the mines and deposits led to preliminary agreements with the different owners of the rights on the fields, followed by a first sampling campaign from all the places that we studied in Albania and Kosovo. For each sample we made XRF analyses at the University of Milan. The results are shown in Tab .9.

	Kis 1	Kis 3	Trepca rock	Trepca flotated	PYRITE Spaç <10 mm	PYRITE Spaç 10-50 mm	Librazhd	Librazhd 1	Librazhd 2	Librazhd 3
S	39,47	32,96	49,4	32,2	47,8	51,4	39	34,9	28	46,7
Fe	34,61	29,61	41,3	26,9	41,6	44,6	33,9	33	24,9	40,9
SiO2	9,01	10,31								
Al2O3	12,62	21,71	0,26	0,83						
As	0,23	0,27	0.01	0,24	0,1	0,11				
CaO	1,61	3,17								
Co	0,002	0,002	0.002	0,002	0.01	0.022				
Cu	0,05	0,12	0.005	0,028	8,16	0,082				
MnO	0,06	0,02								
Ni	0,005	0,005	0.005	0,013	0.005	0.005				
Pb	0,53	1,41	0.01	0,67	0.01	0.01				
Cd	0,003	0,01								
Zn	1,73	2,03								
Sb	0,003	0,005	0,004	0,005	0,001	0,001				
Au (ppm)			0,025	1,525						
Ag (ppm)					5	<1				

**Table. 9** XRF analyses of pyrite ores from Kosovo and Albania.
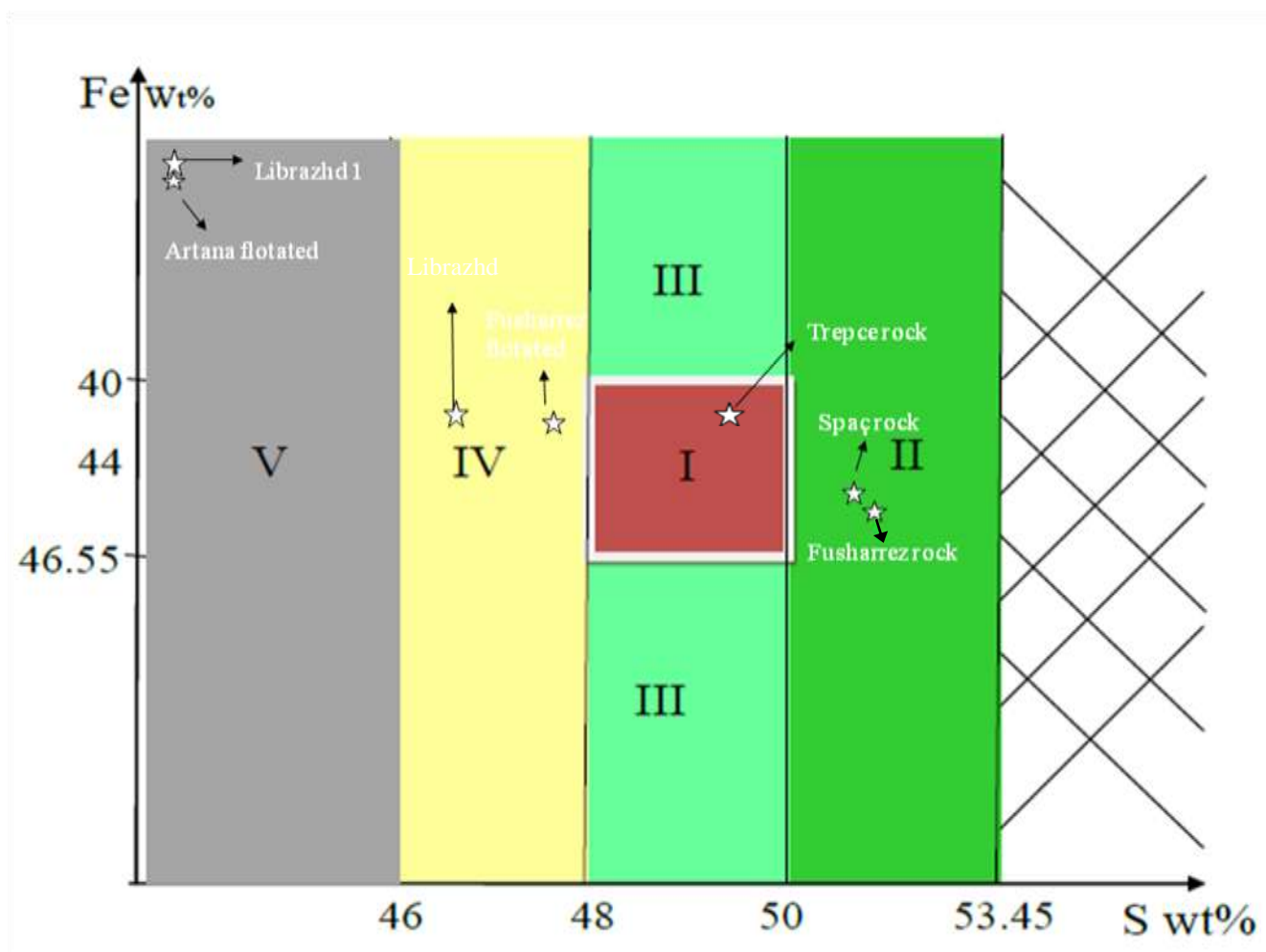
Fig. 58 Chart of geochemical quality parameters of pyrite.

As a conclusion we created a chart of geochemical quality parameters for new pyrite markets. According to the market requirements the pyrite must have a range of S = 48 - 50 wt%, and 40 < Fe < 46,55 wt%. With S that can have lower margin of 46 wt% S, for which pyrite can be still marketed but at a lower commercial value.

As we see in Fig. 58 the chart is divided in five fields.

I – is the perfect field that the market requires.

II – is even better in S content than what markets requires. So the products can be slightly diluted with low cost material

III – is not perfect but is still good because the content of Fe does not influence too much market demand.

IV – is not very good but still acceptable for the market uses.

V – is not useful because of the too low S content.

Samples taken from Trepca Mine as representative of pyrite-rich rock are very good in quality (field I), Samples taken from Spac and Fusharrez are even better than what market demands (field II). Samples taken from the tailings of Fusharrez are not perfect but still suitable for the market (field IV), the same for one sample from Lunik, Librazhd. Samples taken from Artana waste, together with some samples from Librazhd are very low, and cannot be considered useful (field V).

Place	Quality	Export possibilities
1 - Kosovo Trepce **a - rock** **c - Artana** **Albania Fusharrez** **a - rock** **b - flotated**	**Good** **Low** **Very good** **Good**	**Logistic problems of extracting** **No interest** **Negotiation** **Negotiation**
2 - Albania Spaç **- Albania Spaç stock**	**Very good** **Very good**	**Negotiation for re-start mining** **Concluded**
3 – Albania Lunik **Librazhd**	**By hand selection** **can be acceptable**	**Price negotiation** **No Logistic problem, easiest possibility**

Table. 10 Conclusions of the present preliminary study for pyrite-bearing sites considered in Kosovo and Albania.

This preliminary work led to create a list of pyrite sites in Albania and Kosovo where they can be put in order of priority for a possible use as pyrite source (Tab. 10).

Artana flotated pyrite has no interest due to its low S content. Rock sample from Stan Trg, Trepca, has a good quality but at the moment the company is not interest to develop this project due to the high cost of setting up a line for pyrite exploitation. New pyrite deposit at Lunik has a low quality and at the moment the possibility to enrich the possible run of mine is being evaluated. The best products come from Fusharrez and Spac. At Fusharrez anyway negotiations with the Beralb mining company are complicated by the high Au content of the pyrite (both rock and tailing).

As a result of the priority list, attention was driven on Spac pyrite mine and here on the pyrite stock, as re-opening of the mine, that was worked completely underground, is a much more complicated topic that requires more studies.

The work was started in summer 2012 in collaboration between the University of Milan and United Technologies (UT) Group, a company based in Milan that trades industrial minerals. The pyrite stock of this mine was sampled in more detail and analyzed at the laboratories of University of Milan. After the good results and having reached an agreement with the governamental agency that is in charge of the Spac mine works could

begin. The first step was to open a company in Albania called MT Durres. Firstly MT Durres participated in an auction for buying this stock. After this, under the technical supervision of the Author it was organized the work of selecting the material (Fig. 58), loading it on trucks (Figs. 59 to 64) and moving it to Durres port (Fig. 64). In the end about 960 tons of pyrite were brought from Spac mine to the port of Durres and stored there for the last destination in Italy to United Technologies plant. Export to Italy began in end of summer 2012 and is still ongoing. At UT Group plant close to Alessandria pyrite is dried, sieved and packaged for sale.

Fig. 59 Pyrite stock at Spac mine.

Fig. 60 Beginning of loading at Spac pyrite mine stock.

Fig. 61 Works after having loaded about half of the material.

Fig. 62 A truck used to carry pyrite to Durres port.

Fig. 63 Final operations, to be noticed the low quality discharged material on the ground.

Fig. 64 Pyrite stored in open air at the port of Durres, Albania.

The first step of this project was concluded with full satisfaction of the partners. Next step will be a detailed study of all the Spac mine to develop a feasibility plan for re-opening.

The work presented here was just a preliminary study for availability of pyrite ore in Albania and Kosovo for the new pyrite commercial markets. Hereafter the project of pyrite re-cycling will be developed together with another project concerning the environmental study of sulphide mines in Kosovo and Albania that has been funded as a part of Italian PRIN 2009 funds and involves collaboration with the universities of Tirana (Albania) and Pristina (Kosovo). The main target in joining the two projects is to assess the possibility to operate remediation of the contaminated sites also through the re-cycling of pyrite-rich dumps or stocks.

References

Abs-Wurmbach I., Ohmann S., Westerholt K., Meier T., Mouron P. and choisnet J. Magnetic phase diagrams of Mg-, Fe-, (Cu + Ti)- and Cu-substituted braunite $Mn^{2+}Mn_6^{3+}SiO_{12}$. Phys. Chem. Minerals, 2002, **29**, 280-290.

Abs-Wurmbach I., Peters T. The Mn-Al-Si-O system: an experimental study of phase relations applied to parageneses in manganese-rich ores and rocks. Eur. J. Mineral., 1999, **11**, 45-68.

Bhimasankaram V. L. S. and Rao B. S. R. Manganese ore of South-India and its magnetic properties. Geoph. Prosp., 1957, **6(1),** 11-24.

Borsi. S., Ferrara. G., Innocenti. F., Mazzuoli. R., 1972. Geochronology and petrology of recent volcanic in the eastern Aegean Sea (west Anatolia and Leovos Island). Bulletin of Volcanology 36, 473-496.

Bozkurt, E., Sözbilir, H., 2006. Evolution of the large-scale active Manisa fault, southwest Turkey: implications on fault development and regional tectonics. Geodynamica Acta 19 (6), 427–453.

Buhn, B., Okusch, M., Woermann, E., Lehnert, K., Hoernes, S. Metamorphic Evolution of Neoproterozoic Manganese Formations and their Country Rocks at Otjosondu, Namibia. J. Petrol., 1995, **36(2)**: 463-496.

Cox, D. P., and Singer, D. A., eds. Mineral deposit models: U.S. Geological Survey Bulletin 1693, 1986.

Dasgupta, H. Ch. and Manickavasagam, R., Chemical and X-Ray Investigation of Braunite from the Metamorphosed Manganiferous Sediments of India. Neues Jahrb. Mineral. Abh., 1981, **142(2)**, 149–160.

Dasgupta S., Sengupta P., Fukuoka M., Roy, S. Contrasting parageneses in the manganese silicate-carbonate rocks from Parseoni, Sausar Group, India and their interpretation. Contrib. Min. Petrol., 1993, **114**, 533-538.

Dimitrijevic, M. D. (200) – The dinarides and the Vardar Zone: the eternal conundrum. Proc. Intern. Symp. Geology and metallogeny of the Dinarides and the Vardar zone; Banja Luka. Acad. Sciences Arts rep. Srpska, Coll. And Monographs 1/1:5 – 13.

Dimitrijevic, M. D. (2001) – Dinarides and the Vardar Zone. Acta Vulcanologia 13 (1-2): 1-8.

Durmishaj, B., Hyseni. S., Tashko. A., Kelmendi. M., OPerta. M., and Tahiri. I., (2012) – Main geochemical association of the sulphides lead-zinc mineralization in Trepca mineral belt-Artana mine, Kosovo. ARPN Journal of Engineering and apllied Sciences. Vol.7 ISSN 1819-6608.

Emsley J. Manganese. In: Nature's Building Blocks: An A-Z guide to the elements. Oxford, UK: Oxford University Press, 2001, 249-253.

Ercan, E., Satir, M., Sevin, D., Turkecan, A., 1996. Bati Anadolu'daki Tersiyer ve Kuvaterner yasli volkanik kaycladra yeni yapilan radyometrik yas olcumlerinin yorumu (some new radiometric ages from Tertiary and Quaternary volcanic rocks from West Anatolia). Bulletin of Mineral Research and Exploration Institute (Turkey) 119, 103-112.

Eyidoğan, H., Jackson, J.A., 1985. A seismological study of normal faulting in the Demirci, Alaşehir and Gediz earthquake of 1969–70 in western Turkey: implications for the nature and geometry of deformation in the continental crust. Geophysical Journal of the Royal Astronomical Society 81, 569–607.

Forgan C.B. (1959) – Ore deposits at the Stantrg lead – zinc mine. K. C. Dunham editor, 18th intern. Geol. Congress, London, 1948, Part VII, Section F symposium, p. 290 – 307.

Garfunkel, Z.: 2004 Origin of the Eastern Mediterranean basin: a reevaluation. *Tectonophysics*, 391, 11-34.

Gorur, N.: 1988 Timing of opening of the Black Sea basin. *Tectonophysics*, 147, 247-262.

Gutzmer J. and Beukes N. J. Mineral paragenesis of the Kalahari manganese field, South Africa. Ore Geol. Rev., 1996, **11**, 405-428.

Hrouda F. and Kapicka A. The effect of quartz on the magnetic anisotropy of quartzite. Studia Geophysica et geodetica, 1986, **30(1),** 39-45.

Hyseni S., Durmishaj B., Fetahaj B., Shala F., Berisha A., Large D. 2010. Trepça ore belt and Stan Terg mine – Geological overwiev and interpretation, Kosovo (SE Europe). Geologija, 53/1, 87-92.

Kaymakci, N., 2006. Kinematic development and paleostress analysis of Denizli basin (west Turkey): implications of spatial variation of relative paleostress magnitudes and orientations. Journal of Asian Earth Sciences 27, 2007-222.

Ketin, İ.: 1966 Tectonic units of Anatolia. *Maden Tetkik ve Arama Bulletin*, 66, 23-34.

References

Kepuska, H. (1998) – Distribuimi I elementeve shperndarese dhe mikroelementeve percjellese ne mineralet kryesore xheheror formonjese ne vendburimin e plumbit – zinkut Trepca. Doktorrate Universiteti i Prishtines, Fakulteti Xehtarise Metalurgjise, Mitrovice, 80 p.

Kocyigit, A., Ozacar, A., 2003. Extensional neotectonic regime through th NE edge of outer Isparta Angle, SW Turkey: new field and seismic data. Turkish journal of Earth Sciences 12, 67-90.

Kurtanovic, R. (1985) – Zonalni raspored rudnih mineralizacija u funkcji usmeravanja istrazno pripremnih radova i ostvarenog kvaliteta eksploatacije u lezistu Trepca Stari Trg. Zonal distribution of ore minerals in the function of planing preliminary exploration activities and the quality of mining in the Stari Trg deposito f Trepca field. Vesnik Zadova za Geoloska I Geofizika Istrazivanja Beograd, A/43/126: 111 – 119.

Maliqi, G. (2001) – Ndertimi gjeologjik e strukturor I rajonit te Trepces. Geological and structural study of the Trepca ore deposits. Doct. Thesis of Geology, Polytechnical University of Tiranes and Facultu of Metallurgy of Kosova Mitrovica, University of prishtine. Edition Fakulteti I Gjeologjise dhe Minierave, departamenti i Shkencave te Tokes dega e gjeologjise, 137 p.

Monthel, J., Durmishaj, B., Frangu, S., Hoxha, G., Ilic, V. (2001) – The Trepca mining and metallurgical complex in Kosovo : ore resources assessment of Novo Bordo, Hajvalija, Kisnica and Crnac Pb – Zn mines. BRGM Report n° RC – 50641, Tec – Ingeniere, Trepca, UNMIK.

Mosier D. L. and Page N. J. Descriptive and grade-tonnage models of volcanogenic manganese deposits in oceanic environments – A modification. U.S. Geological Survey Bulletin 1811, 1988, 30 pp.

Neubauer, F., Heinrich, C., Geode ABCD working group (2005) – Late Cretaceous and Tertiary geodynamics and ore deposits evolution of the Alpine – Balkan – Carpathian – dinaride orogen. Mineral exploration sustainable development. Eliopoulos et al. Eds, Millpress, Rotterdam, 1133-1136

Okay, A.I., Siyako, M., 1993. The revised location of the İzmir–Ankara Suture in the region between Balıkesir and İzmir. In: Turgut, S. (Ed.), Tectonics and Hydrocarbon Potential of Anatolia and Surrounding Regions. Ozan Sungurlu Symposium Proceedings, Ankara, pp. 333–355.

Okay, A.İ., Satır, M., Maluski, H., Siyako, M., Monie, P., Metzger, R., Akyüz, H.S., 1996. Paleo- and Neo-Tethyan events in northwest Turkey: geological and geochronological constraints. In: Yin, A., Harrison, M. (Eds.), Tectonics of Asia. Cambridge University Press, Cambridge, pp. 420–441.

Ostwald J. and Nayak V. K. Braunite mineralogy and paragenesis from the Kajlidongri mine, Madhya Pradesh, India. Min. Dep., 1993, **28**, 153-156.

Özkaymak, Ç., Sözbilir, H., 2008. Stratigraphic and structural evidence for fault reactivation: the active Manisa Fault Zone, western Anatolia. Turkish Journal of Earth Sciences 17 (3), 615–635.

Özkaymak, Ç., Sözbilir, H., Uzel, B., Akyüz, H.S., 2011. Geological and palaeoseismological evidence for late Pleistocene-Holocene activity on the Manisa fault zone, western Anatolia. Turkish Journal of Earth Sciences 20 (4), 449–474.

Ozturk H. Manganese deposits in Turkey: distribution, types and tectonic setting. Ore Geol. Rev., 1997, **12**, 187-203.

Paton, S., 1992. Active normal faulting, drainage patterns and sedimentation in southwestern Turkey. Journal of the Geological Society of London 149, 1031–1044.

Rao G. V., Mohapatra B. K. and Tripathy A. K.. Enrichment of the manganese content by wet high intensity magnetic separation from Chikla manganese ore, India. Magnetic and Electric Separation, 1998, **9**, 69-82.

Ring, U., Susanne, L., Matthias, B., 1999. Structural analysis of a complex nappe sequence and late orogenic basins from the Agean Island of Samos, Greece. Journal of Structural Geology 21, 1575–1601.

Savascin, Y., 1978. Foca- Urla Neojen Volcanitlerinin Mineralojik ve Jeokimyasal Incelenmesi ve Kokensel Yorumu [Mineralogical and Geochemical Investigations and source Interpretations of Foca- Urla Neogene Volcanites]. PHD Thesis, pp. 1-15.

Schulz N. F. Separation efficiency. 1970. TRANS. SME-AIME. **247**, 56.

Schumacher, F. (1950) – Die Lagerstatte der Trepca und ihre Umgebung. Izdavacko Preduzece Saveta za Energetiku i Ekstraktivnu Industriju vlade FNRJ, Beograd.

Şengör, A.M.C., Görür, N., Şaroğlu, F., 1985. Strike–slip faulting and related basin formation in zones of tectonic escape: Turkey as a case study. In: Biddle, K., Christie-Blick, N. (Eds.), Strike–slip Deformation, Basin Formation and Sedimentation: Society of Economic Paleontologists and Mineralogists, Special Publications, 37, pp. 227–264.

References

Seyitoğlu, G., Scott, B.C., 1991. Late Cenozoic crustal extension and basin formation in west Turkey. Geological Magazine 128, 155–166.

Sözbilir, H., 2002. Geometry and origin of folding in the Neogene sediments of theGediz Graben, western Anatolia, Turkey. Geodinamica Acta 15, 277–288.

Sözbilir, H., Uzel, B., Sümer, Ö., İnci, U., Ersoy, E.Y., Koçer, T., Demirtaş, R., Özkaymak, Ç., 2008. D-B Uzanımlı İzmir fayı ile KD-uzanımlı Seferihisar Fayı'nın birlikte çalıştığına dair veriler: İzmir Körfezi'ni oluşturan aktif faylarda kinematik ve paleosismolojik çalışmalar, Batı Anadolu, Türkiye (Evidence for a kinematically linked E–W-trending İzmir Fault and NE trending Seferihisar Fault: kinematic and paleoseismogical studies carried out on active faults forming the İzmir Bay, Western Anatolia). Geological Bulletin of Turkey 51 (2), 91–114.

Sözbilir, H., Sümer, Ö., Uzel, B., Ersoy, Y., Erkül, F., İnci, U., Helvacı, C., Özkaymak, Ç., 2009. 17–20 Ekim 2005-Sığacık Körfezi (İzmir) Depremlerinin Sismik Jeomorfolojisi Ve Bölgedeki Gerilme Alanları ile Ilişkisi, Batı Anadolu (The seismic geomorphology of the Sığacık Gulf (İzmir) earthquakes of October 17 to 20, 2005 and their relationships with the stress field of their Western Anatolian region). Geological Bulletin of Turkey 52 (2), 217–238.

Sözbilir, H., Sarı, B., Uzel, B., Sümer, Ö., Akkiraz, S., 2011. Tectonic implications of transtensional supradetachment basin development in an extension-parallel transfer zone: the Kocaçay Basin, western Anatolia, Turkey. Basin Research 23 (4), 423–448.

Strucl, I. (1981) – Die schichtgebundenen Blei – Zink – Lagerstatten Jugoslawiens. Mitt. Osterr. Geol. Ges. **74/75**: 307 – 322.

Sudar, M., Kovacs, S. (2006) – Metamorphosed and ductilely deformed conodontd from Triassic limestone situated beneath ophiolite complexes : Kopaonik Mt., Serbia and Bukk Mts., NE Hungary. Geologia Carpathica, **57/3**: 157 – 176.

Tahir Shah M., Moon C. J. Manganese and ferromanganese ores from different tectonic settings in the NW Himalayas, Pakistan. J. Asian Earth Sci., 2007, **29**, 455-465.

Titcomb, H.A., Forgan, Ch. B., Lorimer, J., Page, W. C. (1936) – Trepca Mines Limited I to IV. Mining and Metallurgy, New York, v. 17, **9**:424 – 426, **10**:481 – 484, **11**:514 – 518 & 527, **12**:584 – 585.

Uzel, B., Sözbilir, H., 2008. A first record of strike–slip basin in western Anatolia and its tectonic implication: the Cumaovası basin as an example. Turkish Journal of Earth Sciences 17, 559–591.

Uzel, B., Sözbilir, H., Özkaymak, Ç., 2012. Neotectonic evolution of an actively growing superimposed basin in western Anatolia: the inner bay of İzmir, Turkey. Turkish Journal of Earth Sciences 21, 439–471.

Uysal I., Zaccarini F., Sadiklar M. B., Tarkian M., Thalhammer O. A. R. and Garuti G. The podiform chromitites in the Dagkuplu and Kavak mines, Eskisehir ophiolite (NW-Turkey): genetic implications of mineralogical and geochemical data. Geol. Acta, 2009, **7(3),** 351-362.

Vason M., Martin S. Metamorphosed iron-manganese deposits from the island of Thassos (Western Rhodope region, northern Greece). Ofioliti, 1993, **18(2),** 181-186.

Velilla, N. and Jimenez-Millan, J. Origin and metamorphic evolution of rocks with braunite and pyrophanite from the Iberian Massif (SW Spain). Miner. Petrol., 2003, **78**, 73-91.

Veselinovic – Williams, M., Treloar, P. J., Rankin, A.H. (2007) – The origin and evolution of the Belo Brdo Pb – Zn deposit, northern Kosovo. In: C.J. Andrew et al. (eds), proc. Ninth Biennal SGA Meeting, Dublin 2007, **1:** 161 – 164.

Wedepohl A.. The composition of the continental crust. Geochim. Cosmochim Acta, 1985, **59(7),** 1217-1232.

Wills B. A. Wills' mineral processing technology. 2006. Butterworth-Heinemann, Oxford, 444 pp.

Acknowledgements

Author is grateful to UT Group srl., Sigma metal LTD. and 4 Mevsim Madencilik LTD. for their technical and logistic support.

I am also grateful to Dean. Izet Zeqiri, University of Prishtina, Dean. Ferat Shala Mine of Trepca Coorporation, Kosovo, Prof. Agim Sinojmeri University of Tirana Albania, for their help during my three years of work for my PhD thesis.